THESIS APPROVAL

GRADUATE SCHOOL, KASETSART UNIVERSITY

Master of Engineering (Civil Engineering)

DEGREE

Civil Engineering | Civil Engineering

FIELD | **DEPARTMENT**

TITLE: Behavior of Cold-Formed Steel Built-up Column using Channel Sections With Different Weld Spacing

NAME: Mr. Siripob Kakaew

THIS THESIS HAS BEEN ACCEPTED BY

THESIS ADVISOR

(Assistant Professor Kitjapat Phuvoravan, Ph.D.)

THESIS CO-ADVISOR

(Associate Professor Trakool Aramraks, Ph.D.)

DEPARTMENTHEAD

(Associate Professor Wanchai Yodsudjai, Ph.D.)

APPROVED BY THE GRADUATE SCHOOL ON _____

DEAN

(Associate Professor Gunjana Theeragool, D.Agr.)

THESIS

BEHAVIOR OF COLD-FORMED STEEL BUILT-UP COLUMN USING CHANNEL SECTIONS WITH DIFFERENT WELD SPACING

SIRIPOB KAKAEW

A Thesis Submitted in Partial Fulfillment of
the Requirements for the Degree of
Master of Engineering (Civil Engineering)
Graduate School, Kasetsart University
2013

Siripob Kakaew 2013: Behavior of Cold-Formed Steel Built-up Column using Channel Sections with Different Weld Spacing. Master of Engineering (Civil Engineering), Major Field: Civil Engineering, Department of Civil Engineering. Thesis Advisor: Assistant Professor Kitjapat Phuvoravan, Ph.D. 173 pages.

The research presents on the buckling behavior of cold-formed steel built up column using channel sections with different weld spacings which is subjected to compression between fixed ends. The built-up sections of test specimens were prepared by welding two light lip channel sections together creating a closed column section. More specifically, the welded spacing is varied for each specimen since the weld spacing effects the buckling behavior in different ways. Although this type of built-up column is widely used as a main structural member in the present construction, their behaviors have not been acknowledged by most engineers. This research is conducted to reveal behaviors of built-up sections under concentric compression loading. All the experimental results are compared with the compressive design strength according to the AISI. The effects of the weld spacing on compressive strength and their corresponding buckling behavior are concluded. Furthermore, the stress distributions in the local buckling and post-local buckling states including the failure modes in each column were also studied. However, different weld spacings in each specimen result in different loading capacity.

_____ _____ __ / __ / __

Student's signature Thesis Advisor's signature

ACKNOWLEDGEMENTS

This research would not have been successful without the help, support and guidance rendered by many people were directly or indirectly involved in this work. I would like to express my sincere gratitude and appreciation to my thesis advisor Assistant Professor Dr.Kitjapat Phuvoravan for his invaluable guidance, encouragement and insight provided throughout the research period. My sincere appreciation is also due to Associate Professor Dr.Trakool Aramraks for his invaluable suggestions.

I would like to thanks Bluescope Steel Co., Ltd. and Bluescope Lysaght. Co.,Ltd. who supported the materials for this research and thanks the staff of International Graduate Program in Civil Engineering (IPCE), Kasetsart University. I would like to take this opportunity to thank all my class mates in graduate program in IPCE for making my stay at the university a memorable one.

I would also wish to express my sincere thanks to my parents, friends and well wishers for rendering their support throughout the study period. Lastly, my sincere appreciation goes to my beloved family for their understanding and unwavering support.

Siripob Kakaew

January 2013

TABLE OF CONTENTS

Page

LIST OF TABLES

LIST OF FIGURES

LIST OF FIGURES (Continued)

LIST OF FIGURES (Continued)

LIST OF FIGURES (Continued)

LIST OF FIGURES (Continued)

BEHAVIOR OF COLD-FORMED STEEL BUILT-UP COLUMN USING CHANNEL SECTIONS WITH DIFFERENT WELD SPACING

INTRODUCTION

General

Economic crisis in Thailand nowadays continually effects deceleration in construction industry due to the higher construction cost resulted from the higher prices of construction materials. Accordingly, steel production cost that becomes higher causes the increasing price of the product as well. Therefore, the production of cold-formed steel has been introduced into the industry to replace the production of hot-formed steel which is more expensive. Compared to the latter, the advantages of cold-formed steel over hot-rolled steel are that cold-formed steel has better strength to weight ratio and is lighter, for instance, it is lighter and stronger. Its production also brings about the reduction of labor cost, material cost, and overhead cost.

Cold-formed steel is now extensively used throughout both developed and developing countries in the construction of factory, ready-made house, and shopping mall. Its thickness is from 0.3 to 6.3 mm. The certain thickness of the steel frequently sold in market place is 1.3, 2.0, and 2.8, and especially 1.6, 2.4, and 3.2 mm. The steel sections that find favor public in Thailand are C-channel, U-shaped, and Z-shaped sections, including round steel tube and rectangular steel tube.

In Thailand, there are only a few serious studies of the qualities and structural behaviors of cold-formed steel. Therefore, the steel used as primary structures like columns and beams is more likely to gain less confidence of its users. On the contrary, In European countries and some other countries like Australia, Canada, and the United State of America, or even in Asian countries like China, Japan, and Malaysia, the studies of cold-formed steel have been carried out more earnestly. That

is because although the steel is beneficial in many ways, in a way it is quite thin and there are some problems in its production process. Also, some aspects like its bearing capacity and buckling behaviors need to be further researched.

Nowadays, there are several design and construction standards that have been set in many countries, namely AISI Code, European Code, AS/NZS Code, and so on. as for Thailand, the Engineering Institute of Thailand (EIT) is responsible for the standard setting which is based on Specification for the design of cold-formed steel structural members of American Iron and Steel Institute (AISI). However, the standard set by EIT does not correspond to practical operation, The lack of understanding in structural behaviors and the shortage of practical working knowledge can possibly cause damage to the steel work in the future.

Recently, closed sections made of two similar steel sections attached by welding have been introduced to structural work and more widely used as column and other parts. The weld spacings on the sections can be varied depending on the welders. However, some welders might be unaware or lack the knowledge of how long the spacings should be to make an efficient welding. Hence the seam welding without any spacings can lead to the bending of column members since cold-formed steel is thinner than hot-formed steel.

Accordingly, this study is aimed at the understanding of the behaviors of built-up sections made of C-channel closed sections attached by welding with regular spacings. Included in this study are a number of case studies in different weld spacings on fix supports of both sections. Compression test in laboratory is also conducted to make a comparison of column buckling load and stress in different welding conditions. Buckling behaviors are mainly focused, especially two buckling patterns: local buckling and post local buckling. As well as compression test, tension test in laboratory is conducted to find out mechanical quality of the material.

Finite element method, a numerical method, is used here to solve differential equation. The equation can sometimes be complex, and the numerical answer will be

taken to model or predict the structural behaviors of cold-formed steel. The results are presented in 3-dimensional pictures and the analytical interpretation in color shades of stress. Then the interpretation will be used in finding out critical limits, stress, and failure patterns of the structure. Being compared with the experimental result in laboratory, the result of finite element method can be verified that it is correct and suitable for practical use.

By all reasons, the understanding of the general structural behaviors of cold-formed steel plays an important role in efficient structural design of the steel that is prone to growing use. However, the study of its behaviors is in adequate. Hence this study will bring about comprehensive knowledge in this field that will lead to confidence and safety in the use of cold-formed steel sections.

The cold-rolled steel has several advantages in building construction:

1. Building components made of cold-formed steel can be fabricated with high accuracy in a plant and then assembled on job sites, which generally increases erection efficiency and ensures construction quality (Yu ,1924) .

2. Cold-formed steel structural members are economics in transportation and handing. Light weight cold-formed members or panels are easy to handle and to transport. In addition, they can be nested and bundled, reducing the required shipping and storage space.

3. Thin-walled cold-formed steel sections can be used efficiently as structural members of light–weight structures when hot-rolled sections or others are not efficient.

4. Comparison with thickness hot-rolled shapes, cold-formed light members can be manufactured for relatively light loads and short spans.

5. No formwork needed – The use of cold-formed steel decks eliminates the formwork steel decks eliminates the formwork for pouring concrete floor. In addition,

composite action between the steel deck and concrete increase floor strength and stiffness.

6. All conventional jointing method (i.e. riveting, bolting and welding) can be employed.

7. Durable material–Cold-formed steel is durable because it is termite-proof and rot-proof. In addition, galvanized cold-formed steel products can provide long-term resistance to corrosion.

8. Steel is a non-combustible material and will not contribute fuel to the spread of a fire. This can result in better fire resistance and lower insurance premiums.

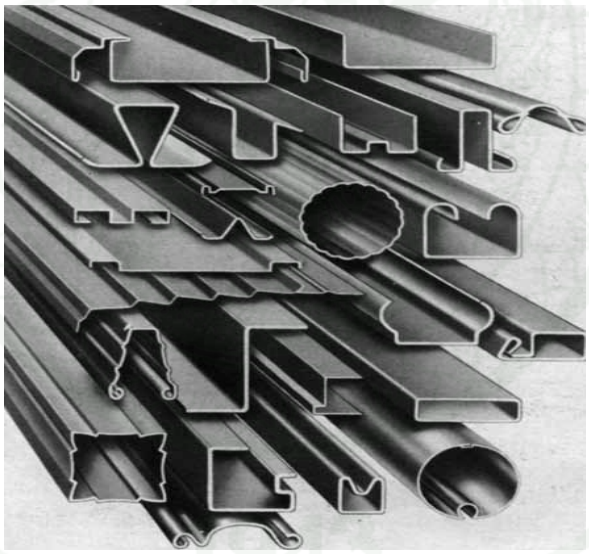

Figure 1 Various shapes of cold-formed sections

Source: Yu (1924)

Panels and Decks

Cold-formed steel sheeting can be used to satisfy both structural and functional requirements. The structural use is more thoroughly considered. Profiled steel sheeting is widely used in roof, wall and floor structures. In these structures, the profiled steel sheeting actually satisfies both the structural and functional requirements. In floor structures the steel sheeting is often used as part of a composite structure with concrete. In northern countries the roof and wall structures are almost always built with thermal insulation. The sound insulation and the fire insulation have also to be considered, when designing structures.

Figure 2 A Steel-concrete composite floor slab with profiled steel sheeting

Source: Helsinki University (1986)

In wall structures, the structure is comprised of an outer layer, the facade sheeting that is usually built with relatively small span, and a substructure which transmits the wind loading to the main building structure. The substructure can be a system of wall rails or horizontal deep profiles, or cassettes with integrated insulation. Another solution combines the load-bearing and protecting function in a sandwich panel built up by metal profiles of various shapes and a core of polyurethane or mineral wool.

Figure 3 A facade made with profiled steel sheeting

Source: Helsinki University (1986)

Cold-formed steel in building structure.

Although cold-formed steel sections are used in building construction began in about the 1850s in both the United States and Great Britain. However, such steel members were not widely used in buildings until around 1940. The early development of steel buildings has been reviewed by Winter (Yu ,1924).

Since 1946 the use and the development of thin-walled cold-formed steel construction in the United States have been accelerated by the issuance of various editions of the"Specification for the Design of Cold-Formed Steel Structural Members" of the American Iron and Steel Institute.

Cold-formed steel structure members are used widely in light-weight construction. In Thailand, the primary use of cold-formed steel sections has extremely in a roof and purlin (Figure 7). The BlueScope Lysaght, Inc. has recently developed a cold-formed steel member. The basic problem of develop is to achieve the least expensive construction.

Figure 4 Cold-formed steel sections used in space frames

Source: Yu (1924)

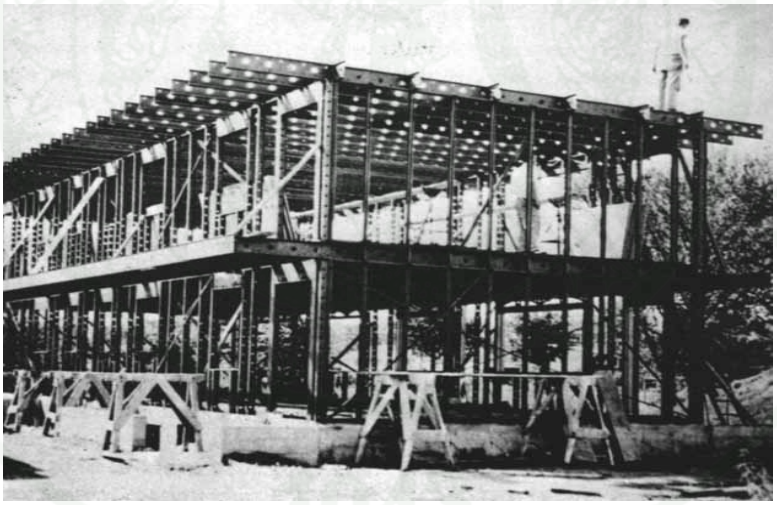

Figure 5 Building composed entirely of cold-formed steel sections

Source: Yu (1924**)**

In Thailand, The Engineering Institute of Thailand under H.M The King ‘s Patronage is preparation a Thailand code of cold-formed steel building design standard

(EIT standard) by reference from Specification for the design of cold-formed steel structural members of American Iron and Steel Institute (AISI).

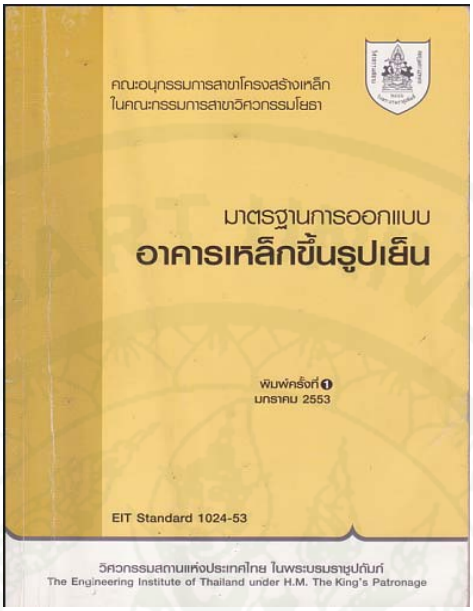

Figure 6 Code of cold-formed steel building design standard (EIT standard)

Source: The Engineering Institute of Thailand (2010)

Statement of problem

Now, box-shaped sections made by connecting two C-sections lip to lip also often found in use in cold-formed steel structures due to the relatively large torsional rigidities and their favorable radius of gyration about both principal axes. The foregoing requirement for maximum spacing of connectors for I shaped members is also applicable to box-type compression members made by C-sections tip to tip, even though it is not specified in the AISI Specification in order to function as a single compression member, the C-sections should be connected at a close enough spacing to prevent buckling of individual C-sections about their own axes parallel to the web at a load equal to or smaller than the buckling load of the entire section. For this reason, built-up members are common compression elements in construction.

The advantages of using cold-formed steel assembled members are well known by the building construction industry:

1. The closed box sections allow spanning greater distances between supports and carrying heavier loads than single C-sections.

2. This connection to conform to a box is usually made by seam welds, being an easy and affordable way to do so. It is especially true in countries where the hourly wage rate for welders is low compared to others. In these countries the use of seam welds applied in-situ is widely used as a good means of coupling two single C-sections in order to make up box sections to be used for structural members as columns and beams.

3. Strong more than single c-channel and two c-channel contacted for I-member.

4. Save material cost more than rectangular tube section for comparative new material subject.

In thailand, for the columns in the structure work used modified two c-channel section contacted by welding for closed-section. But their behaviors have not been acknowledged. Hence, the behaviors of built-up sections when contacted various of different weld spacings will be necessary for the future.

OBJECTIVES

Generally, this study aims to investigate the buckling behavior of cold-formed steel of built up lip-c channel close section by different weld spacing. The specific objectives of the study are:

1. The primary objective of this research is to study the buckling behavior and buckling stress of cold-formed steel built up close-section.

2. The main objective of this research is to investigate the comparative behavior under compression load of close section composed of two lip c-section members in contact by seam welds with different weld spacing (ranging from 100 to 500 mm.).

3. Failure loads and buckling modes were investigated in this study.

4. Comparative buckling behavior and buckling stress of cold-formed steel built up close-section with finite element model.

Scope of Study

This thesis work based on the cold-formed steel built up close section only.

1. This research study the buckling behavior of cold-formed built-up close section columns subject to concentrically loaded compression member.

2. Boundary condition of test are fixed of both support and length of all specimen is 100 cm.

3. The specimen for research are 3 section only:

Section 1 Built-up section from C 203x76x15.5x1.5 mm. (G450)

Section 2 Built-up section from C 152x64x15.5x1.5 mm. (G450)

Section 3 Built-up section from C 102x51x13.5x1.5 mm. (G450)

4. This research was used the finite element analysis program ANSYS for compared buckling shape behavior and buckling load with compression testing in laboratory for understand in behavior of built up section also.

5. Mechanical properties of material determined by tensile coupon test.

6. The residual stressed in material is ignore for this research.

LITERATURE REVIEW

General

In steel construction, there are two main families of structural members. One is the familiar group of hot-rolled shapes and members built up of plates. The other, less familiar but of growing importance, is composed of sections cold-formed from steel sheet, strip, plates, or flat bars in roll-forming machines or by press brake or bending brake operations. These are cold-formed steel structural members. The thickness of steel sheets or strip generally used in cold-formed steel structural members ranges from 0.4 mm to about 6.4 mm. (Yu ,1924) Steel plates and bars as thick as 25 mm. can be cold-formed successfully into structural shapes.

Because material properties play an important role in the performance of structural members, it is important to be familiar with the mechanical properties of the steel sheets, strip, plates, or flat bars generally used in cold-formed steel construction before designing this type of steel structural member.

From a structural standpoint, the most important properties of steel are:

1. Yield point or yield strength
2. Tensile strength
3. Stress–strain characteristics
4. Modulus of elasticity, tangent modulus, and shear modulus
5. Ductility
6. Weld ability

7. Fatigue strength

8. Toughness

Influence of cold work on mechanical properties of steel

The mechanical properties of cold-formed sections are sometimes substantially different from those of the steel sheet, strip, plate, or bar before forming. This is because the cold-forming operation increases the yield point and tensile strength and at the same time decreases the ductility. The percentage increase in tensile strength is much smaller than the increase in yield strength, with a consequent marked reduction in the spread between yield point and tensile strength. Since the material in the corners of a section is cold-worked to a considerably higher degree than the material in the flat elements, the mechanical properties are different in various parts of the cross section. Figure 14 illustrates the variations of mechanical properties from those of the parent material at the specific locations in a channel section and a joist chord after forming tested by Karren and Winter. For this reason, buckling or yielding always begins in the flat portion due to the lower yield point of the material. Any additional load applied to the section will spread to the corners.

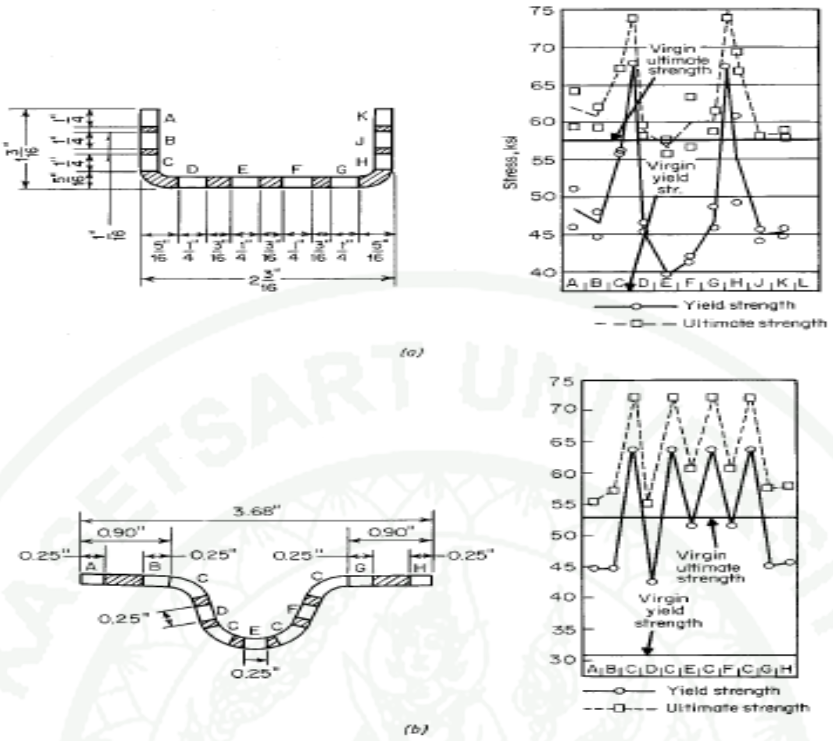

Figure 7 Effect of cold work on mechanical properties in cold-formed steel section (a) channel section (b) joist chord

Source: Yu (1924)

Compression Members

Similar to the heavy hot-rolled steel sections, thin-walled cold-formed steel compression members can be used to carry a compressive load applied through the centroid of the cross section. The cross section of steel columns can be of any shape that may be composed entirely of stiffened elements and unstiffened elements or a combination of stiffened and unstiffened elements. Unusual shapes and cylindrical tubular sections are also often found in use. Cold-formed sections are made of thin material, and in many cases the shear center does not coincide with the centroid of the section. Therefore in the design of such compression members, consideration should be given to the following limit states depending on the configuration of the section, thickness of material, and column length used:

1. Yielding

2. Overall column buckling

   2.1 Flexural buckling: bending about a principal axis

   2.2 Torsional buckling: twisting about shear center

   2.3 Torsional–flexural buckling: bending and twisting simultaneously

3. Local buckling of individual elements

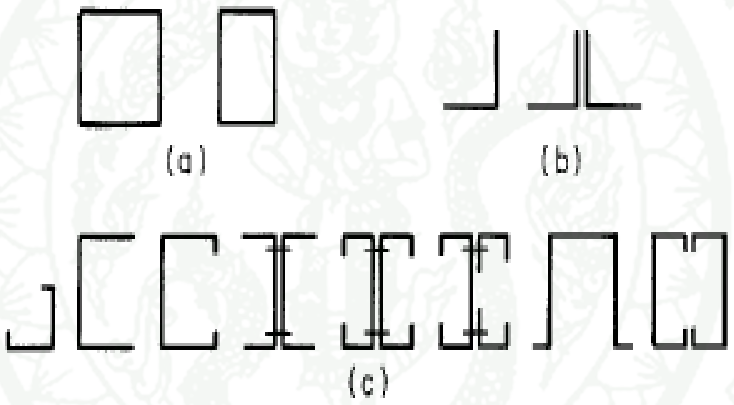

Figure 8 Type of compression member

Source: Yu (1924)

Design provisions for the overall flexural buckling and the effect of local buckling on column strength have long been included in the AISI Specification. The provisions for torsional–flexural buckling were added to the specification in 1968 following a comprehensive investigation carried out by Winter, Chajes, Fang, and Pekoz at Cornell University. The current AISI design provision are based on the unified approach developed in 1986 and discussed by Pekoz (Weng and Pekoz, 1990) This approach consists of the following steps for the design of axially loaded compression members:

1. Calculate the elastic column buckling stress (flexural, torsional, or torsional–flexural) for the full unreduced section.

2. Determine the nominal failure stress (elastic buckling, inelastic buckling, or yielding).

3. Calculate the nominal column load based on the governing failure stress and the effective area.

4. Determine the design column load from the nominal column load using the specified safety factor for ASD or the resistance factor for LRFD.

Flexural column buckling

Elastic Buckling

A slender axially loaded column may fail by overall flexural buckling if the cross section of the column is a doubly symmetric shape (I-section), closed shape (square or rectangular tube), cylindrical shape, or point-symmetric shape (Z-shape or cruciform). For singly symmetric shapes, flexural buckling is one of the possible failure modes.

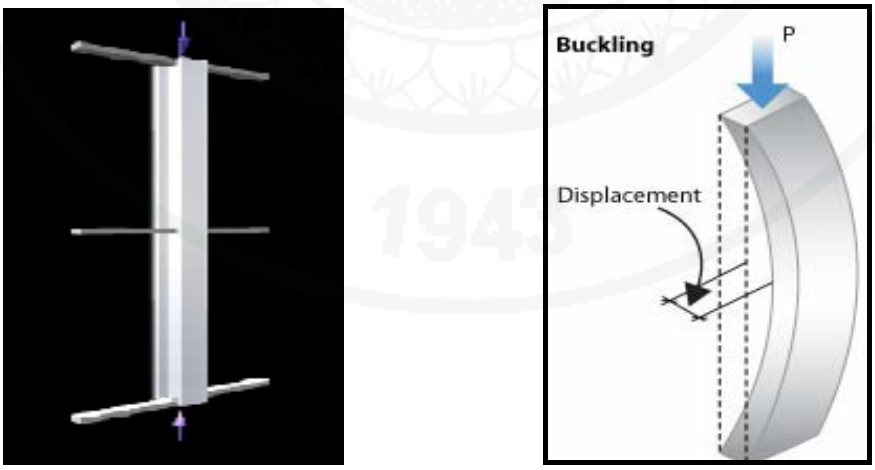

Figure 9 Flexural buckling

Source: Yu (1924)

The elastic critical buckling load for a long column can be determined by the Euler formula:

$$P_e = \frac{\pi^2 EI}{(KL)^2} \quad (1)$$

where P_e = Euler buckling load

E = modulus of elasticity

I = moment of inertia

L = column length

K = effective length factor

Substituting $I = Ar^2$ in equation (1) the following Euler stress for elastic column buckling can be obtained:

$$\sigma_e = \frac{\pi^2 E}{(KL/r)^2} \quad (2)$$

where

KL/r is the effective slenderness ratio and *r* is the least radius of gyration.

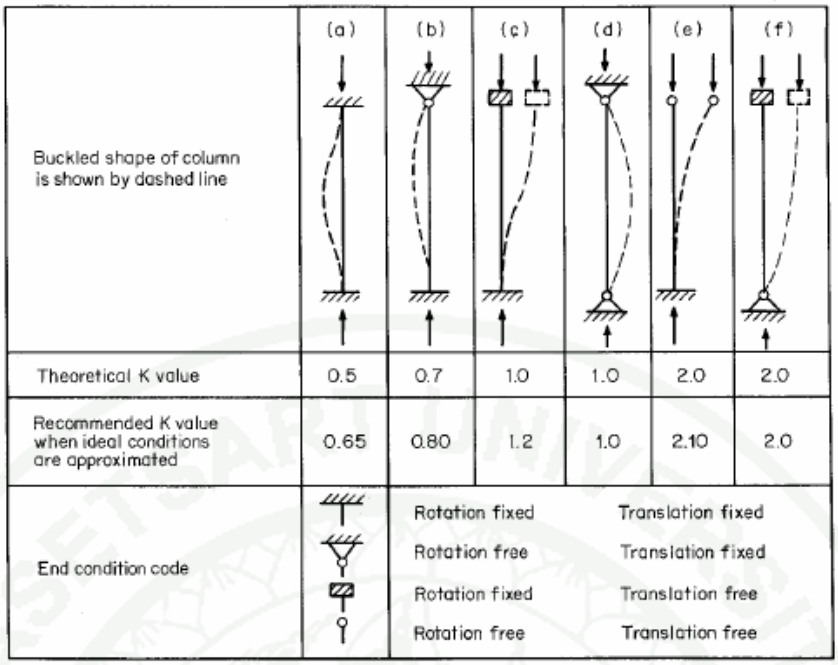

Figure 10 Effective length factor K for Axially loaded columns with various end conditions

Source: Yu (1924)

Local buckling of individual elements

Cold-formed steel design, individual elements of cold-formed steel structural members are usually thin and the width-to-thickness ratios are large. These thin elements may buckle locally at a stress level lower than the yield point of steel when they are subject to compression in flexural bending, axial compression, shear, or bearing. Figure 18 illustrates local buckling patterns of certain beams and columns, where the line junctions between elements remain straight and angles between elements do not change.

Since local buckling of individual elements of cold-formed steel sections has often been one of the major design criteria, the design load should be so determined that adequate safety is provided against failure by local instability with due consideration given to the postbuckling strength.

It is well known that a two-dimensional compressed plate under different edge conditions will not fail like one-dimensional members such as columns when the theoretical critical local buckling stress is reached. The plate will continue to carry additional load by means of the redistribution of stress in the compression elements after local buckling occurs. This is a well-known phenomenon called postbuckling strength of plates (Yu, 1924)**.**

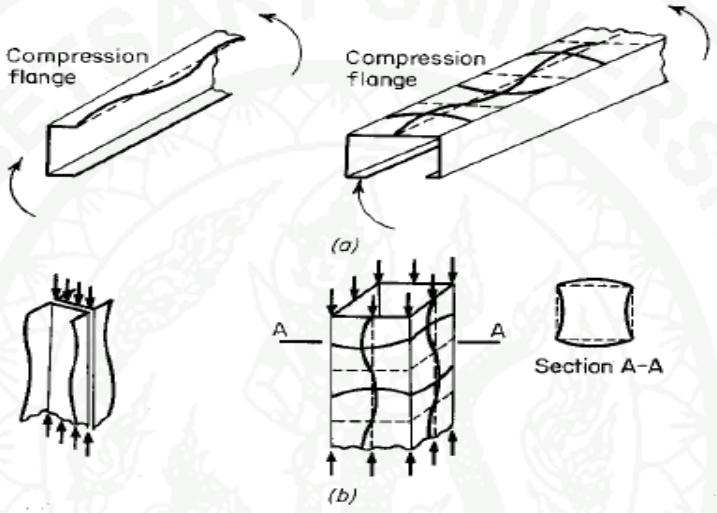

Figure 11 Local buckling of compression elements. (a) Beams. (b) Columns

Source: Yu (1924)

Behavior of compression element.

Elastic Local Buckling Stress of Plates considering a simply supported square plate subjected to a uniform compression stress in one direction, it will buckle in a single curvature in both directions, as shown in Figure 19.

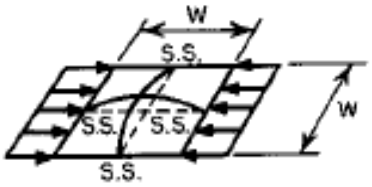

Figure 12 Square plate subject to compression stress

Source: Yu (1924)

The critical buckling stress of a plate as shown in Figure.12 can be determined by solving Bryan's differential equation based on small deflection theory as follows:

$$\frac{\partial^4 \omega}{\partial x^4} + 2\frac{\partial^4 \omega}{\partial x^2\,\partial y^2} + \frac{\partial^4 \omega}{\partial y^4} + \frac{f_x t}{D}\frac{\partial^2 \omega}{\partial x^2} = 0 \qquad (3)$$

Where

$$D = \frac{Et^3}{12(1-\mu^2)} \qquad (4)$$

Where E = modulus of elasticity of steel = 29.5 x 10^3 ksi (203 GPa)

t = thickness of plate

u = Poisson's ratio = 0.3 for steel in the elastic range

w = deflection of plate perpendicular to surface

f_x = compression stress in *x* direction

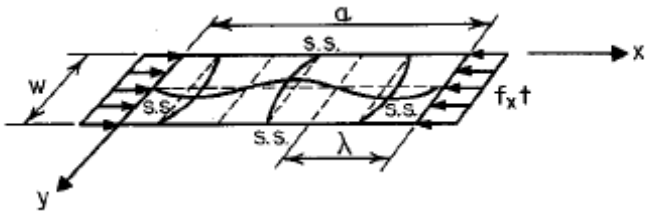

Figure 13 Rectangular plate subjected to compression stress

Source: Yu (1924)

If *m* and *n* are the numbers of half sine waves in the *x* and *y* directions, respectively, the deflected shape of the rectangular plate as shown in Figure.13 may be represented by a double series:

$$\omega = \sum_{m=1}^{\infty} \sum_{n=1}^{\infty} A_{mn} \sin \frac{m\pi x}{a} \sin \frac{n\pi y}{w} \tag{5}$$

From boundary condition at x=0,a and y equal zero.The calculation edge deflection equal zero. Because $\partial^2\omega/\partial x^2 = 0$ and $\partial^2\omega/\partial y^2 = 0$ at four edges, Equation (5) can be solving from edge moment equal zero because

$$M_x = -D\left(\frac{\partial^2\omega}{\partial x^2} + \mu \frac{\partial^2\omega}{\partial y^2}\right) \tag{6}$$

$$M_y = -D\left(\frac{\partial^2\omega}{\partial y^2} + \mu \frac{\partial^2\omega}{\partial x^2}\right) \tag{7}$$

Solving Eq. (3) by using Eq. (5) one can then obtain the following equation:

$$\sum_{m=1}^{\infty} \sum_{n=1}^{\infty} A_{mn}\left[\pi^4 \left(\frac{m^2}{a^2} + \frac{n^2}{w^2}\right)^2 - \frac{f_x t}{D}\frac{m^2\pi^2}{a^2}\right] \sin \frac{m\pi x}{a} \sin \frac{n\pi y}{w} = 0 \tag{8}$$

the quantity in the bracket must be zero. By solving

$$\pi^4 \left(\frac{m^2}{a^2} + \frac{n^2}{w^2}\right)^2 - \frac{f_x t}{D}\frac{m^2\pi^2}{a^2} = 0 \tag{9}$$

You can find a solution for critical local buckling stress as follows:

$$f_{cr} = f_x = \frac{D\pi^2}{tw^2}\left[m\left(\frac{w}{a}\right) + \frac{n^2}{m}\left(\frac{a}{w}\right)\right]^2 \tag{10}$$

the minimum value in square brackets is n =1, that is, only one half sine wave occurs in the y direction. Therefore

$$f_{cr} = \frac{kD\pi^2}{tw^2} \tag{11}$$

where

$$k = \left[m\left(\frac{w}{a}\right) + \frac{1}{m}\left(\frac{a}{w}\right)\right]^2 \tag{12}$$

Represent the value D in Equation(4). to Equation(11). get a general equation for critical local buckling stress for a rectangular plate subjected to compression stress in one direction:

$$f_{cr} = \frac{k\pi^2 E}{12(1-\mu^2)(w/t)^2} \tag{13}$$

k values used in Equation (13). is shown in Figure 14. for different a/w ratios.

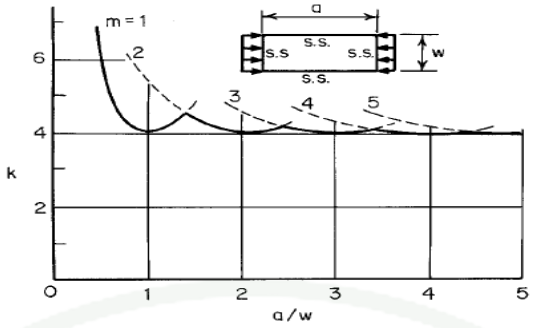

Figure 14 Buckling coefficient for flat rectangular plates

Source: Yu (1924)

Where $\frac{a}{w} \simeq m$

$$\lambda = \frac{a}{m} \simeq w$$

λ = the length of the half sine wave

For long plate having a relatively large a/w ratio is of particular interest as shown in Figure 21 whenever the aspect ratio a/w exceeds about 4, a value of $k = 4$ can be used for determining the critical buckling stress for a plate simply supported along four edges and subjected to compression stress in one direction, that is

$$f_{cr} = \frac{\pi^2 E}{3(1 - \mu^2)(w/t)^2} \tag{14}$$

The values of k for a long rectangular plate are tabulated in Figure 22.

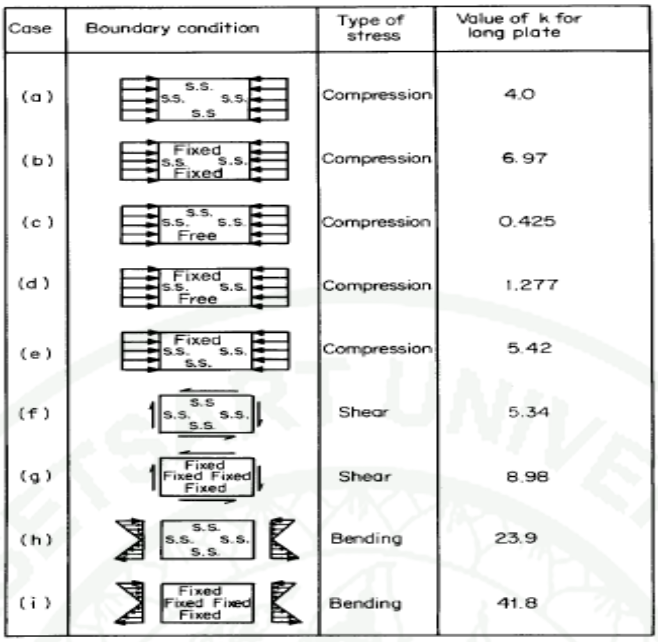

Case	Boundary condition	Type of stress	Value of k for long plate
(a)	s.s. s.s. s.s. s.s	Compression	4.0
(b)	Fixed s.s. s.s. Fixed	Compression	6.97
(c)	s.s. s.s. s.s. Free	Compression	0.425
(d)	Fixed s.s. s.s. Free	Compression	1.277
(e)	Fixed s.s. s.s. s.s.	Compression	5.42
(f)	s.s s.s. s.s. s.s.	Shear	5.34
(g)	Fixed Fixed Fixed Fixed	Shear	8.98
(h)	s.s. s.s. s.s. s.s	Bending	23.9
(i)	Fixed Fixed Fixed Fixed	Bending	41.8

Figure 15 Values of k for Determining Critical Buckling Stress

Source: Yu (1924)

Postbuckling Strength .

Structural members such as columns, stiffened compression elements will not collapse when the buckling stress is reached. An additional load can be carried by the element after buckling by means of a redistribution of stress. This phenomenon is known as postbuckling strength and is most pronounced for elements with large *w*/*t* ratios (Schafer and Adany, 2006).

In the plate Figure 23 the stress distribution is uniform prior to its buckling, as shown in Figure 24 (a). After buckling, a portion of the pre-buckling load of the center strip transfers to the edge portion of the plate. As a result, a nonuniform stress distribution is developed, as shown in Figure 24 (b). The redistribution of stress continues until the stress at the edge reaches the yield point of the steel and then the plate begins to fail Figure 24 (c). The postbuckling behavior of a plate can be analyzed by using large deflection theory. The following differential equation for large deflection buckling of a plate was introduced by von Karman in 1910:

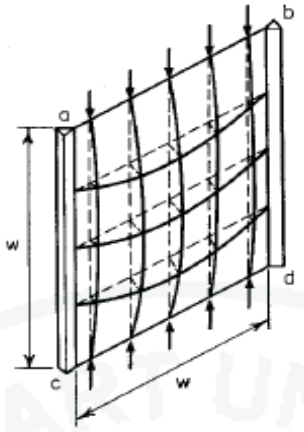

Figure 16 Square plate model for postbuckling action

Source: Yu (1924)

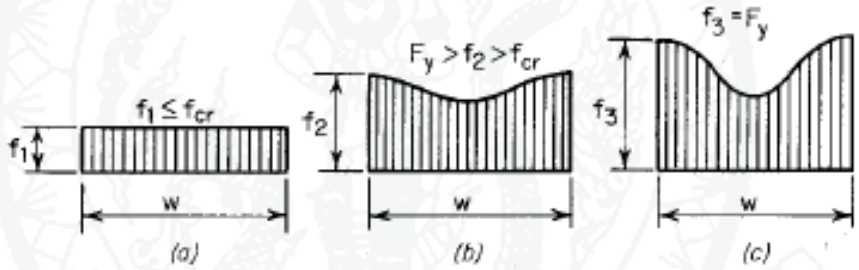

Figure 17 Consecutive stages of stress distribution in stiffen compression element

Source: Yu (1924)

A concept of ‘‘effective width’’ was introduced by von Karman in 1932.In this approach, instead of considering the nonuniform distribution of stress over the entire width of the plate *w*, it is assumed that the total load is carried by a fictitious effective width *b*, subject to a uniformly distributed stress equal to the edge stress f_{max}, as shown in Figure 25.

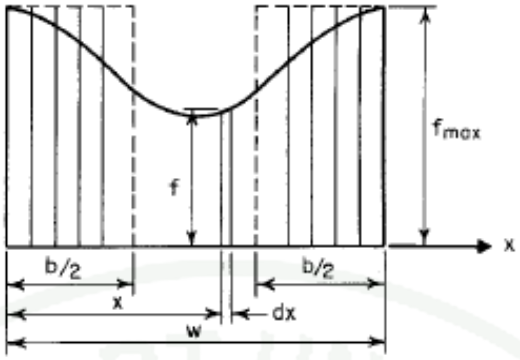

Figure 18 Effective width of stiffeness compression element

Source: Yu (1924)

The plate which just buckles when the compressive stress reaches the yield point of steel. Therefore for a long plate, the theoretical value of *b* may be determined as follows:

$$f_{cr} = F_y = \frac{\pi^2 E}{3(1-\mu^2)(b/t)^2} \quad (15)$$

Whenever w > b,

$$f_{cr} = \frac{\pi^2 E}{3(1-\mu^2)(w/t)^2} \quad (16)$$

AISI design formulas for concentrically loaded compression members.

Concentrically Loaded Compression Members (AISI standard**,** 2007)

This section applies to members in which the resultant of all loads acting on the member is an axial load passing through the centroid of the effective section calculated at the stress, Fn, defined in this section.

(a) The nominal axial strength, *Pn* shall be calculated as follows:

$$Pn = AeFn \tag{17}$$

where *Ae* = Effective area at the stress Fn.

Fn is determined as follows:

For $\lambda_c \leq 1.5$ $F_n = (0.658^{\lambda_c^2})F_y$ (18)

For $\lambda_c > 1.5$ $F_n = \left[\frac{0.877}{\lambda_c^2}\right] F_y$ (19)

Where

$$\lambda_c = \sqrt{\frac{F_y}{F_e}} \tag{20}$$

Fe = the least of the elastic flexural, torsional, and torsional–flexural buckling stress

For doubly symmetric sections, closed cross sections and any other sections which can be shown not to be subject to torsional or torsional–flexural buckling, the elastic flexural buckling stress (AISI standard**,** 2007).

Fe shall be determined as follows:

$$F_e = \frac{\pi^2 E}{(KL/r)^2} \tag{21}$$

Where E = modulus of elasticity

K = effective length factor

L = unbraced length of member

r = radius of gyration of the full, unreduced cross section.

Built-up compression members

For built-up compression members composed of two sections in contact, the available axial strength (factored axial resistance) shall be determined in accordance with Section C4.1(a) of the North American Specification subjected to modification as necessary. Based on Section D1.2 of the 2007 edition of the North American specification(AISI standard**,** 2007), if the buckling mode involves relative deformations that produce shear forces in the connections between individual shapes, the effective slenderness ratio *KL*/*r* is replaced by the modified effective slenderness ratio (*KL*/*r*)m calculated by Equation (22) (Young, 2004)

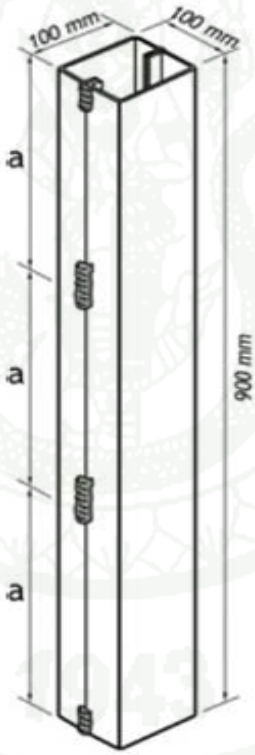

Figure 19 Built-up section member

Source: Reyes and Guzman (2011)

$$\left(\frac{KL}{r}\right)_{\mathrm{m}} = \sqrt{\left(\frac{KL}{r}\right)_{0}^{2} + \left(\frac{a}{r_{\mathrm{i}}}\right)^{2}} \qquad (22)$$

Where

$(KL/r)_0$ = overall slenderness ratio of entire section about built-up member axis.

a = intermediate fastener or spot weld spacings.

ri = minimum radius of gyration of full unreduced cross-sectional area of an individual shape in built-up member

K = the effective length factor

L = the unbraced member length.

In the above design criteria, equation (22) was added to the North American Specification since 2001 on the basis of the 1999 AISC Specification and the 1994 CSA Standard. The overall slenderness ratio, (*KL*/*r*) 0, is computed about the same axis as the modified slenderness ratio, (*KL*/*r*) m. The (*KL*/*r*) m ratio replaces *KL*/*r* in equation (27) for flexural buckling and for both flexural and flexural–torsional buckling replaces *KL/r* in equation (28). Section D1.2 of the North American Specification includes the above three requirements concerning intermediate fastener spacing *a*, end connection of the built-up member and the applied force for the design of intermediate fastener(s). (Kwona *et al.*, 2007) The intermediate fastener spacing requirement for the [*a*/ri ≤0.5*(KL/r)*] (Whittle and Ramseyer, 2009) is to prevent flexural buckling of individual shapes between intermediate connectors to account for any one of the connectors becoming loose or ineffective.

In accordance with section C4.1 of AISI S100-2007 the nominal axial strength shall be calculated by the following

$$Pn = AeFn \tag{23}$$

where Ae = Effective area calculated at stress Fn

Fn shall be calculated as follows:

For $\lambda c \leq 1.5$ (Inelastic buckling mode)

$$F_n = \left(0.658^{\lambda_c^2}\right) F_y. \tag{24}$$

For $\lambda c > 1.5$ (Elastic buckling mode)

$$F_n = \left[\frac{0.877}{\lambda_c^2}\right] F_y \tag{25}$$

Where

$$\lambda_c = \sqrt{\frac{F_y}{F_e}} \tag{26}$$

Fe = The least of the applicable elastic flexural, torsional and flexural–torsional buckling stress.

For sections not subject to torsional or flexural–torsional buckling as doubly-symmetric sections or closed cross-sections:

$$F_e = \frac{\pi^2 E}{(KL/r)^2} \tag{27}$$

For torsional buckling (Ghoraba, 1997)

$$F_e = \frac{1}{A_{gp} r_{op}^2}\left[GJ_p + \frac{\pi^2 EC_{wp}}{(K_t L_t)^2}\right] \quad (28)$$

For torsional buckling stress between fasteners (Ghoraba, 1997)

$$F_e = \frac{1}{A_g r_0^2}\left[GJ + \frac{\pi^2 EC_w}{(a)^2}\right] \quad (29)$$

where E = Modulus of Elasticity
K = Effective length factor
L = Unbraced length of member
r = Radius of gyration of full unreduced cross section about axis of buckling.

Research of cold-formed steel built-up column.

1. Evaluation of the slenderness ratio in built-up cold-formed box sections (Reyes and Guzman, 2011)

According to section D1.2 of AISI S100-2007 for compression members composed of two sections in contact whose buckling mode involves shear forces in the connectors, a reduction must be made, KL/r must be replaced by (KL/r)m. This new modified slenderness ratio takes into account the connection weld spacing and the minimum radius of gyration of an individual shape in the built-up member. Under the provisions of section D1.2 a reduction in load capacity must be made for built-up welded box members, which are the subject of this study. An experimental investigation on 48 samples was addressed to determine the comparative behaviour under compression load of box sections composed of two C-section members in contact by seam welds with different weld spacings (ranging from 100 to 900 mm). The studs were tested simulating rigid and flexible end support conditions. The length

of the samples was 900 mm with a cross-section of 100 mm × 100 mm. The base material thickness was 1.5 mm (gauge 16) for 24 samples and 2.0 mm (gauge 14) for the rest. The testing done on the samples did not show a statistical reduction in the ultimate compression load capacity for these members except for a weld spacing of 900mmand a flexible end support condition. The reduction considered in AISI S100-2007 is not applicable to determine the ultimate load capacity for the rest of the members.

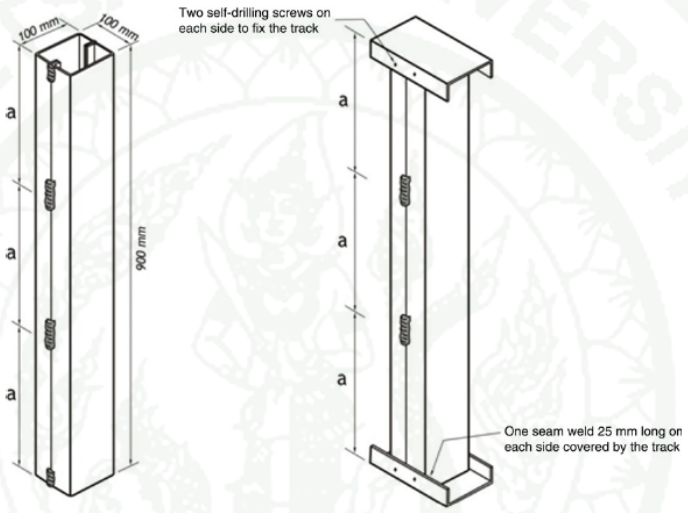

Figure 20 Typical tested sample for rigid end supports (left) and for flexible end supports (right)

Source: Reyes and Guzman (2011)

Experimental investigation

The study performed by Stone and La Boube provided the basic guidance to develop all the research on assembled box members. Fig. 27 presents both the typical stud sample for the first set rigidly supported (left) and the typical sample for the second set under a flexible end supporting condition (right). For the flexible support neoprene plates 15 mm thick at each end were used. The experimentation focused on ultimate axial strength was performed at Universidad del Norte, Barranquilla (Colombia).

The purpose of this research is to determine the variation of the ultimate load capacity for the built-up member evaluating how it is affected by the variability in the weld spacing (distance‘‘a’’ in Fig. 28) taking into consideration different end supporting conditions and also shedding light on determining whether current AISI provisions are applicable for cold-formed box section members. The Figure 29 shows the dimensions of the cross-section.

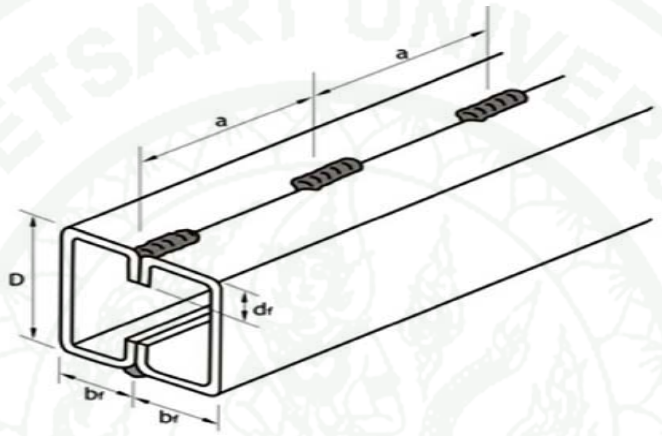

Figure 21 Typical box section

Source: Reyes and Guzman (2011)

Parameter magnitudes of the cross-section.

Parameter	Magnitude (mm)
Stud thickness, t	1.5, 2.0
Depth, D	100
Flange, b_f	50
Edge stiffener, d_f	15
Weld seam spacing, a	100, 300, 600, 900

Figure 22 Parameter magnitudes of the cross-section

Source: Reyes and Guzman (2011)

Test results

Built-up compression-member test results for rigid supports.

Reference	Weld spacing (mm)	P_{test1}, Failure load (kN)		
		1st test	2nd test	3rd test
Box 100 × 100–1.5 mm	100	131.4	141.6	133.2
Box 100 × 100–1.5 mm	300	133.1	134.0	129.8
Box 100 × 100–1.5 mm	600	131.0	123.6	121.1
Box 100 × 100–1.5 mm	900	141.9	130.2	144.3
Box 100 × 100–2.0 mm	100	240.1	265.4	256.9
Box 100 × 100–2.0 mm	300	264.0	267.9	264.1
Box 100 × 100–2.0 mm	600	263.8	246.2	263.9
Box 100 × 100–2.0 mm	900	257.5	269.6	263.9

Figure 23 Built-up compression-member test results for rigid supports

Source: Reyes and Guzman (2011)

Built-up compression-member test results for flexible supports.

Reference	Weld spacing (mm)	P_{test2}, Failure load (kN)		
		1st test	2nd test	3rd test
Box 100 × 100–1.5 mm	100	131.2	125.8	129.7
Box 100 × 100–1.5 mm	300	120.9	128.2	121.4
Box 100 × 100–1.5 mm	600	124.8	121.8	129.7
Box 100 × 100–1.5 mm	900[a]	115.8	119.5	118.2
Box 100 × 100–2.0 mm	100	239.4	247.8	251.8
Box 100 × 100–2.0 mm	300	250.8	262.9	259.5
Box 100 × 100–2.0 mm	600	243.6	253.3	254.9
Box 100 × 100–2.0 mm	900[a]	238.3	235.8	240.0

[a] These samples presented a significant statistical reduction in the average of the maximum load capacity.

Figure 24 Built-up compression-member test results for flexible supports

Source: Reyes and Guzman (2011)

Figure30 and figure31 summarise the failure loads for each specimen. These results collect all the maximum loads obtained from the tests for rigid and flexible supports. The results of the first set of samples, under a rigid support condition, are summarised in figure30 (Ptest1). Figure31 presents the results obtained from the second set of samples according to a flexible support condition (Ptest2).

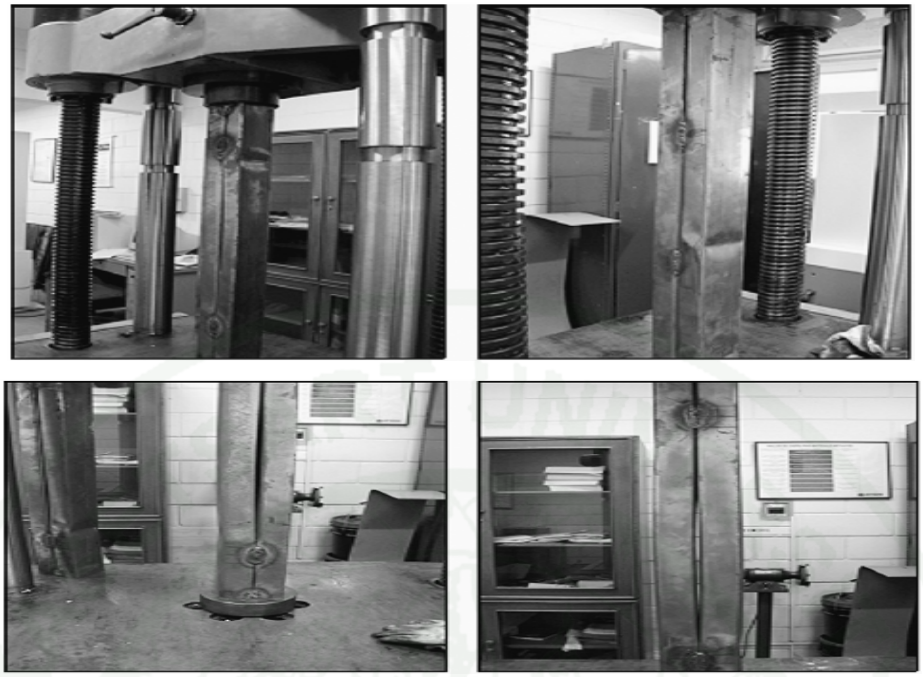

Figure 25 Typical failure mode for rigidly supported specimens

Source: Reyes and Guzman (2011)

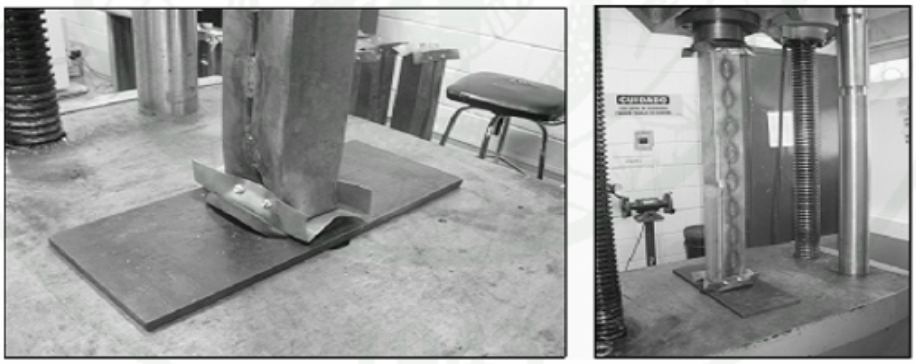

Figure 26 Local buckling at ends for samples with flexible supports (left) and buckling close to seam welds along the specimen (right)

Source: Reyes and Guzman (2011)

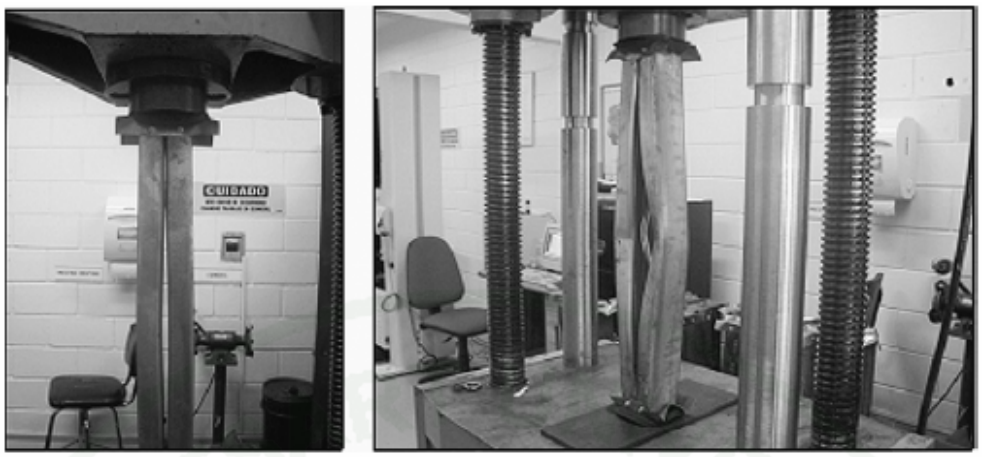

Figure 27 Typical failure curvature mode on samples with flexible supports and welds spaced 900 mm (there was a reduction in the maximum load capacity under this configuration)

Source: Reyes and Guzman (2011)

Conclusion and discussion for this paper

For both end support conditions the statistical values of failure load are about the same magnitude except for the 900 mm spacing with a flexible end support. This latter spacing showed a reduced capacity with a flexible support compared to that with an end rigid support. The reduction considered in section D1.2 of the North American Specification (AISI S100-2007) due to the weld spacing would not be applicable to predict the failure load up to a weld spacing of 600 mm no matter the type of support. In other words, the actual overall slenderness ratio of the entire section might not be modified due to the weld spacing as it is less than or equal to 600 mm. The analysis of the results obtained from the 48 specimens shows that the modified slenderness ratio is not always necessary for material 1.5 and 2.0 mm thick and therefore the actual slenderness ratio could be used to compute the ultimate load capacity for these structural members if the seam weld spacing is less than or equal to 600 mm since there is not a significant statistical reduction in the failure load in laboratory tests. The values were slightly affected by the type of support but this reduction did not represent a significant statistical difference except for the samples

on flexible supports with a seam weld spacing of 900mm.Disregarding this latter spacing there is no need to use the modified slenderness ratio to determine the maximum load capacity of the members under consideration no matter the type of support. This observation concurs and expands the application of the AISC approach for built-up members conformed from two C-section members in contact by seam welds.

2. Buckling capacities of axially loaded, cold-formed, built-up C-channels Whittle and Ramseyer (2009)

Cold-formed, built-up members are common compression elements in cold-formed steel joists, and these built-up members are susceptible to unique buckling behaviors. Built-up member design is addressed in Section C4.5 of the American Iron and Steel Institute 2001 Specification. Over 150 experimental compression tests on closed-section, built-up members formed of intermediately welded c-channels were conducted, and these experimental values were compared to theoretical buckling capacities based on the Section C4.5 modified slenderness ratio. Use of the modified slenderness ratio was exceedingly conservative. Capacities based on the unmodified slenderness ratio and C4.5 fastener and spacing provisions were consistently conservative. The 2007 AISI Specification Section D1.2 specifies that built- up members be designed with a modified slenderness ratio if shear forces are induced between the weld or screw connectors. The section also introduces a minimum fastener strength requirement and a fastener spacing requirement for built-up members . Refer to Eqs.(29) and (30) for the modified slenderness ratio and intermediate fastener spacing provision as stated in AISI Specification D1.2:

$$\left(\frac{KL}{r}\right)_m = \sqrt{\left(\frac{KL}{r}\right)_o^2 + \left(\frac{a}{r_i}\right)^2} \qquad (29)$$

Condition for AISI D1.2 — modified slenderness ratio

$$\frac{a}{r_i} \leqslant 0.5\left(\frac{KL}{r}\right)_o \qquad (30)$$

AISI C4.5 fastener spacing provision where (KL/r)o is the over all slenderness ratio of entire section about the built-up member axis ;a is the intermediate fastener or spot weld spacing ; ri is the minimum radius of gyration of the full unreduced cross-sectional area of an individual shape in a built- up member ; K is the effective length factor; and L is the unbraced member length. However, the modified slenderness ratio is heavily adopted.

Test objective and experimental setting.

An experimental investigation of over 150 cold-formed, built- up c-channels loaded in compression was conducted at the University of Oklahoma's Fears Structural Engineering Laboratory. All specimens were tested in pure axial compression with pinned end conditions. The primary objective was to find maximum buckling capacities for a variety of built-up members to determine the accuracy of the AISI2007 Specification's design methods for built-up members. In addition, the effects of built-up member characteristics, such as member thickness, member geometry, column length, and location and number of intermediate weld attachments were explored to obtain abroad- range of experimental data that could more thoroughly represent built-up c-channel buckling behaviors. Three repetitions of each member type were tested to obtain reliable average buckling values, and single c-channel tests served as a baseline measure for each built-up member type. A total of 153 experimental tests were conducted and 55 specimen types investigated. Eight of the 55 specimen types had fewer than three repeated specimens tested. The experimental testing focused on closed-section built-up members, as this configuration provides exceptional torsional resistance, and limited research has been performed in this built-up member area. Not all of the built-up members tested met the fastener spacing provisions present in AISI Specification Section D1.2. The purpose of experimentally testing built-up members that did and did not meet the provision was to better relay the accuracy of

SectionD1.2 for properly designed, built-up compression members. In addition, the type of built-up members were chosen to provide experimental verifica-tion of specific built-up section behavior for the research sponsor, who was interested in constructability limitations and not necessarily interested in the D1.2 limitations.

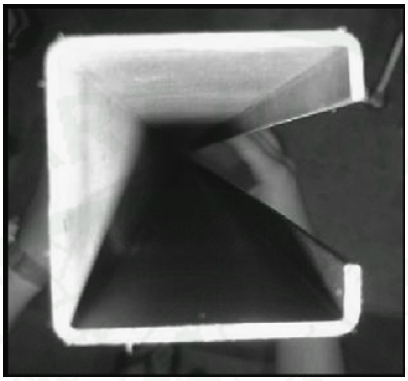

Figure 28 Single section

Source: Whittle and Ramseyer (2009)

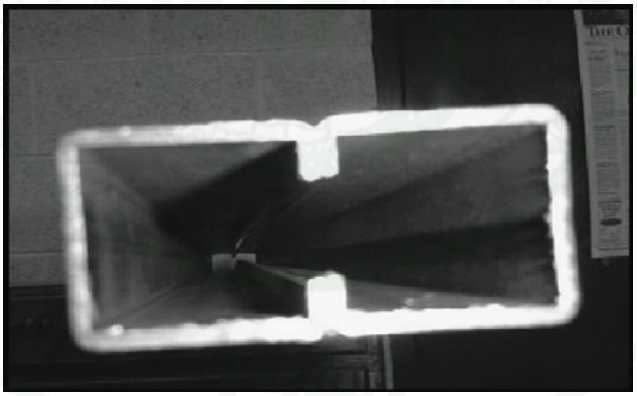

Figure 29 Built-up member

Source: Whittle and Ramseyer (2009)

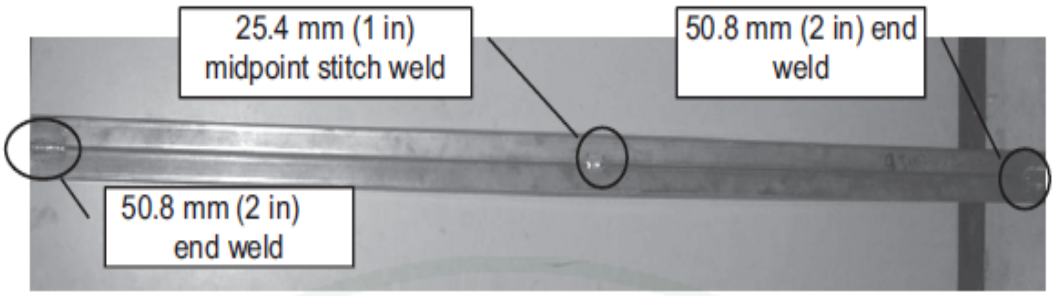

Figure 30 Complete built-up member with midpoint attachment

Source: Whittle and Ramseyer (2009)

The built-up members were created with two, lipped c- channels welded together at the top and bottom with 50.8 mm (2 in.) long welds and at intermediate locations along the member with 25.4 mm.(1 in.) long welds to form a closed box-section. All welds were approximately 4.76 mm (0.1875in.) thick. Figs.35and36 display a single c-channel and a closed, built-up member, respectively. Fig.37 illustrates a complete built-up member with a typical midpoint intermediate weld. All intermediate welds were equally spaced along the length of the member. The number and location of intermediate weld attachments and length of the member represented the diversity of built-up members. Midpoint, third-point, and sixth-point welds were all tested in addition to welding on a single side of the member or both sides of the members. The efficient, single-sided welding has recently become more prevalent as robotic fabrication processes for built-up members have grown in popularity. Member lengths of 1803 mm (71 in.) and 1397 mm (55 in.) were also researched.

Test results

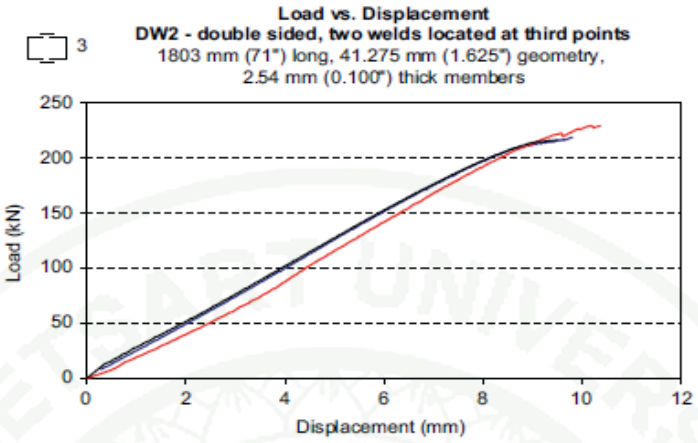

Figure 31 Load-displacement of DW2- double sided

Source: Whittle and Ramseyer (2009)

Figure 32 Intermediate attachment orientations and descriptions

Source: Whittle and Ramseyer (2009)

Length (mm) (in.)	Width (mm) (in.)	Thickness (mm) (in.)	Weld type	Axial capacity (kN) (kip)		P_{test}/P_n
				Average P_{test} (kN) (kip)	AISI P_n (kN) (kip)	
1397 (55)	41.275 (1.625)	2.032 (0.080)	Single	33.98 (7.64)	19.04 (4.28)	1.78
1397 (55)	41.275 (1.625)	2.032 (0.080)	Double	104.1 (23.40)	63.52 (14.28)	1.64
1397 (55)	41.275 (1.625)	2.032 (0.080)	SW 1	141.9 (31.89)	102.8 (23.11)	1.38
1397 (55)	41.275 (1.625)	2.032 (0.080)	DW 1	175.3 (39.41)	97.46 (21.91)	1.80
1397 (55)	41.275 (1.625)	2.032 (0.080)	SW 2	136.8 (30.75)	113.1 (25.42)	1.21
1397 (55)	41.275 (1.625)	2.032 (0.080)	DW 2	174.4 (39.20)	107.3 (24.13)	1.62
1397 (55)	41.275 (1.625)	2.032 (0.080)	SW 5	137.4 (30.88)	119.7 (26.91)	1.15
1397 (55)	41.275 (1.625)	2.032 (0.080)	DW 5	164.4 (36.96)	115.6 (25.98)	1.42

Figure 33 Axial capacities-maximum buckling loads and AISI nominal loads (1397 mm length) (55in.)

Source: Whittle and Ramseyer (2009)

Length (mm) (in.)	Width (mm) (in.)	Thickness (mm) (in.)	Weld type	Axial capacity (kN) (kip)		P_{test}/P_n
				Average P_{test} (kN) (kip)	AISI P_n (kN) (kip)	
1803 (71)	41.275 (1.625)	1.626 (0.064)	Single	14.99 (3.37)	9.56 (2.15)	1.57
1803 (71)	41.275 (1.625)	1.626 (0.064)	Double	56.36 (12.67)	31.09 (6.99)	1.81
1803 (71)	41.275 (1.625)	1.626 (0.064)	SW 1	76.51 (17.20)	52.27 (11.75)	1.46
1803 (71)	41.275 (1.625)	1.626 (0.064)	DW 1	102.9 (23.13)	50.18 (11.28)	2.05
1803 (71)	41.275 (1.625)	1.626 (0.064)	SW 2	66.28 (14.90)	59.78 (13.44)	1.11
1803 (71)	41.275 (1.625)	1.626 (0.064)	DW 2	144.0 (32.37)	50.98 (11.46)	2.83
1803 (71)	41.275 (1.625)	1.626 (0.064)	SW 5	77.98 (17.53)	65.48 (14.72)	1.19
1803 (71)	41.275 (1.625)	1.626 (0.064)	DW 5	131.2 (29.49)	59.92 (13.47)	2.19
1803 (71)	41.275 (1.625)	2.032 (0.080)	Single	24.11 (5.42)	14.28 (3.21)	1.69
1803 (71)	41.275 (1.625)	2.032 (0.080)	SW 1	119.3 (26.82)	62.99 (14.16)	1.89
1803 (71)	41.275 (1.625)	2.032 (0.080)	DW 1	143.2 (32.20)	62.99 (14.16)	2.27
1803 (71)	41.275 (1.625)	2.032 (0.080)	SW 2	95.73 (21.52)	72.11 (16.21)	1.33
1803 (71)	41.275 (1.625)	2.032 (0.080)	DW 2	146.4 (32.92)	72.11 (16.21)	2.03
1803 (71)	41.275 (1.625)	2.032 (0.080)	SW 5	133.2 (29.95)	79.00 (17.76)	1.69
1803 (71)	41.275 (1.625)	2.032 (0.080)	DW 5	142.6 (32.05)	79.00 (17.76)	1.81
1803 (71)	41.275 (1.625)	2.54 (0.100)	Single	40.88 (9.19)	21.44 (4.82)	1.91
1803 (71)	41.275 (1.625)	2.54 (0.100)	Double	116.6 (26.21)	44.35 (9.97)	2.63
1803 (71)	41.275 (1.625)	2.54 (0.100)	SW 1	144.8 (32.54)	74.91 (16.84)	1.93
1803 (71)	41.275 (1.625)	2.54 (0.100)	DW 1	206.2 (46.36)	74.91 (16.84)	2.75
1803 (71)	41.275 (1.625)	2.54 (0.100)	SW 2	161.8 (36.38)	85.85 (19.30)	1.89
1803 (71)	41.275 (1.625)	2.54 (0.100)	DW 2	221.6 (49.81)	85.85 (19.30)	2.58
1803 (71)	41.275 (1.625)	2.54 (0.100)	SW 5	182.2 (40.95)	94.08 (21.15)	1.94
1803 (71)	41.275 (1.625)	2.54 (0.100)	DW 5	223.7 (50.28)	94.08 (21.15)	2.38

Figure 34 Axial capacities- maximum buckling loads and AISI nominal loads (1803 mm (71in.) length, 41.275 mm (1.625in.) width

Source: Whittle and Ramseyer (2009)

Length (mm) (in.)	Width (mm) (in.)	Thickness (mm) (in.)	Weld type	Axial capacity (kN) (kip)		P_{test}/P_n
				Average P_{test} (kN) (kip)	AISI P_n (kN) (kip)	
1803 (71)	66.675 (2.625)	1.626 (0.064)	Single	43.37 (9.75)	16.86 (3.79)	2.57
1803 (71)	66.675 (2.625)	1.626 (0.064)	Double	128.4 (28.87)	82.34 (18.51)	1.56
1803 (71)	66.675 (2.625)	1.626 (0.064)	SW 1	143.9 (32.34)	119.4 (26.84)	1.20
1803 (71)	66.675 (2.625)	1.626 (0.064)	DW 1	171.8 (38.62)	109.3 (24.58)	1.57
1803 (71)	66.675 (2.625)	1.626 (0.064)	SW 2	152.4 (34.26)	126.2 (28.36)	1.21
1803 (71)	66.675 (2.625)	1.626 (0.064)	DW 2	177.5 (39.91)	118.7 (26.69)	1.50
1803 (71)	66.675 (2.625)	1.626 (0.064)	SW 5	161.2 (36.23)	128.2 (28.83)	1.26
1803 (71)	66.675 (2.625)	1.626 (0.064)	DW 5	176.6 (39.69)	124.7 (28.03)	1.42
1803 (71)	66.675 (2.625)	2.032 (0.080)	Single	64.90 (14.59)	25.80 (5.80)	2.51
1803 (71)	66.675 (2.625)	2.032 (0.080)	Double	185.9 (41.80)	112.3 (25.24)	1.66
1803 (71)	66.675 (2.625)	2.032 (0.080)	SW 1	205.3 (46.15)	150.8 (33.91)	1.36
1803 (71)	66.675 (2.625)	2.032 (0.080)	DW 1	225.8 (50.76)	144.1 (32.40)	1.57
1803 (71)	66.675 (2.625)	2.032 (0.080)	SW 2	195.9 (44.05)	165.0 (37.09)	1.19
1803 (71)	66.675 (2.625)	2.032 (0.080)	DW 2	229.1 (51.51)	152.8 (34.34)	1.50
1803 (71)	66.675 (2.625)	2.032 (0.080)	SW 5	215.6 (48.46)	163.3 (36.72)	1.32
1803 (71)	66.675 (2.625)	2.032 (0.080)	DW 5	240.2 (54.00)	155.7 (35.01)	1.54
1803 (71)	66.675 (2.625)	2.54 (0.100)	Single	96.48 (21.69)	38.21 (8.59)	2.53
1803 (71)	66.675 (2.625)	2.54 (0.100)	Double	280.9 (63.14)	135.9 (30.56)	2.07
1803 (71)	66.675 (2.625)	2.54 (0.100)	SW 1	330.6 (74.31)	208.4 (46.86)	1.59
1803 (71)	66.675 (2.625)	2.54 (0.100)	DW 1	409.2 (92.00)	189.9 (42.70)	2.15
1803 (71)	66.675 (2.625)	2.54 (0.100)	SW 2	352.3 (79.19)	218.4 (49.10)	1.61
1803 (71)	66.675 (2.625)	2.54 (0.100)	DW 2	434.2 (97.60)	200.9 (45.16)	2.16
1803 (71)	66.675 (2.625)	2.54 (0.100)	SW 5	345.8 (77.74)	230.8 (51.88)	1.50
1803 (71)	66.675 (2.625)	2.54 (0.100)	DW 5	384.6 (86.45)	220.3 (49.52)	1.75

Figure 35 Axial capacities- maximum buckling loads and AISI nominal loads (1803 mm (71in.) length, 66.675 mm (2.625in.) width

Source: Whittle and Ramseyer (2009)

Data analysis

Analysis of AISI specification D1.2 the modified slenderness ratio.

The primary goal of the test results was to validate the effectiveness of using the modified slenderness ratio in D1.2 to calculate axial buckling capacities. The ratio of Ptest/Pn indicate show conservative the AISI2007 Specification is for designing built-up columns using the modified slenderness ratio in D1.2. There was a trend for the design of columns using the average modified slenderness ratio to be more conservative for thicker members than thinner members. This upward trend of material thickness compared to the ratio of experimental capacity to nominal capacity followed the pattern first mentioned in Stone and LaBoube's research of built-up studs. This trend between material thickness and degree of AISI capacities being conservative was also dually noted in Brueggen and Ramseyer's research. Comparison of the seven various built-up member configurations indicated that built-up members with shorter widths (more stub by sections) result in more conservative AISI nominal strength predictions based on the modified slenderness ratio. In

addition, the axial buckling capacities based on the modified slenderness ratio were more conservative for longer columns than shorter columns, as seen in the comparison between the 1803 mm (71in.) and 1397 mm (55in.) specimens.

The relationship between calculating axial capacities based on the modified slenderness ratio, based on the unmodified slenderness ratio, and the pure experimental test values is displayed. The average buckling capacities for each member thickness were compared. The method using the modified slenderness ratio was consistently conservative. It was 72.5% conservative on average when compared to the experimental buckling capacities for all built-up members tested, and it was 77% conservative on average for all built-up members meeting the provisions of Section D1.2. The percentage of being conservative increased as member thickness increased. This conservative percentage was based on both double-and single-sided attachments. The average axial capacities based on the modified slendernesss ratio of section D1.2 were 60% conservative on average for all 1.626mm (0.064in.) thick members tested, 64% conservative on average for all 2.032mm (0.080in.) thick members tested, and 107% conservative on average for all 2.54mm (0.100 in.) thick member tested. There were no Ptest/Pn values below. Similarly, the axial capacities based on the unmodified slenderness ratio were also very conservative on average. Use of the unmodified slenderness ratio would represent ignoring Section D1.2 for built-up members and designing a member solely on the column design specification. Overall ,the method using the unmodified slenderness ratio was on average 46% conservative for all built-up members tested, and it was 65% conservative on average for all built-up members meeting the provisions of Section D1.2. The degree of the design method based on the unmodified slenderness ratio being conservative also increased with the increased thickness of the member. The average axial capacities using the unmodified slenderness ratio were 34% conservative on average for all 1.626 mm (0.064in.) thick members tested, 44% conservative on average for all 2.032 mm (0.080in.) thick members tested, and 72% conservative on average for all 2.54 mm (0.100in.) thick member tested.

Analysis of intermediate weld pattern and buckling modes

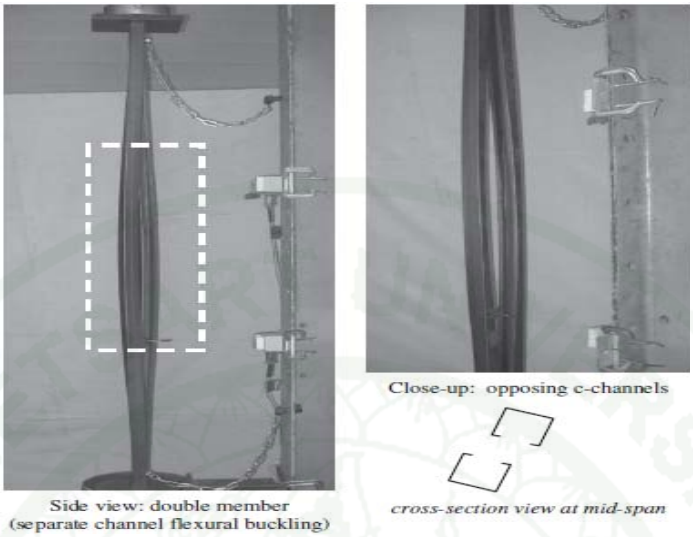

Figure 36 Double member buckling

Source: Whittle and Ramseyer (2009)

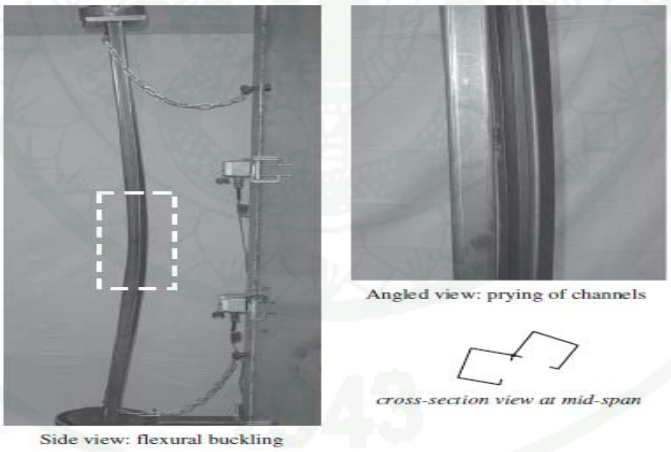

Figure 37 Side view: flexural–torsional buckling of SW5, 41.275 mm (1.625 in.) wide built-up member

Source: Whittle and Ramseyer (2009)

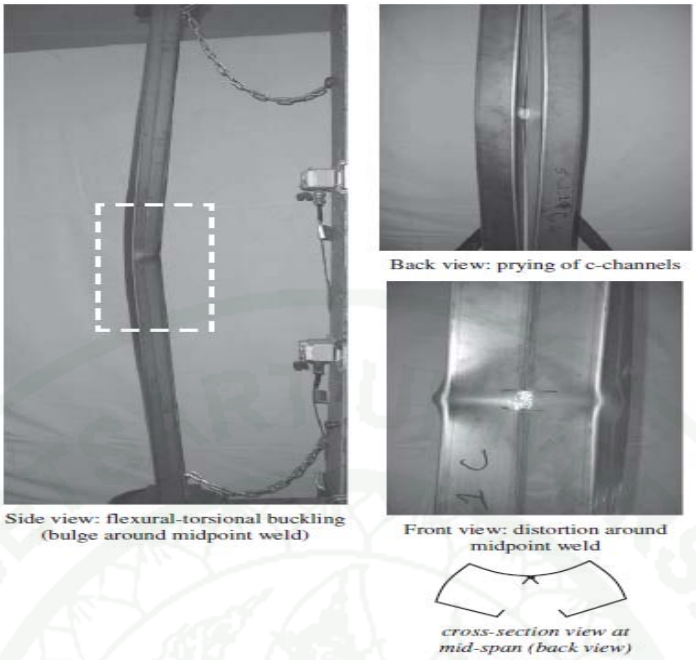

Figure 38 Buckling of SW1, 66.675mm (2.625 in.) wide built-up member

Source: Whittle and Ramseyer (2009)

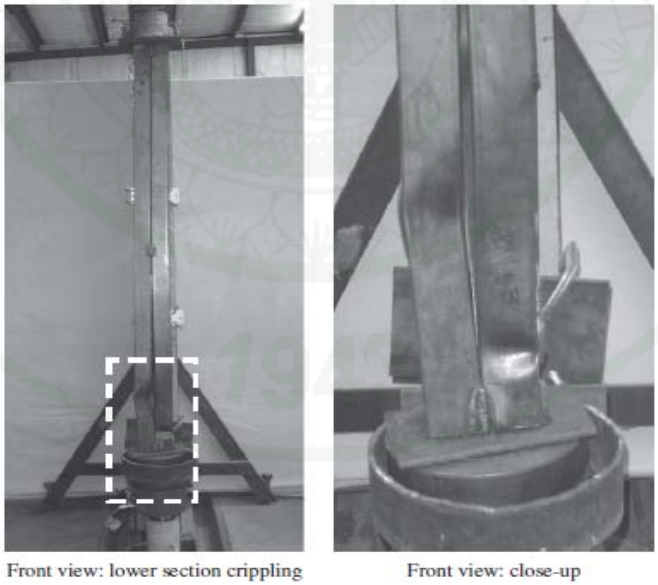

Figure 39 Front view: crippling and separate channel buckling of DW1 member

Source: Whittle and Ramseyer (2009)

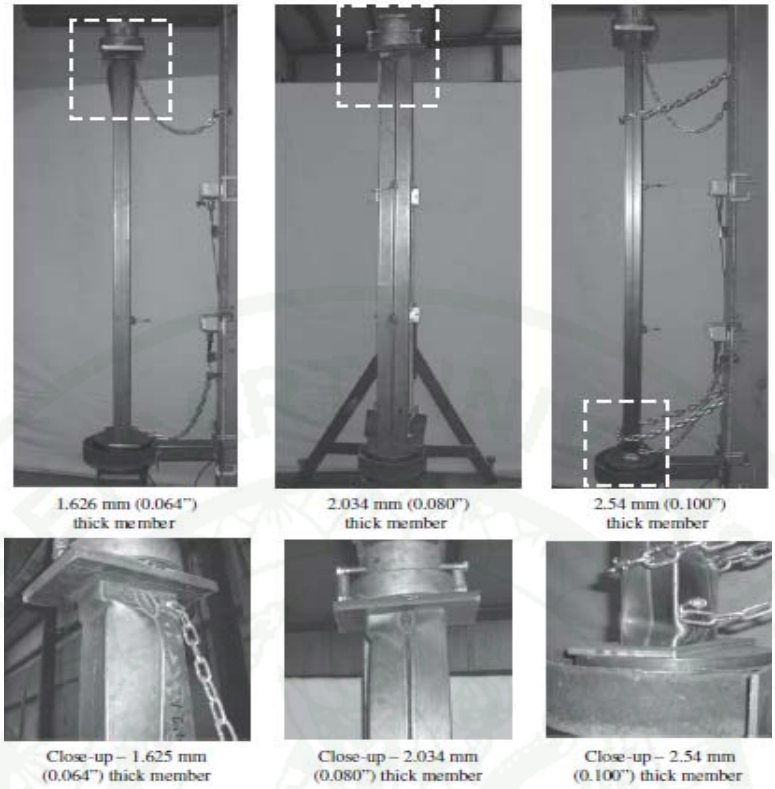

Figure 40 Isolated deformation of members with double-sided attachments

Source: Whittle and Ramseyer (2009)

Conclusions

1. The average axial capacity based on the modified slenderness ratio of sectionD1.2 is exceedingly conservative for built-up members, in general, greater than 70% conservative. The unity check range for all built-up members tested that the meetD1.2 provisions is 1.11–2.83. The value of 1.0 represents a legal built - up member according to the AISI Specification.

2. Use of the modified slenderness ratio is more conservative for longer built-up members and thicker built-up sections. Using the modified slenderness ratio of Specification D1.2 for built-up members is marginally more conservative than using

the standard column procedures of C4 with the unmodified slenderness ratio, if the built-up member fastener and spacing provisions of D1.2 are followed.

2.1 The axial capacities determined using the unmodified slenderness ratio are on average 12% less conservative than the axial capacities calculated based on the modified slenderness ratio for all built-up members tested that meet D1.2 provisions.

2.2 The axial capacities calculated using the unmodified slenderness ratio are unconservative for only one specimen meeting the provisions of D1.2 for built-up members. The unity check for this specimen is 0.98.

3. The built-up member fastener and spacing provisions of D1.2 are effective. These provisions in combination with the unmodified slenderness ratio are very conservative for closed-section, intermediately welded, built-up members. The results range from a unity of 0.98–2.5, with values greater than 1.0 representing conservatively designed members.

3. Investigation on slenderness ratios of built-up compression members
Liu, Lue, Lin (2009)

This paper provides a direct experimental verification of the AISC slenderness ratio formulas for built-up compressive members. The comparison on various code-specified slenderness ratios or provisions, which used in the AISC-ASD, AISC-LRFD, AS-4100, and CSA S1601, are presented.

Slenderness ratios of built-up compressive members For clarity and convenience, various slenderness ratios for built-up compression members summarized as follows and related parameters used are briefly specified.

Bleich's formula

$$\left(\frac{KL}{r}\right)_m = \sqrt{\left(\frac{L}{r}\right)_0^2 + \left(\frac{\pi^2}{12}\right)\left(\frac{a}{r_{ib}}\right)^2} \quad (31)$$

where

(KL/r)m : modified column slenderness ratio of built-up member acting as a unit

(L/r)o : column slenderness ratio of built-up member acting as a unit

a : distance between connectors

rib : radius of gyration of individual component relative to its centroidal axis parallel to member axis of buckling.

Section E6 of 2005 AISC specification

For intermediate connectors that are snug-tight bolted:

$$\left(\frac{KL}{r}\right)_m = \sqrt{\left(\frac{KL}{r}\right)_0^2 + \left(\frac{a}{r_i}\right)^2} \quad (32)$$

For intermediate connectors that are welded or fully-tensioned bolted:

$$\left(\frac{KL}{r}\right)_m = \sqrt{\left(\frac{KL}{r}\right)_0^2 + 0.82\frac{\alpha^2}{1+\alpha^2}\left(\frac{a}{r_{ib}}\right)^2} \quad (33)$$

where α : separation ratio = (h/2rib)

h : distance between centroids of individual components perpendicular to the member axis of buckling.

a/ri : largest column slenderness of individual components.

Australian code (AS-4100)

The maximum slenderness ratio (le/r)c of a main component, based on its minimum radius of gyration and the length between consecutive points where battens

are attached, shall not exceed the lesser of 50 or 0.6 times the slenderness ratio of the built-up member as a whole. The slenderness ratio (le/r)bn of a laced or battened compression member about the axis normal to the plane of the battens shall be calculated as follows:

$$\left(\frac{l_e}{r}\right)_{bn} = \sqrt{\left[\left(\frac{l_e}{r}\right)_m^2 + \left(\frac{l_e}{r}\right)_c^2\right]} \tag{34}$$

where (le/r)m = slenderness ratio of the whole member about the above axis calculated by assuming that the main components act as an integral member.

(le/r)c = maximum slenderness ratio of the main component.

The slenderness ratio (le/r)bp of a battened compression member about the axis parallel to the plane of the battens shall be taken as not less than 1.4(le/r)c.

Canadian code (CSA S16-01)

For built-up members composed of two interconnected shapes, such as back-to-back angles or channels, in contact or separated only by filler plates, the maximum slenderness ratio of component parts between fasteners or welds shall be based on an effective length factor of 1.0 when the fasteners are snug-tight bolts and 0.65 when welds or pretensioned bolts are used.

For built-up members composed of two interconnected shapes separated by lacing or batten plates, the maximum slenderness ratio of component parts between fasteners or welds shall be based on an effective length factor of 1.0 for both snug-tight and pretensioned bolts and for welds. The equivalent slenderness ratio of built-up member, ρ*e*, is taken as:

$$\rho_e = \sqrt{\rho_o^2 + \rho_i^2} \tag{35}$$

where ρe = equivalent slenderness ratio of built-up member where
ρi = maximum slenderness ratio of component part of a built-up member between interconnectors
ρo = slenderness ratio of built-up member acting as an integral unit

Summary for axial compression strengths

Axial strength based on SSRC: Pcr = Fcr Ag

For inelastic bukling.

$$F_{cr} = \left(1 - \frac{(KL/r)^2}{2C_c^2}\right) F_y \quad \text{when } \frac{KL}{r} \leq C_c. \tag{36}$$

For elastic bukling.

$$F_{cr} = \frac{\pi^2 E}{(KL/r)^2} \quad \text{when } \frac{KL}{r} > C_c \tag{37}$$

Where Pcr = critical load,
Fcr = critical stress,
Ag = gross area unit
(*KL*/*r*) = column slenderness ratio
Cc = $\sqrt{\frac{2\pi^2 E}{F_y}}$.

Design axial strength based on AISC Section E3

For inelastic buckling.

$$F_{cr} = \left[0.658^{\frac{F_y}{F_e}}\right] F_y \quad \text{when } \frac{KL}{r} \leq 4.71\sqrt{\frac{E}{F_y}}. \tag{38}$$

For elastic buckling.

$$F_{cr} = 0.877F_e \quad \text{when } \frac{KL}{r} > 4.71\sqrt{\frac{E}{F_y}} \tag{39}$$

Where Pu = design compressive strength = φ Pn = φ Fcr Ag, φ = 0.90

Fcr = critical stress,

Fe = elastic critical buckling st $F_e = \frac{\pi^2 E}{(KL/r)^2}$.

Description of testing.

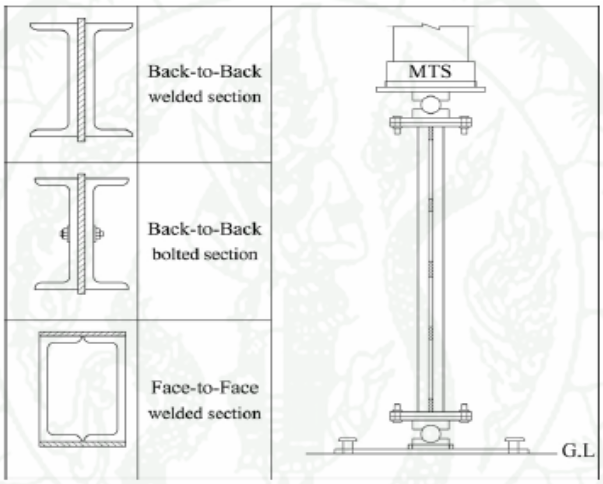

Figure 41 Isolated deformation of members with double-sided attachments

Source: Liu *et al.* (2009)

Sectional properties of the built-up members investigated

Section size	Shape	Area (cm^2)	I_x (cm^4)	r_x (cm)	I_y (cm^4)	r_y (cm)	Dimension specification
C75 × 6.9[a]		8.82	75.30	2.92	12.00	1.17	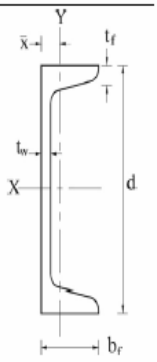
C100 × 9.4[b]		11.92	188.00	3.97	26.00	1.48	
	Single Channel						
2C75 × 6.9		17.64	150.60	2.92	68.44	1.97	
2C100 × 9.4		23.84	376.00	3.97	132.71	2.36	
	Double Channels Back-to-Back						
2C75 × 6.9		17.64	150.60	2.92	154.91	2.96	
2C100 × 9.4		23.84	376.00	3.97	337.40	3.76	
	Double Channels Face-to-Face						

Figure 42 Isolated deformation of members with double-sided attachments

Source: Liu *et al.* (2009)

Test resulted

Grouping and test results for the specimens

Group no.	Axial compression loads (kN)								
	Specimen[a]	P_{test}					F_y (MPa)	F_u (MPa)	E_s (MPa)
		No. 1	No. 2	No. 3	No. 4	Avg.			
1	2C75 × 6.9/B–B, bolted, 4 @52.5 cm	379	425	405	374	396	347.3	456.2	200436
2	2C75 × 6.9/B–B, bolted, 2 @105.0 cm	341	362	332	349	346	347.3	456.2	200436
3	2C75 × 6.9/B–B, welded, 4 @52.5 cm	394	378	369	418	390	347.3	456.2	200436
4	2C75 × 6.9/B–B, welded, 2 @105.0 cm	312	349	391	364	354	347.3	456.2	200436
5	2C100 × 9.4/B–B, bolted, 4 @52.5 cm	626	601	587	NA[b]	605	347.3	456.2	200436
6	2C100 × 9.4/B–B, bolted, 2 @105.0 cm	558	511	505	NA	524	347.3	456.2	200436
7	2C75 × 6.9/F–F, welded, 4 @52.5 cm	500	518	506	NA	508	347.3	456.2	200436
8	2C75 × 6.9/F–F, welded, 3 @70.0 cm	478	515	511	542	512	408.7	521.5	199539
9	2C75 × 6.9/F–F, welded, 2 @105.0 cm	391	340	396	NA	376	347.3	456.2	200436
10	2C100 × 9.4/F–F, welded, 4 @52.5 cm	683	760	686	NA	710	347.3	456.2	200436
11	2C100 × 9.4/F–F, welded, 3 @70.0 cm	766	771	716	769	756	408.7	521.5	199539
12	2C100 × 9.4/F–F, welded, 2 @105.0 cm	684	612	579	NA	625	347.3	456.2	200436

[a] B–B = Back-to-Back; F–F = Face-to-Face.
[b] NA = Not Available.

Figure 43 Isolated deformation of members with double-sided attachments

Source: Liu *et al.* (2009)

This figure shown the built-up buckling strengths obtained from the tests are shown the difference of the strengths between the bolted and welded built-up members appears to be small (2.3%). Strength comparisons for sections having same component shapes, but with different arrangements (e.g., back-to-back, face-to-face, interval, bolted, and welded), can be very different as shown in table .

The Ptest values for sections with 2C75 × 6.9 range from 346 to 508 kN, a potential 47% difference. Similarly, the Ptest values for sections with 2C100×9.4 vary from 524 to 710 kN, reaching a difference of 35%. The Ptest values for Groups 8 and 11 are not included in the comparison as different Fy values were used.

Various slenderness ratios for the built-up and component members

Group no.	Slenderness ratio					Range classification
	$(KL/r)_{(0)}$	$0.75 \times (KL/r)_{(0)}$	(a/r)	$(KL/r)_{(3)}$	$0.75 \times (KL/r)_{(3)}$	
1	106.6	80.0	44.9	115.7	86.8	a_1 and b_1
2	106.6	80.0	89.7	139.4	104.6	a_2 and b_1
3	106.6	80.0	44.9	111.5	83.6	a_1 and b_1
4	106.6	80.0	89.7	125.0	93.8	a_2 and b_1
5	89.0	66.8	35.5	95.8	71.9	a_1 and b_1
6	89.0	66.8	71.0	113.8	85.4	a_2 and b_1
7	71.0	53.3	44.9	80.2	60.2	a_1 and b_1
8	71.0	53.3	59.8	86.7	65.0	a_2 and b_1
9	71.0	53.3	89.7	103.0	77.3	a_3 and b_2
10	55.9	41.9	35.5	63.2	47.4	a_1 and b_1
11	55.9	41.9	47.3	68.3	51.2	a_2 and b_1
12	55.9	41.9	71.0	81.3	61.0	a_3 and b_2

Figure 44 Isolated deformation of members with double-sided attachments

Source: Liu *et al.* (2009)

This figure shown summarized of slenderness ratio value for all group,

a/r < 0.75(KL/r)o or a/r < 0.75(KL/r)m ,
0.75(KL/r)(o) < a/r < (KL/r)(o) or
0.75(KL/r)(m) < a/r < (KL/r)(m)
a/r > (KL/r)o or a/r > (KL/r)m

Compression of code-specified strengths with the test results

Group no.	Specimen	Load ratio	Load ratios for various n values					
			$n = 0$ Un-modified	$n = 1$ Bleich (1952)	$n = 2$ LRFD (1986)	$n = 3$ LRFD (2005)	$n = 4$ AS-4100 (1998)	$n = 5$ CSA S16-01 (2001)
1	2C75 × 6.9/B–B, Bolted, 4 @52.5 cm	$P_{test}/P_{a(n)}$	2.47	2.83	2.91	2.91	2.91	2.91
		$P_{test}/P_{u(n)}$	1.66	1.87	1.92	1.92	1.92	1.92
		$P_{test}/P_{cr(n)}$	1.29	1.48	1.52	1.52	1.52	1.52
2	2C75 × 6.9/B–B, Bolted, 2 @105.0 cm	$P_{test}/P_{a(n)}$	2.16	3.42	3.69	3.69	3.69	3.69
		$P_{test}/P_{u(n)}$	1.45	2.26	2.44	2.44	2.44	2.44
		$P_{test}/P_{cr(n)}$	1.13	1.78	1.93	1.93	1.93	1.93
3	2C75 × 6.9/B–B, Welded, 4 @52.5 cm	$P_{test}/P_{a(n)}$	2.43	2.79	2.43	2.66	2.87	2.62
		$P_{test}/P_{u(n)}$	1.63	1.84	1.63	1.76	1.89	1.74
		$P_{test}/P_{cr(n)}$	1.27	1.46	1.27	1.39	1.50	1.37
4	2C75 × 6.9/B–B, Welded, 2 @105.5 cm	$P_{test}/P_{a(n)}$	2.21	3.50	2.52	3.04	3.78	2.87
		$P_{test}/P_{u(n)}$	1.48	2.31	1.66	2.01	2.50	1.90
		$P_{test}/P_{cr(n)}$	1.15	1.82	1.31	1.59	1.97	1.50
5	2C100 × 9.4/B–B, Bolted, 4 @52.5 cm	$P_{test}/P_{a(n)}$	2.14	2.30	2.34	2.34	2.34	2.34
		$P_{test}/P_{u(n)}$	1.45	1.57	1.59	1.59	1.59	1.59
		$P_{test}/P_{cr(n)}$	1.12	1.20	1.22	1.22	1.22	1.22
6	2C100 × 9.4/B–B, Bolted, 2 @105.0 cm	$P_{test}/P_{a(n)}$	1.85	2.57	2.76	2.76	2.76	2.76
		$P_{test}/P_{u(n)}$	1.26	1.71	1.82	1.82	1.82	1.82
		$P_{test}/P_{cr(n)}$	0.97	1.34	1.44	1.44	1.44	1.44
7	2C75 × 6.9/F–F, Welded, 4 @52.5 cm	$P_{test}/P_{a(n)}$	2.00	2.23	2.00	2.19	2.28	2.28
		$P_{test}/P_{u(n)}$	1.33	1.51	1.33	1.48	1.55	1.55
		$P_{test}/P_{cr(n)}$	1.06	1.17	1.06	1.16	1.20	1.20
8	2C75 × 6.9/F–F, Welded, 3 @70.0 cm	$P_{test}/P_{a(n)}$	1.82	2.32	1.83	2.22	2.46	2.46
		$P_{test}/P_{u(n)}$	1.22	1.58	1.23	1.52	1.67	1.67
		$P_{test}/P_{cr(n)}$	0.96	1.21	0.97	1.16	1.28	1.28
9	2C75 × 6.9/F–F, Welded, 2 @105.0 cm	$P_{test}/P_{a(n)}$	1.48	2.41	1.64	2.20	2.70	2.70
		$P_{test}/P_{u(n)}$	0.99	1.61	1.11	1.49	1.79	1.79
		$P_{test}/P_{cr(n)}$	0.79	1.26	0.86	1.15	1.41	1.41
10	2C100 × 9.4/F–F, Welded, 4 @52.5 cm	$P_{test}/P_{a(n)}$	1.83	1.96	1.83	1.94	1.98	1.98
		$P_{test}/P_{u(n)}$	1.20	1.29	1.20	1.28	1.31	1.31
		$P_{test}/P_{cr(n)}$	0.99	1.05	0.99	1.04	1.06	1.06
11	2C100 × 9.4/F–F, Welded, 3 @70.0 cm	$P_{test}/P_{a(n)}$	1.72	1.97	1.72	1.93	2.04	2.04
		$P_{test}/P_{u(n)}$	1.13	1.33	1.13	1.29	1.37	1.37
		$P_{test}/P_{cr(n)}$	0.93	1.04	0.93	1.02	1.07	1.07
12	2C100 × 9.4/F–F, Welded, 2 @105.0 cm	$P_{test}/P_{a(n)}$	1.61	2.11	1.66	2.02	2.24	2.24
		$P_{test}/P_{u(n)}$	1.05	1.43	1.09	1.36	1.53	1.53
		$P_{test}/P_{cr(n)}$	0.87	1.11	0.89	1.06	1.18	1.18

Figure 45 Isolated deformation of members with double-sided attachments

Source: Liu *et al.* (2009)

This figure shown the calculated axial compressive capacities by using the slenderness ratio formulas of AS-4100 are more conservative as compared with those using the AISC equations. For back-to-back sung-tight bolted sections, the axial compressive capacities computed from the slenderness ratio formulas of CSA S16-01 are virtually same as those determined by the AISC formulas. The CSA S16-01 design strengths appear to be less conservative for back-to-back welded sections, and more conservative for face-to-face welded sections as compared with those evaluated by the AISC.

Conclusion for this paper.

1. It can be seen from the tests as shown in resulted table that a lower strength is obtained if a larger component slenderness ratio (a/r) is applied. In other words, a larger longitudinal spacing of connectors connecting components of built-up members will results in a lower buckling strength. This is within our expectation.

2. Although the AISC-ASD Specification requires that Ka/r should not exceed 0.75(KL/r)(0), the Ptest/Pu ratios seem justifiable when 0.75(KL/r)(0)< Ka/r < (KL/r)(0).

3. Since (KL/r)(3) is the AISC modified slenderness ratio and is larger than (KL/r)(0), the above concluding point is also applicable when (KL/r)(0) is replaced by (KL/r)(3). As such, higher Ptest/Pu ratios can be achieved. The rule which states that the component slenderness ratio (Ka/r) not exceeding three-fourths times the governing slenderness ratio of built-up member, seems rationale according to the tests conducted in this study. The governing slenderness ratio ofbuilt-up member could be the modified or unmodified one as explained in the AISC specification.

MATERIALS AND METHODS

Compression test

Compression test is study on the buckling behavior of cold-formed steel columns with the fixed-end support condition under compressive loading. The built-up sections of test specimens were prepared by welding the cross sections of two C-steel together for closed section. The compression test by Instron machine which have capacity for maximum compressive load 200 KN and used velocity 0.5 mm/minute. for testing. This machine can recorded loading and displacements at the test time until maximum loading.

Instruments of compression testing.

1. Instron machine. (Compression tool)
2. Specimens.
3. Strain gauges.
4. Data loggers.
5. Adhesive for strain gauges.
6. Computer.

Test Specimens.

Single section

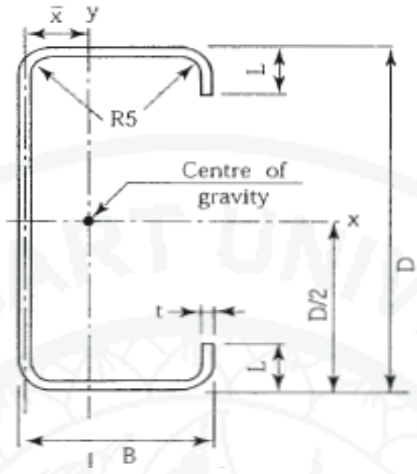

Figure 46 Shown the all dimensions of the single specimens

Source: Bluescope Lysaght Co.Ltd. (1987)

Table 1 Shown the all dimensions of the single specimens

BUILT-UP SPECIMEN No.	SINGLE SECTION SECTION DxBxLxt	B mm	D mm	t mm	L mm
BC200	C-203x76x15.5x1.5	76	203	1.5	15.5
BC150	C-152x64x15.5x1.5	64	152	1.5	15.5
BC100	C-102x51x13.5x1.5	51	102	1.5	13.5

Built-up section

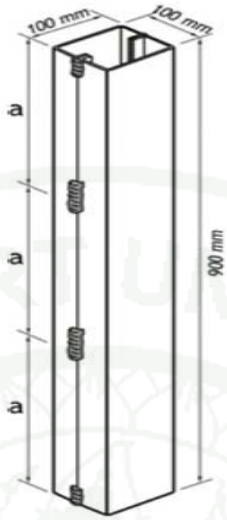

Figure 47 Built-up section

Source: Reyes and Guzman (2011)

This figure show built-up section from 2 section of light lip channel c by used welding method. Welding length used 20 mm. for all point and equal spacing in section. The other specimens have differented weld spacing for study affected to buckling load of different weld spacing .

Welding methodology

General requirement

Methodology for welding method using AWS D1.3 standard for structural welding code sheet steel. This code contains the requirements for arc welding of structural sheet/strip steel including cold formed member hereafter collectively referred to as sheet steel, which are equal to or less than 4.88 mm. in norminal thickness. The provisions of this code are intended for used sheet steel having a minimum yield point equal or less than 550 Mpa. (American Welding Society, 2008)

Table 1.1
Code Application Matrix of D1.3 and D1.1 Codes
Based on Material Thickness Being Joined (see 1.1)

Material Thickness	$t_2 < 1/8$ in [3 mm]	1/8 in $\le t_2 \le$ 3/16 in [3 mm $\le t_2 \le$ 5 mm]	$t_2 > 3/16$ in. [5 mm]
$t_1 < 1/8$ in [3 mm]	D1.3	D1.3 or Annex A	Annex A
1/8 in. $\le t_1 \le$ 3/16 in [3 mm $\le t_1 \le$ 5 mm]	D1.3 or Annex A	D1.3 or Annex A or D1.1	Annex A or D1.1
$t_1 > 3/16$ in [5 mm]	Annex A	Annex A or D1.1	D1.1

Note: Annex A, Note 1 applications may be used without removal of coating or galvanizing, provided the application meets the requirements of Note 1.

Figure 48 AWS D1.3 specification

Source: American Welding Society D1.3 (2008)

Gas Metal Arc Welding

Gas metal arc welding uses an arc between a continuous filler metal (consumable) electrode and the weld pool. Shielding is provided by an externally supplied shielding gas. This process is also known as MIG welding or MAG welding. MIG (Metal Inert Gas) welding means the use of an inert (i.e. non active) gas. MAG (Metal Active Gas) welding requires the use of an active gas (i.e. carbon dioxide and oxygen). CO_2 is a more commonly used shortening of MAG welding gas.

Figure 49 Mig/ Mag Welding method

Source: American Welding Society D1.3 (2008)

The process consists of a DC arc burning between a thin bare metal wire electrode and the workpiece. The arc and weld area are enveloped in a protective gas shield. The wire electrode is fed from a spool, through a welding torch which is connected to the positive terminal into the weld zone. MIG/MAG welding is the most widely used process in the world today. It is a versatile method which offers a lot of advantages. The technique is easy to use and there is no need for slag-cleaning. Another advantage is the extremely high productivity that MIG/MAG welding makes possible.

Figure 50 Mig/Mag Welding machine

MIG/MAG welding is used on all thicknesses of steels, aluminium, nickel, stainless steels etc. The MAG process is suitable both for steel and unalloyed, low-alloy and high-alloy based materials. The MIG process, on the other hand, is used for welding aluminium and copper materials.

Welding Types

Flare-Groove Welds. For matching filler-metal, base-metal combinations, the allowable load capacity of flare-groove welds made in any welding position is considered to be governed by the thickness of the sheet steel adjacent to the welds, provided that a weld size at least equal to the thickness of the sheet steel as was obtained with the WPS qualification.

Single-Flare-V-Groove Welds.

Single-flare-V-groove weld positions shall be followed in figure xx. The minimum length shall be 3/4 in [19 mm] (American Welding Society, 2008)

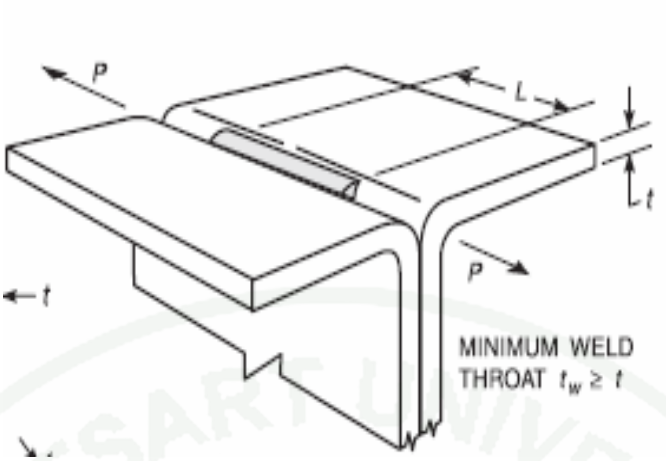

Figure 51 Single-Flare-V-Groove Welds

Source: Reyes and Guzman (2011)

Figure 52 Built-up section

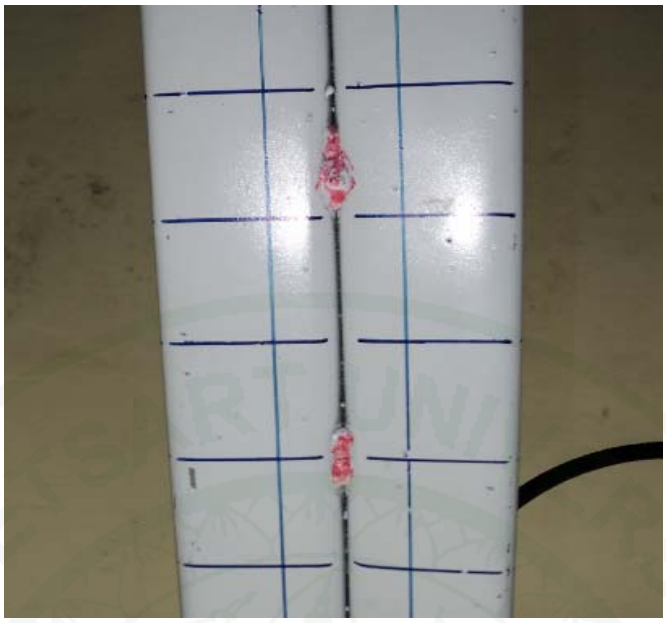

Figure 53 Welded point of built-up section

Specimens Quantity.

Table 2 Specimens Quantity

Built-up section	Length (L) (cm.)	Weld spacing (a) (cm.)	Length of seam welds (cm)
BC100@125	100	12.5	2
BC100@250	100	25	2
BC100@500	100	50	2
BC150@125	100	12.5	2
BC150@250	100	25	2
BC150@500	100	50	2
BC200@125	100	12.5	2
BC200@250	100	25	2
BC200@500	100	50	2

Preparation of specimens

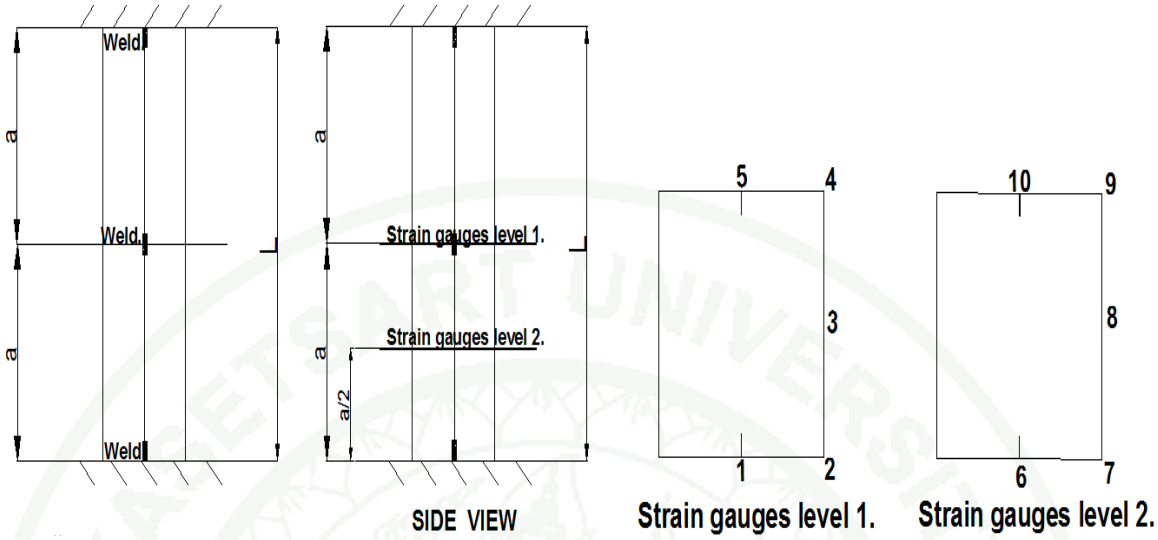

Figure 54 Position of strain gauges

This figure show the position of strain gauges on specimens were installed. All strain gauges measurement for the distribution of stress on section and study affected to buckling load of different weld spacing.

All strain gauges were installed divided 2 level, first level for 1-5 positions were installed 5 point followed this figure at mid length of specimen or same level with welding point by choose symmetry of section only. Remain 5 position of strain gauges were installed level between weld spacings or a spacing and same position of section for study buckling stress distribution on section at 2 level different.

Tension test

The tension test related to the mechanical testing of steel products subjects a machined or full-section specimen of the material under examination to a measured load sufficient to cause rupture. In general, the testing equipment and standard for usein this research is ASTM370 (American Society of Testing and Materials) for result in mechanical properties of steel.

Standard dimension of tension test are show in Figure 12 and used automatic extensometer for strain measurement.

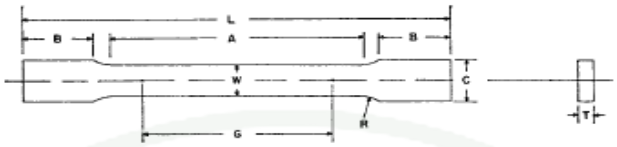

DIMENSIONS

	Standard Specimens						Subsize Specimen	
	Plate-Type, 1½-in. (40-mm) Wide							
	8-in. (200-mm) Gauge Length		2-in. (50-mm) Gauge Length		Sheet-Type, ½ in. (12.5-mm) Wide		¼-in. (6-mm) Wide	
	in.	mm	in.	mm	in.	mm	in.	mm
G—Gauge length (Notes 1 and 2)	8.00 ± 0.01	200 ± 0.25	2.000 ± 0.005	50.0 ± 0.10	2.000 ± 0.005	50.0 ± 0.010	1.000 ± 0.003	25.0 ± 0.08
W—Width (Notes 3, 5, and 6)	1½ + ⅛ − ¼	40 + 3 − 6	1½ + ⅛ − ¼	40 + 3 − 6	0.500 ± 0.010	12.5 ± 0.25	0.250 ± 0.002	6.25 ± 0.05
T—Thickness (Note 7)	Thickness of Material							
R—Radius of fillet, min (Note 4)	½	13	½	13	½	13	¼	6
L—Overall length, min (Notes 2 and 8)	18	450	8	200	8	200	4	100
A—Length of reduced section, min	9	225	2¼	60	2¼	60	1¼	32
B—Length of grip section, min (Note 9)	3	75	2	50	2	50	1¼	32
C—Width of grip section, approximate (Notes 4, 10, and 11)	2	50	2	50	¾	20	⅜	10

Figure 55 Standard dimension of tension test

Source: ASTM370 (1890)

Instruments of tension testing.

1. Instron machine.

2. Coupon specimens

3. Extensometer and micrometer or vernier caliper

4. Computer

The tension test results showed relationship between stress and strain curve of steel from flat part and corner part. From tensile result can indicated mechanical properties , example tensile strength, yield point, yield strength, Modulus of elasticity (E) ,percentage elongation and reduction of area from material.

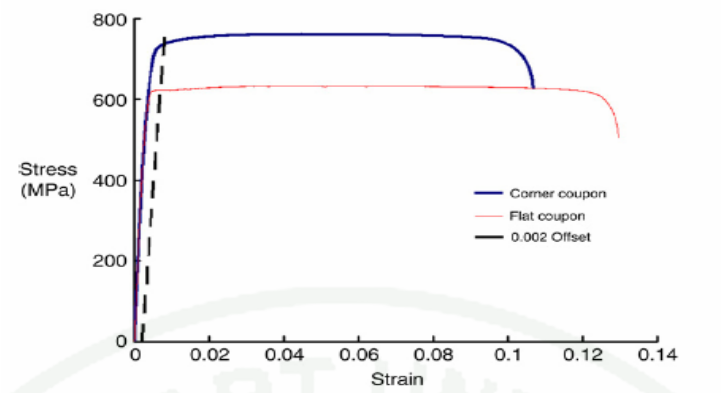

Figure 56 Stress and strain curve of steel

Source: Timoshenko and Gere (1961)

Finite element Program.

This research was used the finite element analysis program ANSYS only for study behaviors of built-up specimens for expected buckling load and failure mode shape of all specimens before testing and compared behavior with testing in laboratory. Since main objectives of this research focus on testing in laboratory more than the finite element analysis

Finite element method, a numerical method, is used here to solve differential equation. (Cook *et al.*, 2003) The equation can sometimes be complex, and the numerical answer will be taken to model or predict the structural behaviors of cold-formed steel. The results are presented in 3-dimensional pictures and the analytical interpretation in color shades of stress (Logan, 1976). Then the interpretation will be used in finding out critical limits, stress, and failure patterns of the structure. Being compared with the experimental result in laboratory, the result of finite element method can be verified that it is correct and suitable for practical use.

By all reasons, the understanding of the general structural behaviors of cold-formed steel plays an important role in efficient structural design of the steel that is prone to growing use. However, the study of its behaviors is in adequate. Hence this study will bring about comprehensive knowledge in this field that will lead to confidence and safety in the use of cold-formed steel sections.

RESULTS AND DISCUSSION

Tensile tested

This tensile strength test is an examination of material properties of the specimens. It is objectived at finding fundamental data, namely proof stress at 0.2%, ultimate tensile strength, and elastic young modulus which are needed to calculated of ultimate compressive strength and buckling stress of the sections.

In this test, Electromechanical Universal Testing Machine SCHENCK RSA 250 was used at the speed of 0.5 mm./minute with the specimens taken from BC100, BC150, and BC200, two pieces for each type as shown in picture 57. The test was conducted under ASTM A370 (AISI standard**,** 2007) Standard and elastic young modulus was calculated by a tool called Extensometer, As shown in picture 57.

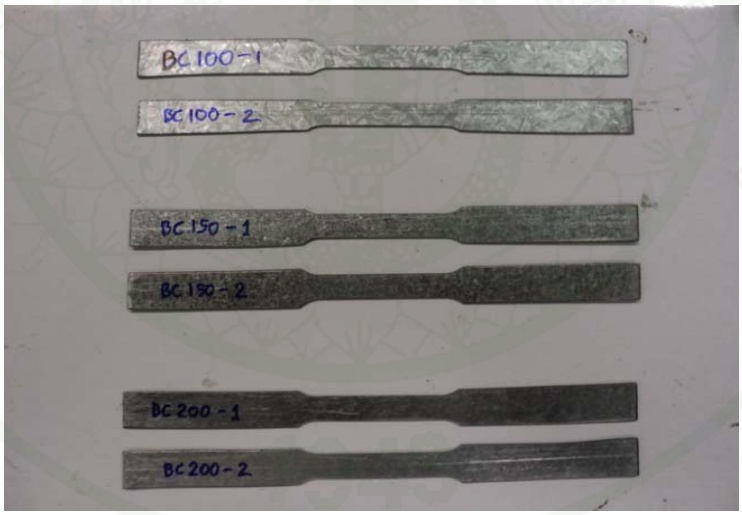

Figure 57 Tensiles specimens

Figure Tensile coupon sample shows six specimens taken from three groups of steel: BC100, BC150, and BC200. Each specimen was prepared in accordant with ASTM A370 Standard as shown in figure. All specimens cut off from web element of Light lip channel in each group.

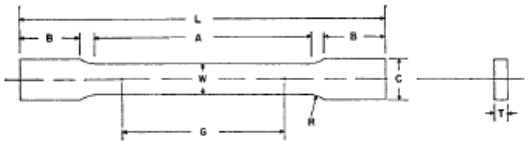

DIMENSIONS

	Standard Specimens						Subsize Specimen	
	Plate-Type, 1½-in. (40-mm) Wide							
	8-in. (200-mm) Gauge Length		2-in. (50-mm) Gauge Length		Sheet-Type, ½ in. (12.5-mm) Wide		¼-in. (6-mm) Wide	
	in.	mm	in.	mm	in.	mm	in.	mm
G—Gauge length (Notes 1 and 2)	8.00 ± 0.01	200 ± 0.25	2.000 ± 0.005	50.0 ± 0.10	2.000 ± 0.005	50.0 ± 0.010	1.000 ± 0.003	25.0 ± 0.08
W—Width (Notes 3, 5, and 6)	1½ + ⅛ − ¼	40 + 3 − 6	1½ + ⅛ − ¼	40 + 3 − 6	0.500 ± 0.010	12.5 ± 0.25	0.250 ± 0.002	6.25 ± 0.05
T—Thickness (Note 7)	Thickness of Material							
R—Radius of fillet, min (Note 4)	½	13	½	13	½	13	¼	6
L—Overall length, min (Notes 2 and 8)	18	450	8	200	8	200	4	100
A—Length of reduced section, min	9	225	2¼	60	2¼	60	1¼	32
B—Length of grip section, min (Note 9)	3	75	2	50	2	50	1¼	32
C—Width of grip section, approximate (Notes 4, 10, and 11)	2	50	2	50	¾	20	⅜	10

Figure 58 ASTM A370 standard

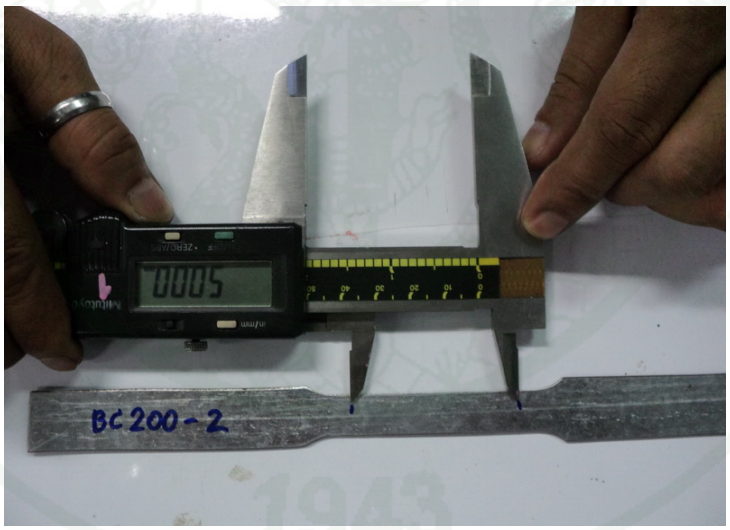

Figure 59 Gauge length measurement

This figure shows gauge length measurement of BC200-2 specimen by digital vernier caliper and used gauge length at 50 mm. which is equal value of all specimens. This measurement was recorded to show the comparison between gauge lengths before and after test in order to calculate elongation of the specimens in percentage extension of each specimen.

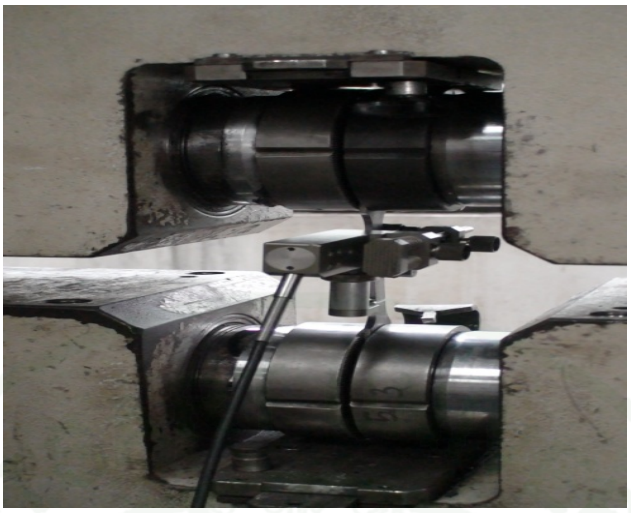

Figure 60 Extensometer machine

Figure shows the tensile testing behaviored by using Electromechanical Universal Testing Machine SCHENCK RSA 250 at the speed of 0.5 mm./minute with Extensometer installed to find out Young's modulus of specimen.

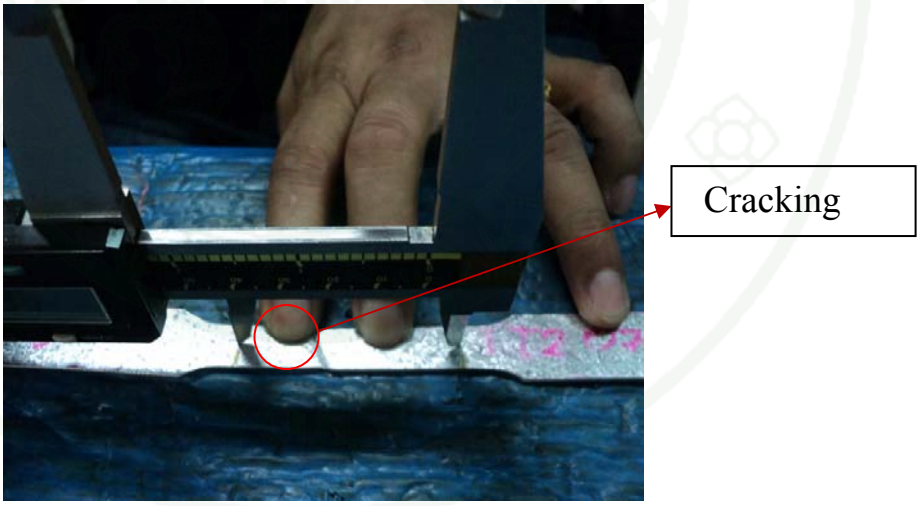

Figure 61 Elongation measurement

Figure Elongation measurement shown gauge lengths measurement of the specimens after test for compared between before test to calculate elongation of specimen. It suggests that mostly the cracking of specimen occurred at half length of each specimen.

Resulted

Mechanical properties of steel for BC100

The results of tensile test of BC100-1 and BC100-2 are shown in figures 62 and 63 Figure shows relationship between strength (Mpa) on y-axis and extention (%) on x-axis at testing speed of 0.5 mm./minute. From this graph it can find yield strength of material at 0.2 % proof stress and young‘s modulus of this material and conclusion in x table for used all values for calculated norminal buckling load of built-up section continuously.

Mechanical properties of steel for BC100 -1

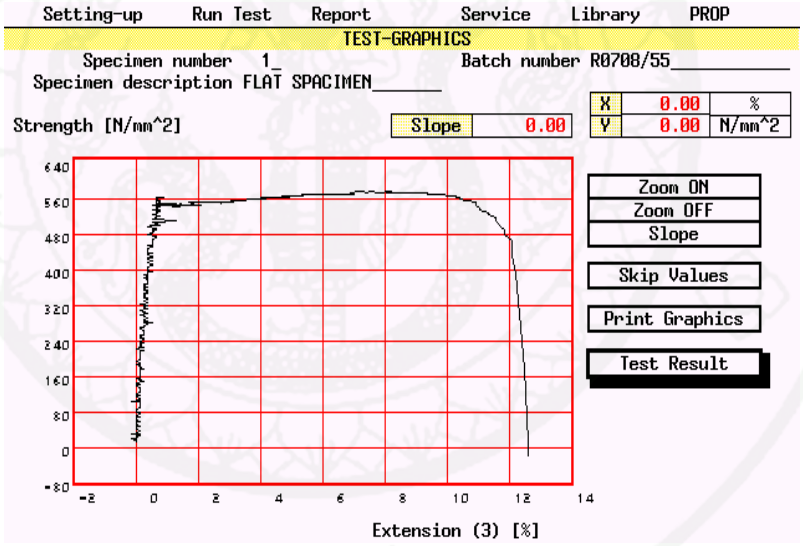

Figure 62 Tensile resulted of BC100-1

The figure as shown the resulted of tensile test of BC100-1 specimen, the ultimate strength was approximately 570 Mpa. from graph and data from the graph could also be taken to calculate compressive strength, Young's modulus, as well as yield strength, all are displayed in table .

Mechanical properties of steel for BC100 - 2

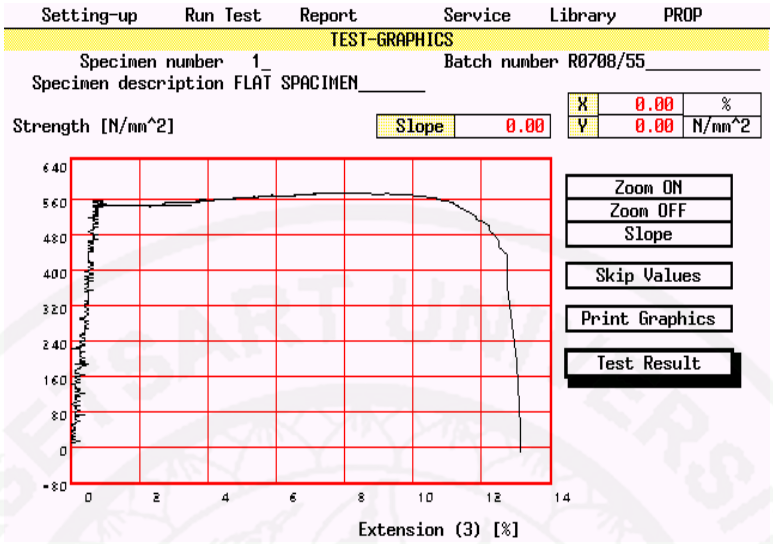

Figure 63 Tensile resulted of BC100-2

The figure as shown the resulted of tensile test of BC100-2 specimen, the ultimate strength was approximately 567 Mpa. From graph and data from the graph could also be taken to calculate compressive strength, Young's modulus, as well as yield strength, all are displayed in table.

Table 3 Conclusion mechanical properties of steel for BC100-1 , BC100-2

Specimen	BC100-1	BC100-2
Thickness (mm.)	1.554	1.553
Width (mm.)	12.64	12.63
Cross section area (mm^2)	19.64	19.61
Load at 0.2 % offset yield Strength (N)	10,643	10,581
Maximum tensile load (kN)	11.205	11.130
0.2% offset yield Strength (N/mm^2)	541.91	539.58
Tensile strength (N/mm^2)	570.52	567.57
Young's Modulus (MPa)	220,600	218,360
Elongation (%)	13.08	13.14

Mechanical properties of steel for BC150

The results of tensile test of BC150-1 and BC150-2 are shown in figures 64 and 65 Figure shows relationship between strength (Mpa) on y-axis and extention (%) on x-axis at testing speed of 0.5 mm./minute. From this graph it can find yield strength of material at 0.2 % proof stress and young‘s modulus of this material and conclusion in x table for used all values for calculated norminal buckling load of built-up section continuously.

Mechanical properties of steel for BC150-1

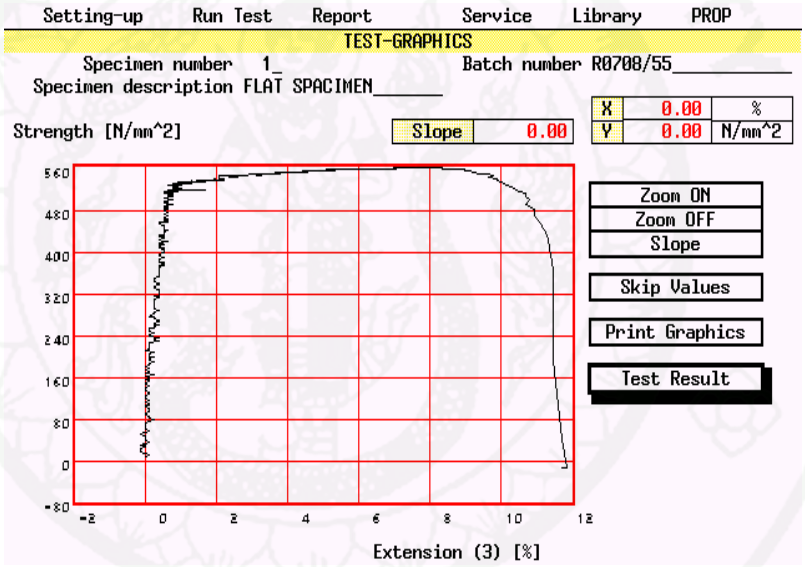

Figure 64 Tensile result of BC150-1

The figure as shown the resulted of tensile test of BC150-1 specimen, the ultimate strength was approximately 560 Mpa. From graph and data from the graph could also be taken to calculate compressive strength, Young's modulus, as well as yield strength, all are displayed in table.

Mechanical properties of steel for BC150-2

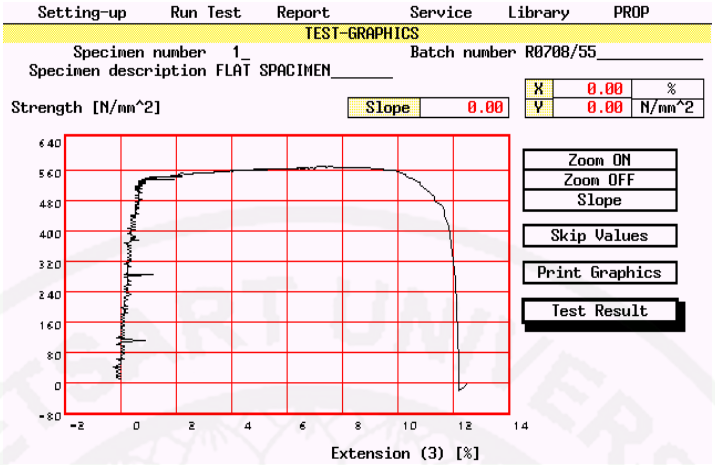

Figure 65 Tensile result of BC150-2

The figure 65 as shown the resulted of tensile test of BC150-2 specimen, the ultimate strength was approximately 563 Mpa. From graph and data from the graph could also be taken to calculate compressive strength, Young's modulus, as well as yield strength, all are displayed in table.

Table 4 Conclusion Mechanical properties of steel for BC150-1, BC150-2

Specimen	BC150-1	BC150-2
Thickness (mm.)	1.547	1.545
Width (mm.)	12.63	12.66
Cross section area (mm^2)	19.54	19.56
Load at 0.2 % offset yield Strength (N)	10,279	10,352
Maximum tensile load (kN)	10.965	11.015
0.2% offset yield Strength (N/mm^2)	526.05	529.23
Tensile strength (N/mm^2)	561.16	563.14
Young's Modulus (MPa)	217,250	221,330
Elongation (%)	11.06	12.66

Mechanical properties of steel for BC200

The results of tensile test of BC200-1 and BC200-2 are shown in figures 66 and 67 Figure shows relationship between strength (Mpa) on y-axis and extention (%) on x-axis at testing speed of 0.5 mm./minute. From this graph it can find yield strength of material at 0.2 % proof stress and young‘s modulus of this material and conclusion in x table for used all values for calculated norminal buckling load of built-up section continuously.

Mechanical properties of steel for BC200-1

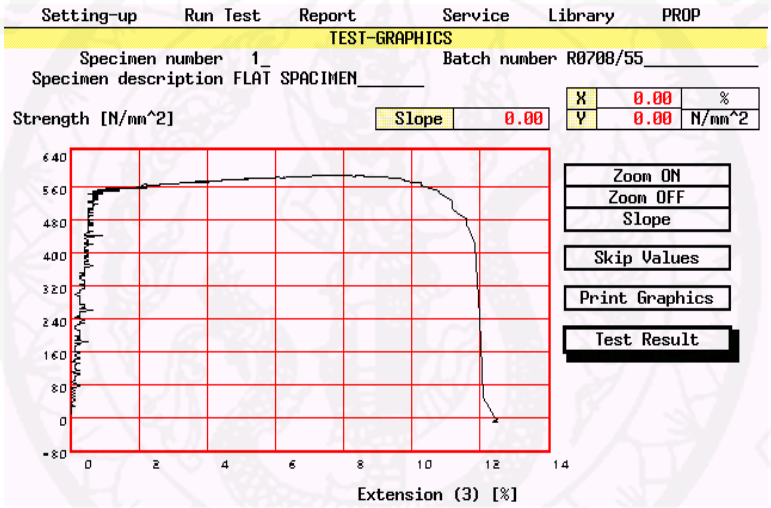

Figure 66 Tensile result of BC200-1

The figure 66 as shown the resulted of tensile test of BC200-1 specimen, the ultimate strength was approximately 581 Mpa. From graph and data from the graph could also be taken to calculate compressive strength, Young's modulus, as well as yield strength, all are displayed in table.

Mechanical properties of steel for BC200-2

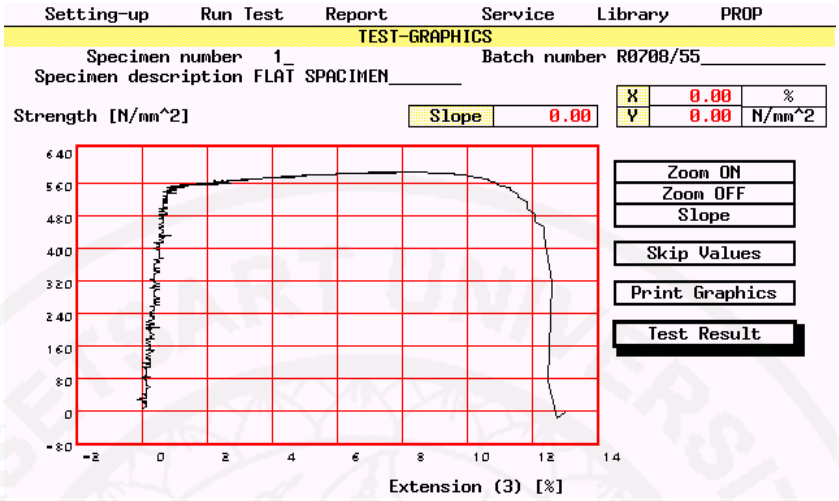

Figure 67 Tensile result of BC200-2

The figure 67 as shown the resulted of tensile test of BC200-2 specimen, the ultimate strength was approximately 581 Mpa. from graph and data from the graph could also be taken to calculate compressive strength, Young's modulus, as well as yield strength, all are displayed in table .

Table 5 Conclusion mechanical properties of steel for BC200-1, BC200-2

Specimen	BC200-1	BC200-2
Thickness (mm.)	1.537	1.538
Width (mm.)	12.63	12.62
Cross section area (mm^2)	19.41	19.41
Load at 0.2 % offset yield Strength (N)	10,582	10,559
Maximum tensile load (kN)	11.290	11.290
0.2% offset yield Strength (N/mm^2)	545.20	544.01
Tensile strength (N/mm^2)	581.66	581.66
Young's Modulus (MPa)	220,110	203,440
Elongation (%)	12.56	13.18

Conclusion of tensile test resulted

Tensile test resulted suggest that material properties of each specimen are almost equal in term of 0.2% offset yield strength, ultimate tensile strength, Young's modulus which are important in the calculation of buckling loads of each section and data for mechanical properties of specimen.

Table 6 Conclusion mechanical properties of steel all specimens

Specimen	BC100-1	BC100-2	BC150-1	BC150-2	BC200-1	BC200-2
Thickness (mm.)	1.554	1.553	1.547	1.545	1.537	1.538
Width (mm.)	12.64	12.63	12.63	12.66	12.63	12.62
Cross section area (mm^2)	19.64	19.61	19.54	19.56	19.41	19.41
Load at 0.2 % offset yield Strength (N)	10,643	10,581	10,279	10,352	10,582	10,559
Maximum tensile load (KN)	11.205	11.130	10.965	11.015	11.290	11.290
0.2% offset yield Strength (N/mm^2)	541.91	539.58	526.05	529.23	545.20	544.01
Tensile strength (N/mm^2)	570.52	567.57	561.16	563.14	581.66	581.66
Young's Modulus (MPa)	220,600	218,360	217,250	221,330	220,110	203,440
Elongation (%)	13.08	13.14	11.06	12.66	12.56	13.18

Compression tested

Results and discussion

1. Load - displacement relationships

The load-displacement relationships obtained through the test are shown in figs. 6-8. All figures show the maximum buckling capacity loads of specimens. The load-displacement relationships used speed 0.5 mm./minute for tested by UTS machine.

1.1 Load - displacement relationships of BC100 - 1

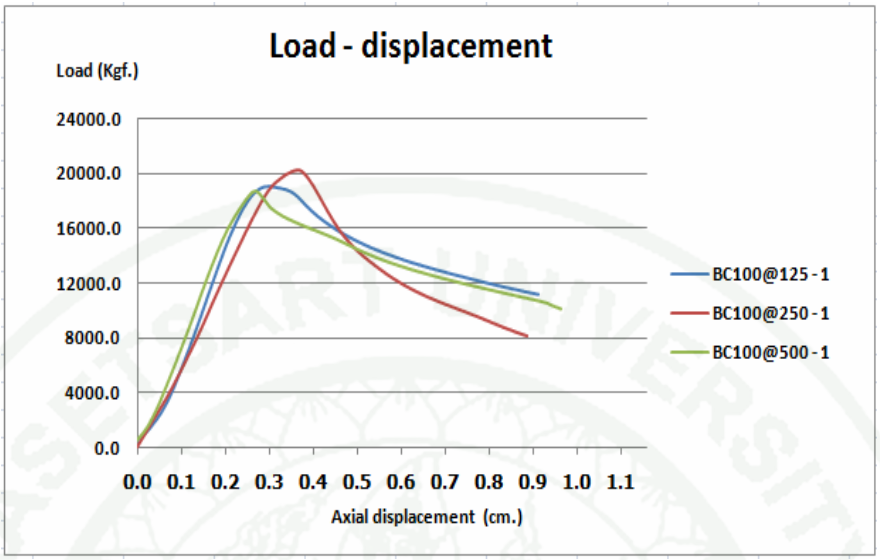

Figure 68 Load-displacement relationships of BC100-1

Figure 68 shows that at the very beginning BC100@250 had the highest ultimate buckling load and developed axial load quite less than the others. Then load displacement continued in linear direction. And then @125, @500, and @250 began to generate local buckling at 10,000 kg., 11,000 kg., and 14,000 kg. respectively. It is noticeable that the buckling was in wave shape at web element with larger w/t ratio than other parts, and it led to earlier buckling behavior as seen in figure x. After that the column was still able to hold the load until ultimate buckling behavior was generated in each specimen. The subsidence of all four sides of the column was called Roof mechanism behavior. The area between welding points began to part while the points themselves remained complete. The ultimate buckling loads of @250, @125, and @500 were 20,260 kg., 18,500 kg., and 18,000 kg. respectively.

1.2 Load - displacement relationships of BC100 - 2

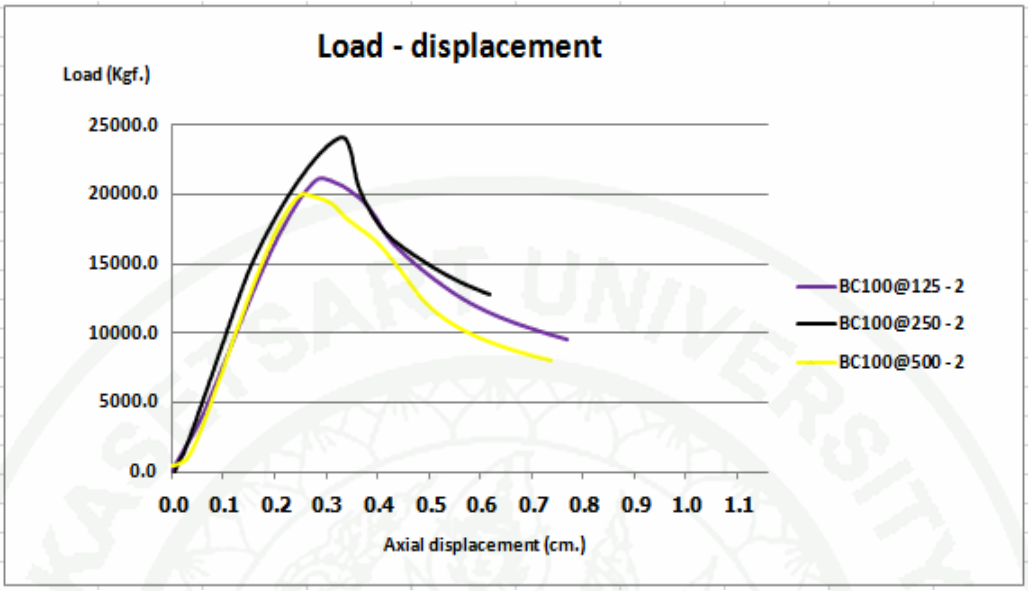

Figure 69 Load - displacement relationships of BC100-2

Figure shows that at the very beginning BC100@250 had the highest ultimate buckling load. Then load- displacement continued in linear direction. And then @125, @250, and @500 began to generate local buckling at 14,000 kg., 15,000 kg., and 11,200 kg. respectively. It is noticeable that the buckling was in wave shape at web element with larger w/t ratio than other parts, and it led to earlier buckling behavior as seen in figure x. After that the column was still able to hold the load until ultimate buckling behavior was generated in each specimen. The big wave of all four sides of the column was called Roof mechanism behavior. The area between welding points began to part while the points themselves remained complete. The ultimate buckling loads of @125, @250, and @500 were 21,000 kg., 24,000 kg., and 20,000 kg. respectively. All resulted in second time tested, it have ultimate buckling load more than first time tested about 2000 Kg.

Conclusion of Load-displacement relationships of BC100–1 and BC100-2

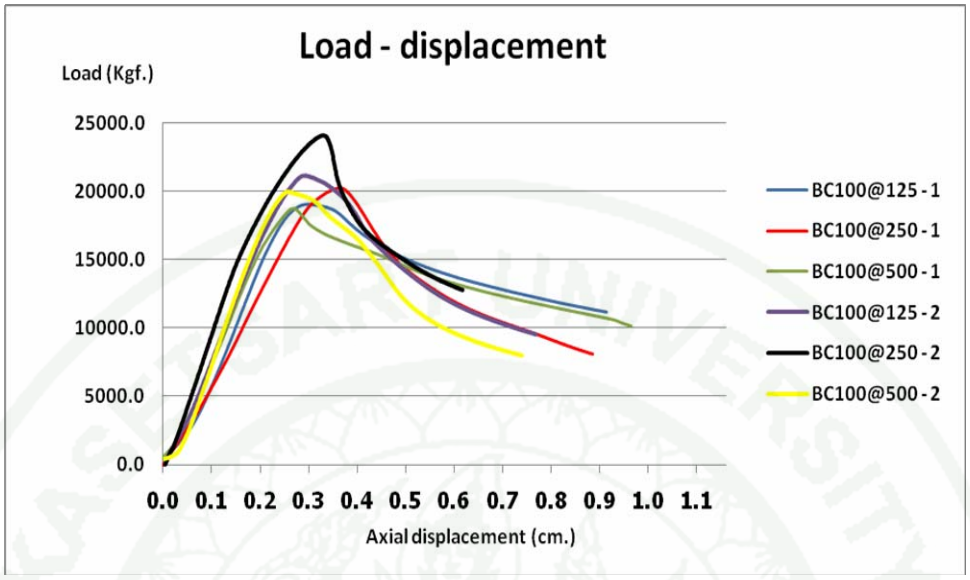

Figure 70 Load-displacement relationships of BC100 all specimen

From this figure as shown in relationships load-displacement all specimen of BC100 in first time tested group (BC100@125–1, BC100@250–1, BC100@500–1) and the second time tested group (BC100@125–2, BC100@250–2, BC100@500–2). In each group have 3 weld spacings, @125, @250, @500 respectively.

For the first time tested group, BC100@250–1 had highest ultimate buckling load About 20,200 Kg. and followed to BC100@125–1 had ultimate buckling load about 18,500 Kg. and then BC100@500–1 had buckling load about 18,000 Kg. respectively.

For the second time tested group, BC100@250–2 had highest ultimate buckling load about 23,500 Kg. and followed to BC100@125–2 had ultimate buckling load about 21,300 Kg. and then BC100@500–2 had buckling load about 20,000 Kg. respectively.

All specimen observed resulted that in each test group could arranged the ultimated buckling load from highest buckling load as @250 and then @125 and @500 were same direction in two tested group. The specimen in each group, first time test group and second time test group were prepared welding procedure in each group per each time tested, it affected to different resulted in each group but resulted in two tested group same direction in buckling load. The second time tested group have buckling load more than first time tested group about 3,000 Kg. when compared in each weld spacing, it causing from preparation of specimen such as baseplate for specimen or vertical line of specimen should be perpendicular with baseplate, it need for specimen preparation procedure of tested.

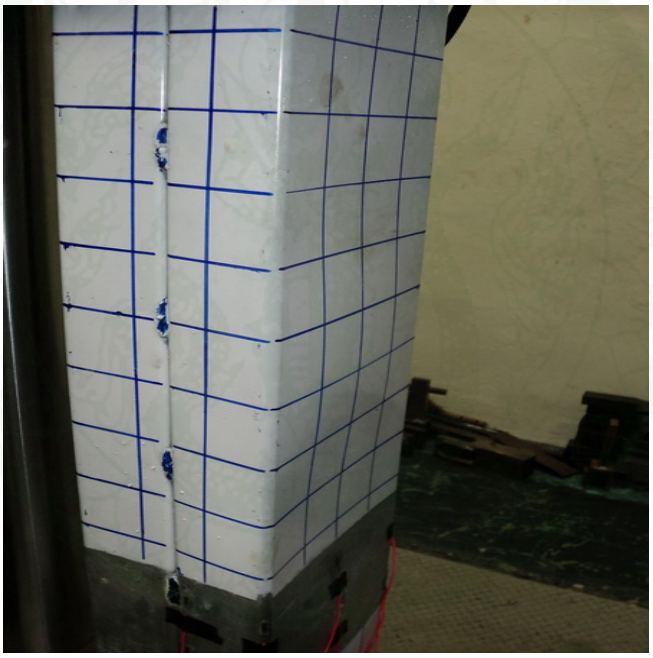

Figure 71 Local buckling behavior

As shown from this figure called “Local buckling behavior” was occurred this behavior when loading at 40%-60% of ultimate buckling load by displayed in shape of sine wave at the web element of light lip c channel steel on both sides.

Local buckling behavior is first mode of failure for thin plate structure or cold-formed steel. Because of web element had large w/t ratio which caused to local buckling more easily when compared with flanged element .

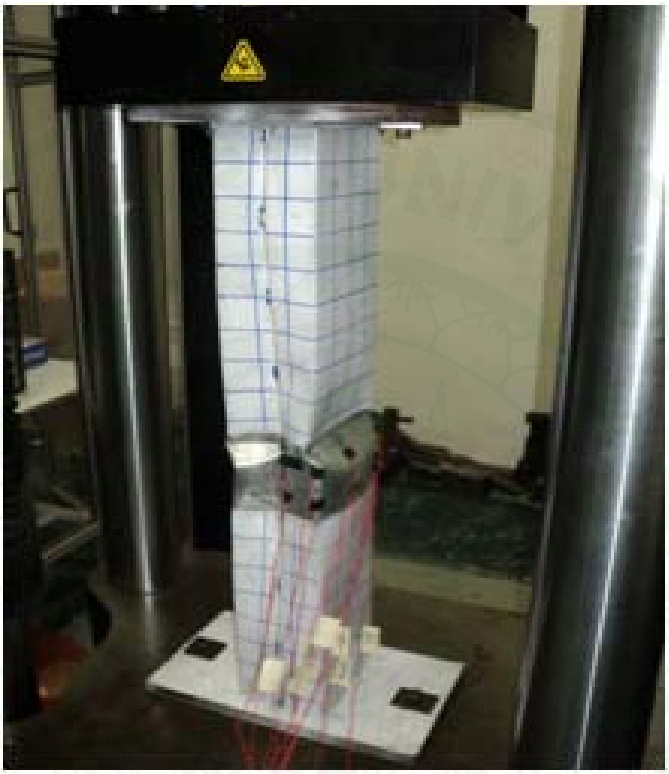

Figure 72 Ultimate buckling behavior

Ultimate buckling behavior of the specimens was local buckling first generated in the depth of the sections. The column could continually restrain the compressive strength until inelastic local buckling called “Roof mechanism” was generated on all four sides of the sections by in-out of four surface around specimen.

Roof mechanism behavior is generally alike in all sections at inelastic behavior of specimen followed in this figure.

1.3 Load - displacement relationships of BC150 - 1

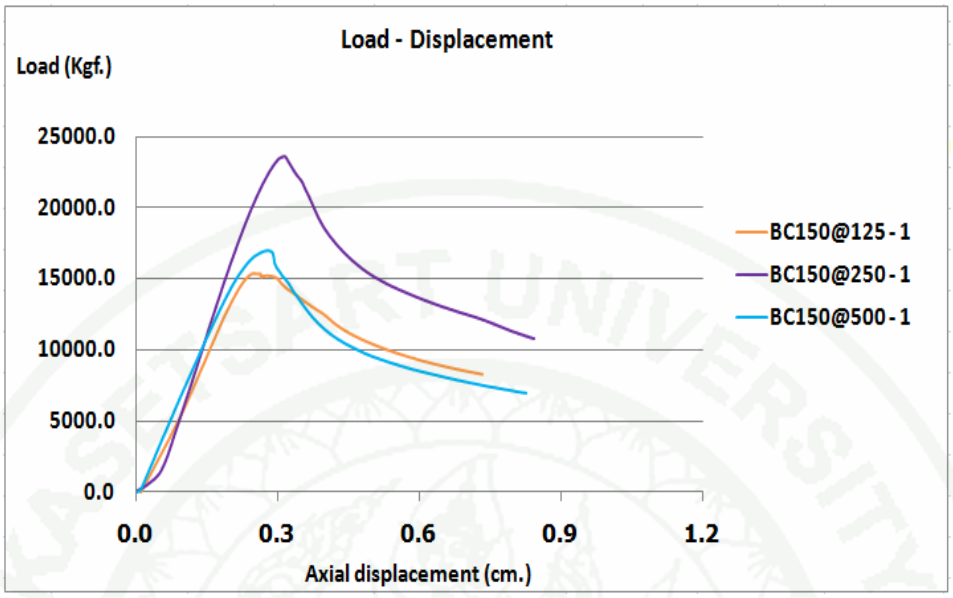

Figure 73 Load-displacement relationships of BC150–1

At the beginning, the load displacement relationship of all specimens continued almost in the same direction. After that @500, @125, and @250 began to generate local buckling behavior at 6,000 kg., 7,000 kg., and 8,000 kg. respectively.

Local buckling behavior was in shape of wave at web element of C-shaped steel on both sides, as shown in figure 73. Roof mechanism behavior also occurred during buckling behavior. The ultimate buckling loads occurred were 15,500 kg., 17,000 kg., and 23,000 kg. of @125, @500 and @250 respectively.

1.4 Load - displacement relationships of BC150 - 2

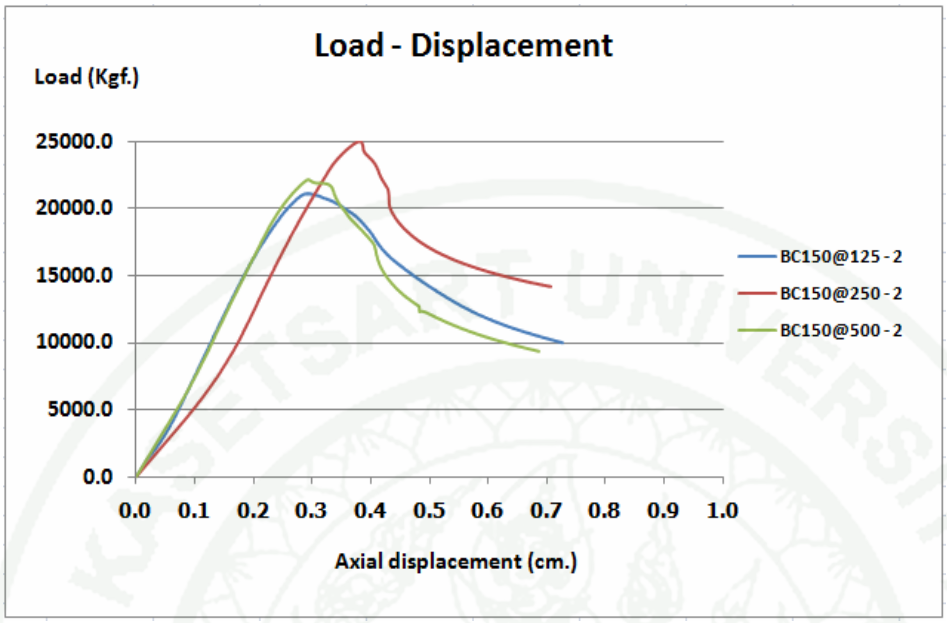

Figure 74 Load-displacement relationships of BC150–2

At the beginning, the load displacement relationship of all specimens continued almost in the same direction. After that @500, @125, and @250 began to generate local buckling behavior at 10,000 kg., 11,000 kg., and 9,000 kg. respectively.

Local buckling behavior was in shape of wave at web element of C-shaped steel on both sides, as shown in figure. And like BC100, Roof mechanism behavior also occurred during buckling behavior. The ultimate buckling loads of @125, @500 and @250 were 21,000 kg., 22,000 kg., and 25,000 kg. respectively.

Conclusion of Load - displacement relationships of BC150 – 1 and BC150 - 2

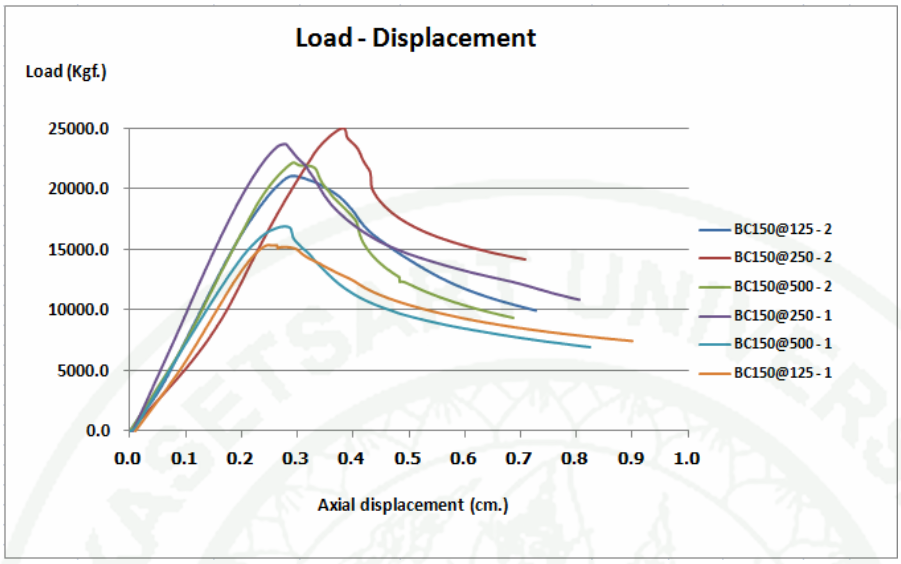

Figure 75 Load-displacement relationships of BC150 all specimen

From this figure as shown in relationships load-displacement all specimen of BC150 in first time tested group (BC150@125–1, BC150@250–1, BC150@500–1) and the second time tested group (BC150@125–2, BC150@250–2, BC150@500–2). In each group have 3 weld spacings, @125, @250, @500 respectively.

For the first time tested group, BC150@250– 1 had highest ultimate buckling load About 23,000 Kg. and followed to BC150@500–1 had ultimate buckling load about 17,000 Kg. and then BC150@125–1 had buckling load about 15,000 Kg. respectively.

For the second time tested group, BC150@250–2 had highest ultimate buckling load about 25,000 Kg. and followed to BC150@500–2 had ultimate buckling load about 22,400 Kg. and then BC150@125–2 had buckling load about 21,500 Kg. respectively.

All specimen observed resulted that in each test group could arranged the ultimated buckling load from highest buckling load as @250 and then @500 and @125 were same direction in two tested group. The specimen in each group, first time test group and second time test group were prepared welding procedure in each group per each time tested, it affected to different resulted in each group but resulted in two tested group same direction in buckling load. The second time tested group have buckling load more than first time tested group when compared in each weld spacing, it causing from preparation of specimen such as baseplate for specimen or vertical line of specimen should be perpendicular with baseplate, it need for specimen preparation procedure of tested.

1.5 Load-displacement relationships of BC200-1

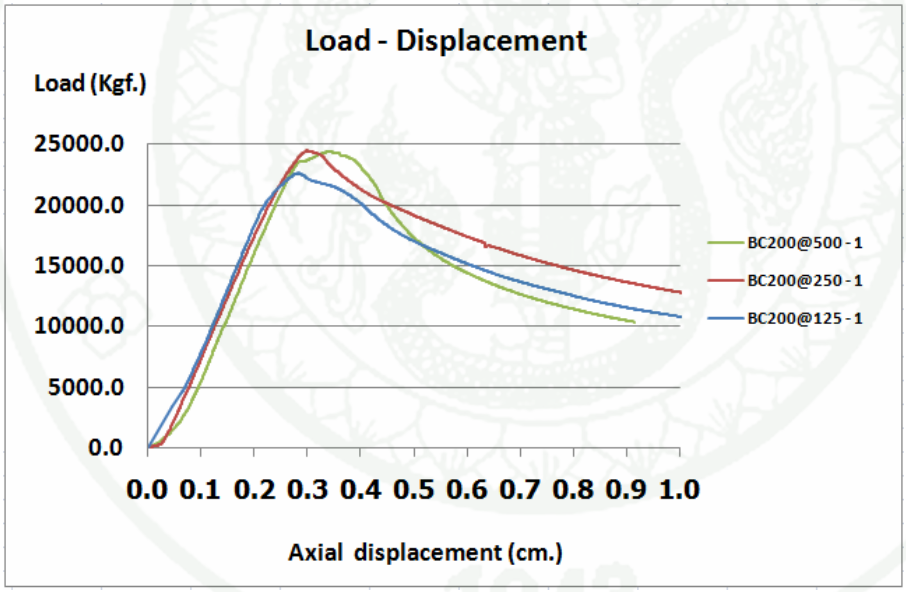

Figure 75 Load-displacement relationships of BC200–1

For BC200, load displacement continued almost in the same direction on every section. @500 first began to generate local buckling behavior at 7,000 kg., followed by @125 at 9,500 kg. and @250 at 13,000 kg. Roof mechanism, like BC100, BC150 and BC200 occurred during buckling behavior at the middle length of all four sides of the column.

The ultimate buckling loads of @125, @500 and @250 were 22,500 kg., 23,000 kg., and 24,463 kg. respectively.

1.6 Load-displacement relationships of BC200-2

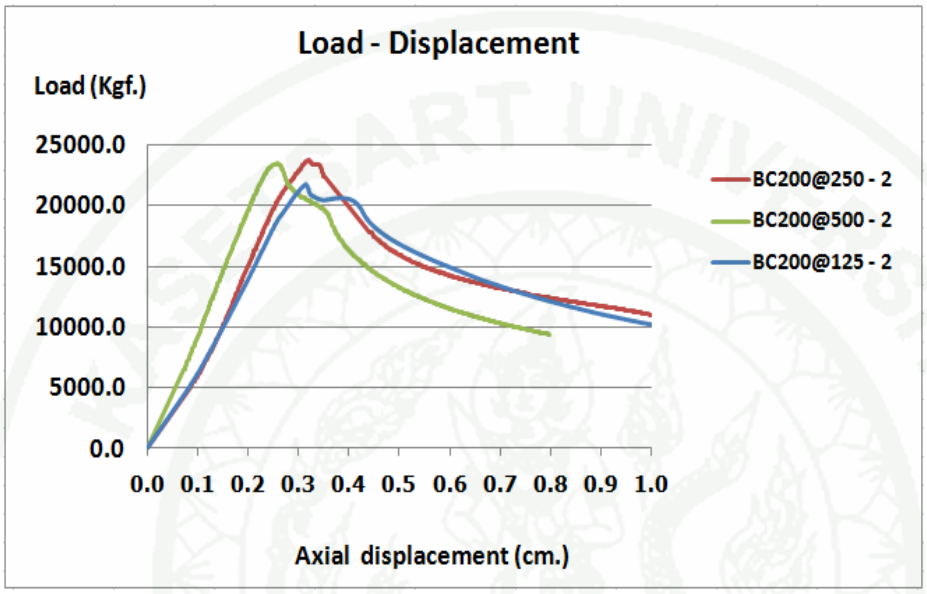

Figure 76 Load-displacement relationships of BC200-2

For BC200, load displacement continued almost in the same direction on every section. @500 first began to generate local buckling behavior at 5,000 kg., followed by @250 at 7,500 kg. and @125 at 8,000 kg. Roof mechanism, like BC100, BC150 and BC200 occurred during buckling behavior at the middle length of all four sides of the column.

The ultimate buckling loads of @125, @500 and @250 were 21,500 kg., 23,000 kg., and 23,500 kg. respectively.

Conclusion of Load-displacement relationships of BC200–1 and BC200-2

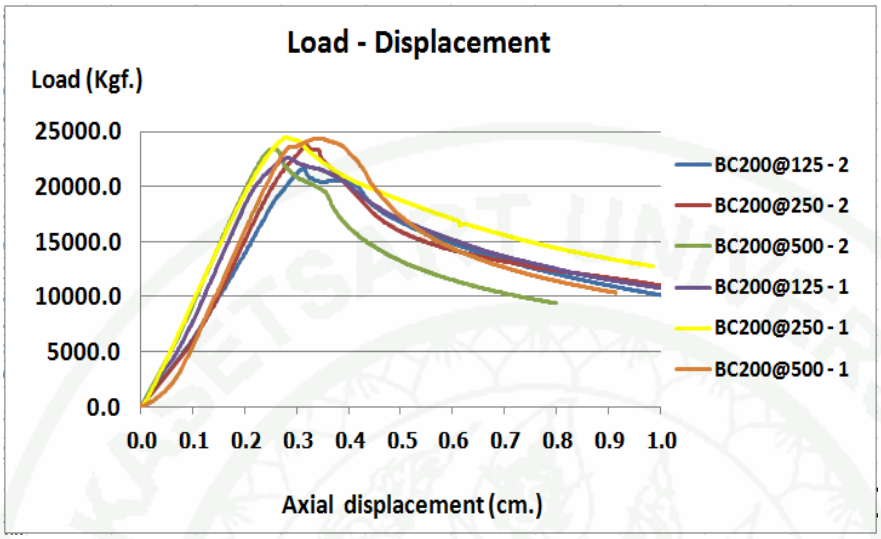

Figure 77 Load–displacement of BC200 all specimen

From this figure as shown in relationships load-displacement all specimen of BC200 in first time tested group (BC200@125–1, BC200@250–1, BC200@500–1) and the second time tested group (BC200@125–2, BC200@250–2, BC200@500–2). In each group have 3 weld spacings such as @125, @250, @500 respectively.

For the first time tested group, BC200@250–1 had highest ultimate buckling load About 24,463 Kg. and followed to BC200@500–1 had ultimate buckling load about 23,000 Kg. and then BC200@125–1 had buckling load about 22,500 Kg. respectively.

For the second time tested group, BC200@250–2 had highest ultimate buckling load about 22,700 Kg. and followed to BC200@500–2 had ultimate buckling load about 22,200 Kg. and then BC200@125–2 had buckling load about 21,400 Kg. respectively.

All specimen observed resulted that in each test group could arranged the ultimated buckling load from highest buckling load as @250 and then @500 and @125 were same direction in two tested group. The specimen in each group, first time test group and second time test group were prepared welding procedure in each group per each time tested, it affected to different resulted in each group but resulted in two tested group same direction in buckling load. The second time tested group have buckling load more than first time tested group when compared in each weld spacing, it affected from preparation procedure of specimen such as baseplate for specimen or vertical line of specimen should be perpendicular with baseplate, its need for specimen preparation procedure of tested.

Result of compression test.

Figure 78 showns the conclusion result of compression test compared with AISI code calculation of all specimens. The local buckling load and ultimate buckling load from test as shown in table and properties of the specimen as well as weld spacing, failure mode and name of specimen are shown in this table. The AISI code calculation of specimens took all design parameters in following section.

No.	Specimens	Weld spacings (cm.)	Local buckling load (Kg.) (Tested)	Ultimate buckling load (Kg.) (Tested)	Average of tested (Kg.)	AISI code Calculation
1	BC100@125 - 1	12.5	10,000	18,500	19900 (FB +FTB)	18430 (FTB)
2	BC100@125 - 2	12.5	12,000	21,300		
3	BC100@250 - 1	25	14,000	20,260	21880 (FB +FTB)	18200 (FTB)
4	BC100@250 - 2	25	15,000	23,500		
5	BC100@500 - 1	50	11,000	18,000	19000 (FB +FTB)	17210 (FTB)
6	BC100@500 - 2	50	11,200	20,000		
7	BC150@125 - 1	12.5	7,000	15,000	18250 (LB +FTB)	24620 (FTB)
8	BC150@125 - 2	12.5	10,500	21,500		
9	BC150@250 - 1	25	8,000	23,000	24000 (LB +FTB)	24580 (FTB)
10	BC150@250 - 2	25	11,500	25,000		
11	BC150@500 - 1	50	5,000	17,000	19700 (LB +FTB)	23750 (FTB)
12	BC150@500 - 2	50	10,000	22,400		
13	BC200@125 - 1	12.5	9,500	22,500	21950 (LB +FTB)	25610 (FTB)
14	BC200@125 - 2	12.5	8,000	21,400		
15	BC200@250 - 1	25	13,000	24,463	23581.5 (LB +FTB)	25330 (FTB)
16	BC200@250 - 2	25	7,500	22,700		
17	BC200@500 - 1	50	7,000	23,000	22600 (LB +FTB)	24740 (FTB)
18	BC200@500 - 2	50	5,000	22,200		

Remark : FB = Flexural buckling , FTB = Flexural - Torsional buckling , LB = Local buckling

Figure 78 Result of compression test.

Table 7 Comparison of the compression test results

No.	Specimen	w/t ratio	Local bucking load (kg.) (Mean of @125, @250, @500)	Ultimate bucking load (kg.) (Mean of @125, @250, @500)	(Strength / weight) / m.
1	BC100	68	12,730 Kg.	21,600 Kg.	4.12
2	BC150	101.3	10,670 Kg.	22,960 Kg.	3.19
3	BC200	135.3	9,830 Kg.	23,320 Kg.	2.59

From table 7, as for the local buckling load capacity, BC100 gave the highest capacity load followed by BC150 and BC200 respectively. This is a direct result of the w/t ratio of the specimen. According to thin plate theory, BC200 that has the highest w/t ratio is more likely to have local buckling occurring for the first mode at the web element of the section compared with BC100 that has the lowest w/t ratio. In terms of length of the specimen, which is currently assigned to 100 cm, results show that the difference between load capacities of the specimens is around 1,000–2,000 kg. If the length of the specimen is increased to 150 cm or 200 cm, obvious flexural buckling mode on BC100 is expected, with similar roof mechanism at the midpoint of the length of the specimen; however, the difference between the load capacities of the larger section will be larger than 1,000–2,000 kg. since longer specimen is prone to flexural buckling. In the case of BC150 and BC200, similar failure behavior is flexural – torsional buckling, as well as roof mechanism behavior at the midpoint of the length of the specimen; however, the ultimate buckling load capacity of BC200 will be higher than that of BC150 because of the larger section area.

For the strength to weight ratio based on the length of 1 m, BC100 has the largest strength to weight ratio, followed by BC150 and BC200 respectively. BC200 and BC150 that has the highest w/t ratio is more likely to have local buckling

occurring for the first mode at the web element of the section compared with BC100 that has the lowest w/t ratio. Therefore, BC100 which is the lightest section, holds the largest strength to weight ratio. However, if the length is increased to over 1 m, the strength to weight ratio of BC100 might be reduced or less than other sections. This is because BC100 has the smallest area section compared with BC150 and BC200, and it is more likely to suffer from flexural buckling.

Behavior of stress distribution

Behavior of stress distribution focused here are the behavior of stress on section at the same level of welding and the midway welding level around section and the behavior of two level to show that welding has influence on difference between compressive strength of section at the two levels.

The stress–distribution showns in figure12. is of the specimen BC150@125. This figure shows the stress distribution of pre-buckling load (3500 kg.) with the condition: 50 percent of local buckling load = pre – buckling load.

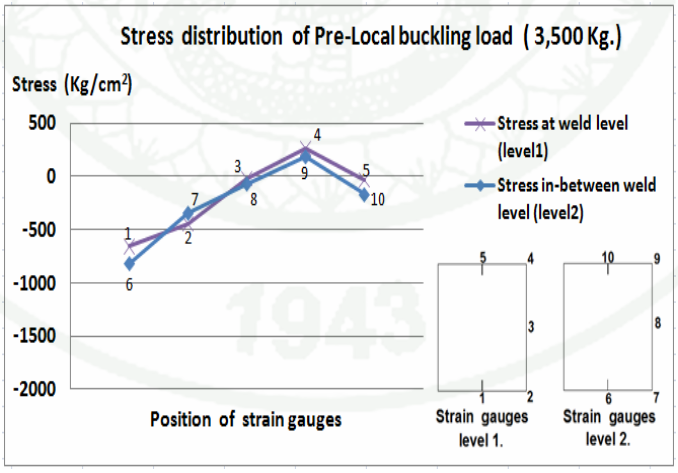

Figure 79 Stress-distribution of BC150@125 at Pre–local buckling load (3500 Kgf.)

Figure 12 shows the stress distribution in two comparative levels, which were weld level and in-between level. At weld level1 was at 50 cm. which was half of the full height (stg1-stg5). And level2 was in between the weld (stg6-stg10). The stress of both levels were nearly value. However, the stress at stg.1 was less than the one at stg.6 which was in the same position. Since there was no seam welds at stg.6 to attached the specimens, they could be more elastic. This behavior similar to, stg10 which had more stress than stg.5 had a tendency to occur more obvious behavior when the compression load to increased.

After that ,this behavior continually until go to local buckling mode as shown in figure14 shows that the stress of both levels had a tendency to develop more due to the compression at local buckling load (7000 Kgf.) shown in figure13, especially for Stg.6 and Stg.10 which were at the edge.

These two positions had more stress than the others at the same level. As for the stress at weld level (level 1), Figure14 stress all positions also had a tendency to developed more stress. But for stg.1 and stg. 5, these two positions were joined by seam welds so the behavior could not be moved. It affected to a result, the stress there developed less than stg. 6 and stg. 10 which were not attached by seam welds.

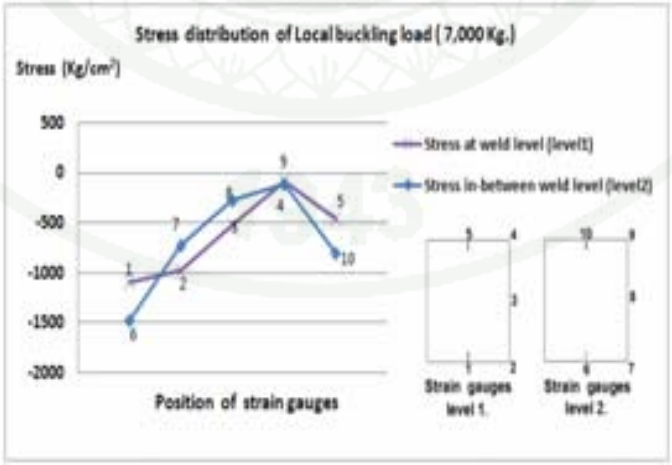

Figure 80 Stress-distribution of BC150@125 at Local buckling load (7000 Kgf.)

Local buckling behavior was in shape of sine wave which occurred at the web element of C-shaped steel on both sides. That was because the web element had large w/t ratio which led to local buckling more easily. As shown in figure.this behavior occurred linearly along the column on both sides.

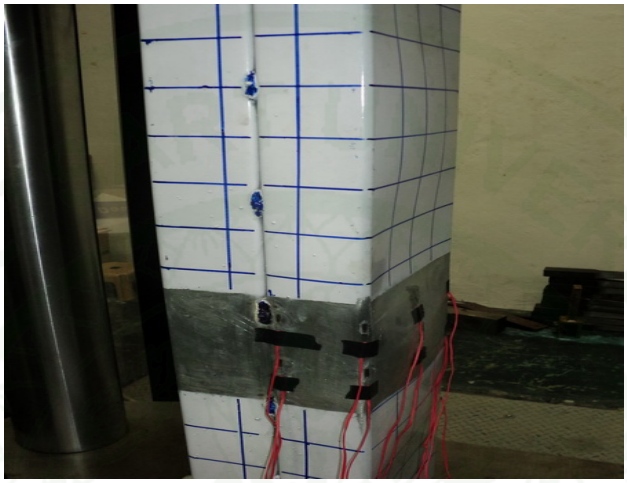

Figure 81 Local buckling behavior

After local buckling behavior occurred its continued behavior will go to ultimate buckling as Figure15. shown stress-distribution of BC150@125 for the ultimate buckling load (15,000 kgf.) at the positions 6 and 10 (level 2) was the edge portion that generated redistribution of stress, causing the highest at the positions. Then, the stress of stiffened element (stg.8) decreased, accordant with the method of post buckling behavior, with the pattern of failure behavior that was in form of Roof mechanism as shown in figure16. For the stress at weld level (level 1), that the seam weld was on lip part it similar to level 2 in stress distribution. The stress at was quite low, contrasting with the stress at stg. 1 and stg. 5 which were attached by seam welds.

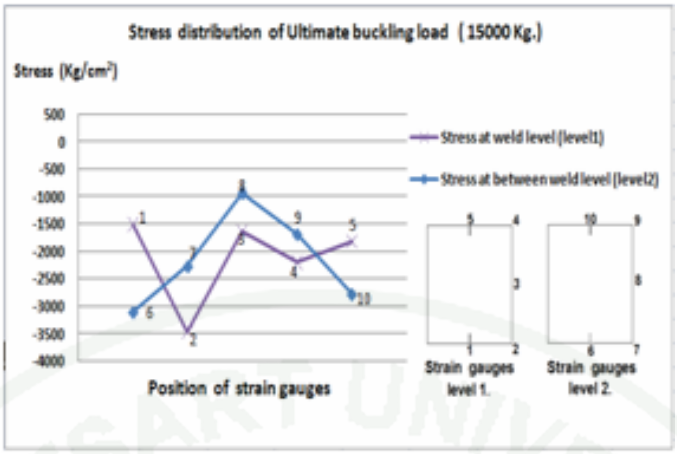

Figure 82 Stress-distribution of BC150@125 at Ultimate buckling load (15000 Kgf.)

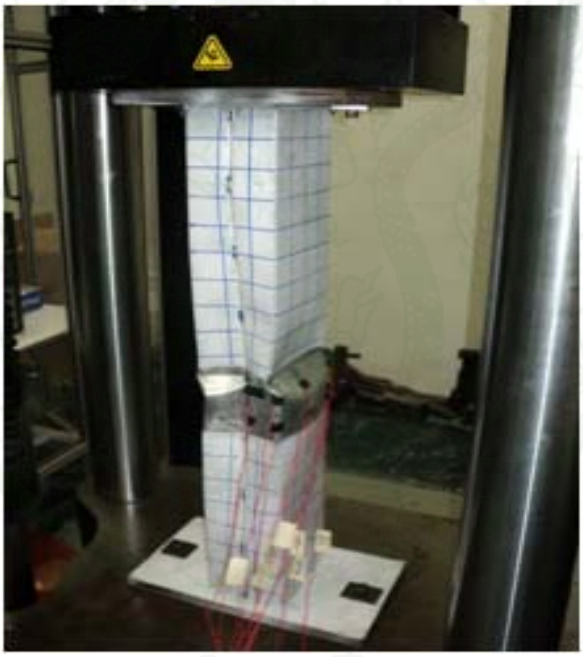

Figure 83 Inelastic buckling behavior (Shown at ultimate load)

Figure as shown ultimate Buckling behavior of the specimens was local buckling first generated in the depth of the sections. The column could continually restrain the compressive strength until occurred inelastic local buckling called Roof mechanism (Iwamoto *et al.*, 1978) was generated on all four sides of the sections. Roof mechanism behavior is generally alike in all sections followed figure.

Conclusion of stress distribution behavior

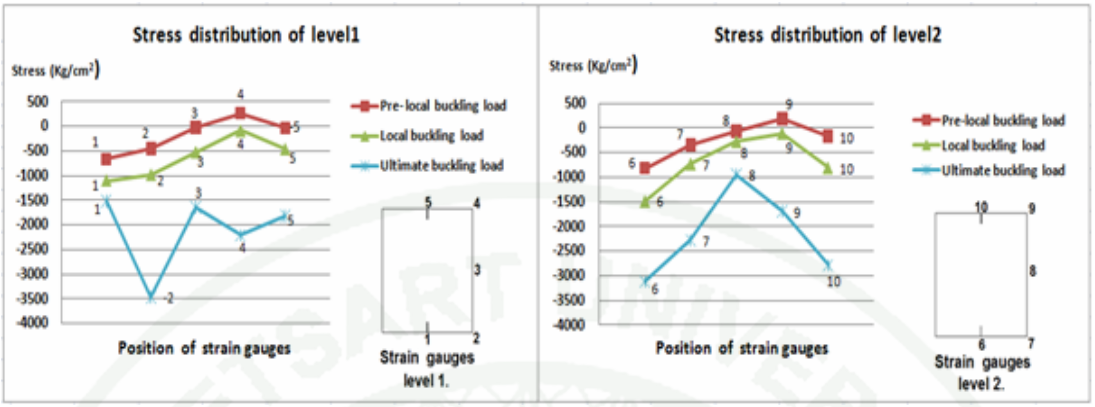

Figure 84 Compare stress distribution behavior of BC150@125 between level1 and level2 for all load

According to figure. the graph shows the relationship between stress distributions of level 1 and level 2 which are influenced by different seam welds. It is noticeable that stress distributions at pre-local buckling load and at local buckling load of both levels develop in the same direction. However, stress distributions of both levels begin to differ from each other in ultimate load behavior: the stress at positions 1 and 5 which are attached by seam welds is quite little, in contrast to the stress at positions 6 and 10 which are not attached by seam welds. That is because most of the stress here is transferred to nearby position, position 2. And the stress distribution at this position is in accordance with the experiment on the specimens attached by too many seam welds: the load capacity here is not high and failure behavior usually occurs at the corner first. For level 2 which is not attached by seam welds, the behavior of stress distribution at ultimate buckling load is post-buckling behavior, which is a normal behavior. Positions 6 and 10 which are at the corners contain rather high stress. And the stress begins to decrease at position 8 which is in the middle of element. This is quite different from stress distribution of level 1 due to the influence of seam welds.

Failure behavior

Failure behavior of all specimens was local buckling first generated in the depth of the sections. The column could continually restrain the compressive strength until inelastic local buckling called Roof mechanism was generated on all four sides of the sections. Buckling behavior is generally alike in all sections.

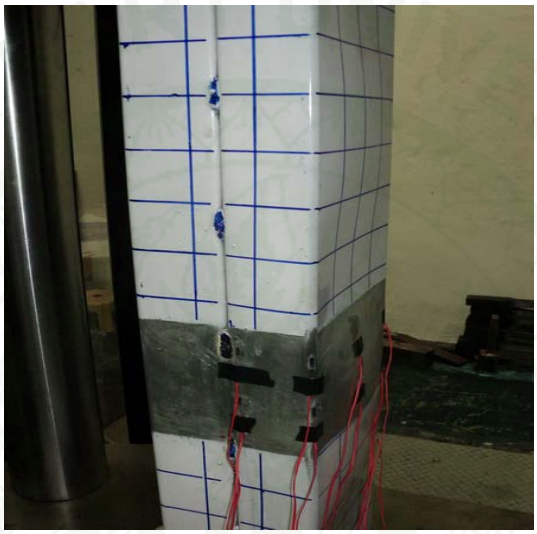

Figure 85 Local buckling behavior

Figure 86 Weld spacing behavior

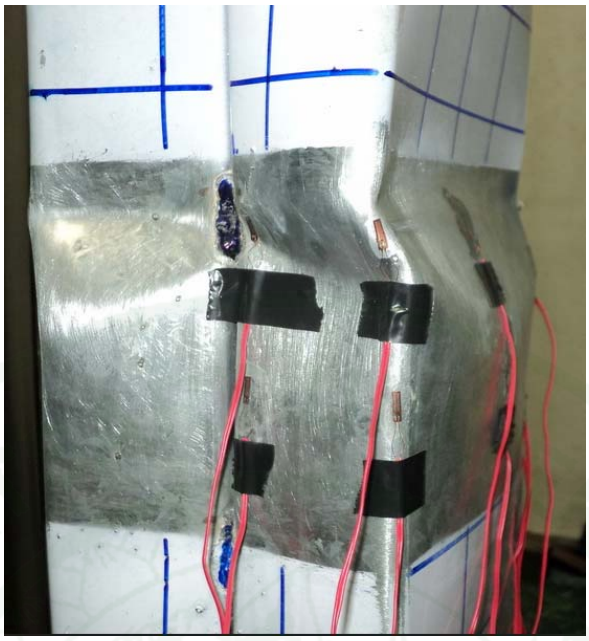

Figure 87 Roof mechanism behavior

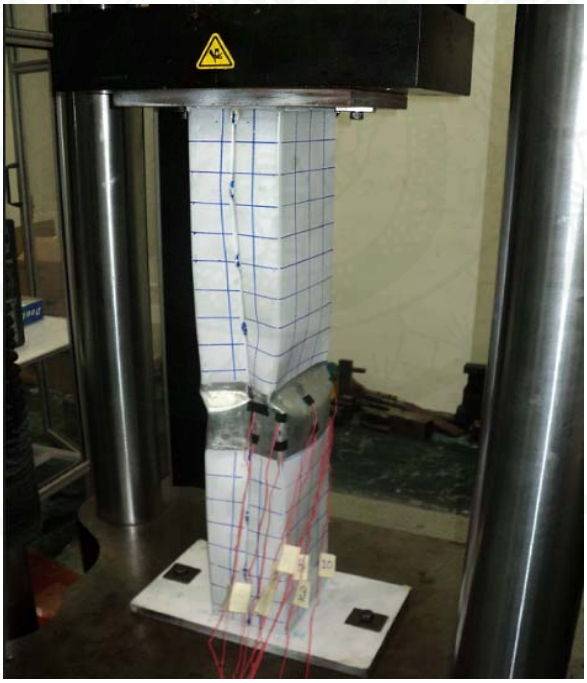

Figure 88 Inelastic buckling behavior (Roof mechanism)

Finite element Program.

This research was used the finite element analysis program ANSYS only for study behaviors of built-up specimens for expected buckling load and failure mode shape of all specimens before testing and compared behavior with testing in laboratory. Since main objectives of this research focus on testing in laboratory more than the finite element analysis.

Finite element method, a numerical method, is used here to solve differential equation. The equation can sometimes be complex, and the numerical answer will be taken to model or predict the structural behaviors of cold-formed steel. The results are presented in 3-dimensional pictures and the analytical interpretation in color shades of stress. Then the interpretation will be used in finding out critical limits, stress, and failure patterns of the structure. Being compared with the experimental result in laboratory, the result of finite element method can be verified that it is correct and suitable for practical use.

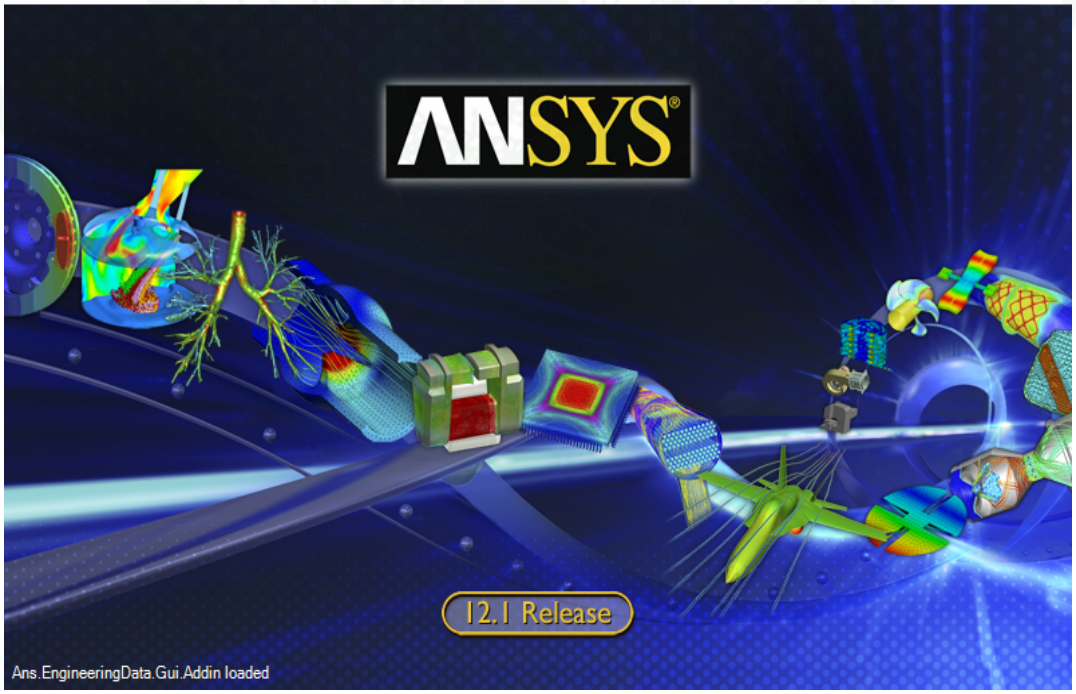

Figure 89 ANSYS version 12.1 Finite element program

Resulted of Finite element program

1. BC100@125

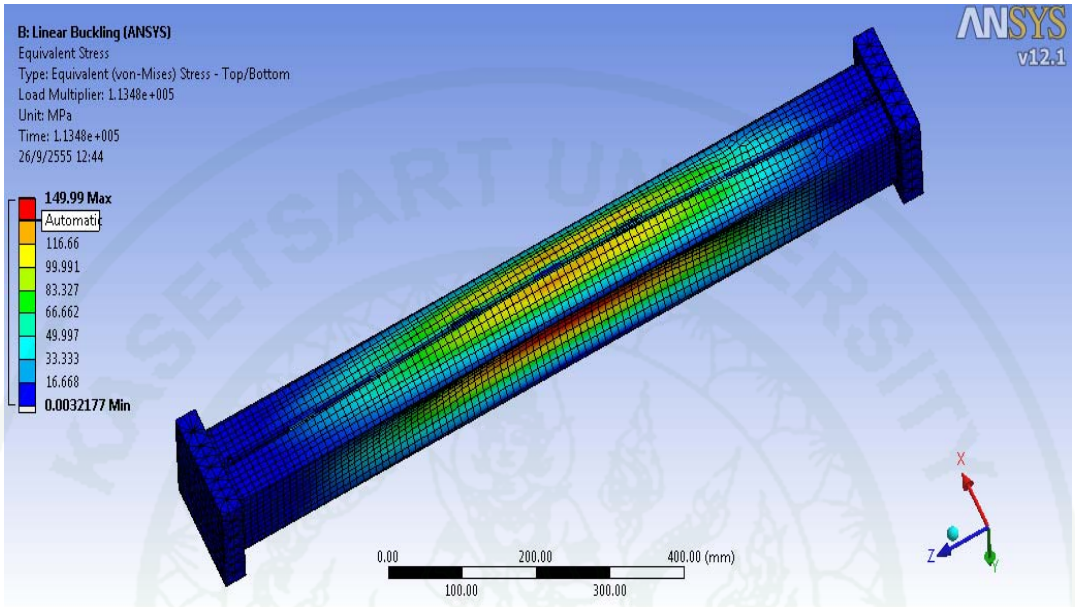

Figure 90 Mode 1 Local buckling load 11,340 Kg.

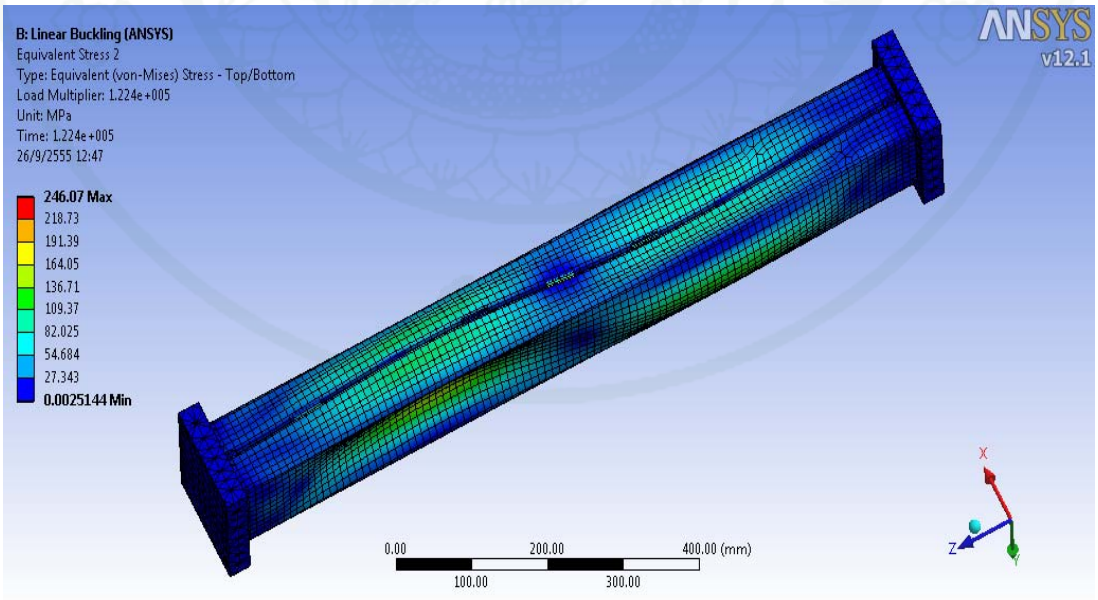

Figure 91 Mode 2 Local buckling load 12,240 Kg.

2. BC100@250

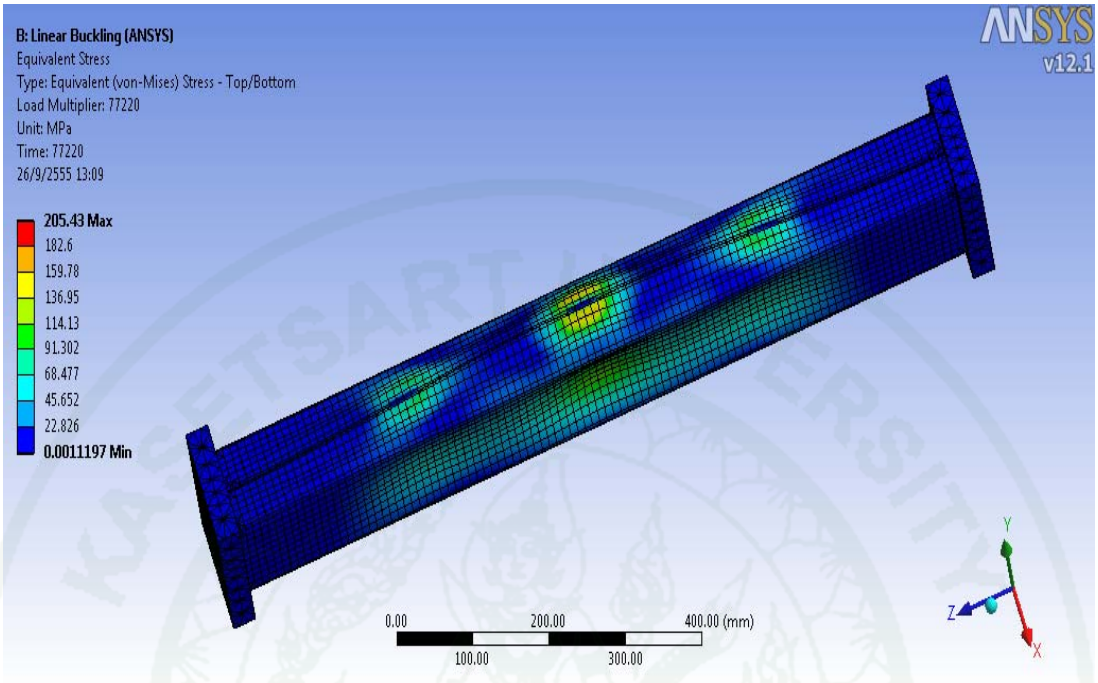

Figure 92 Mode 1 Local buckling load 7,722 Kg.

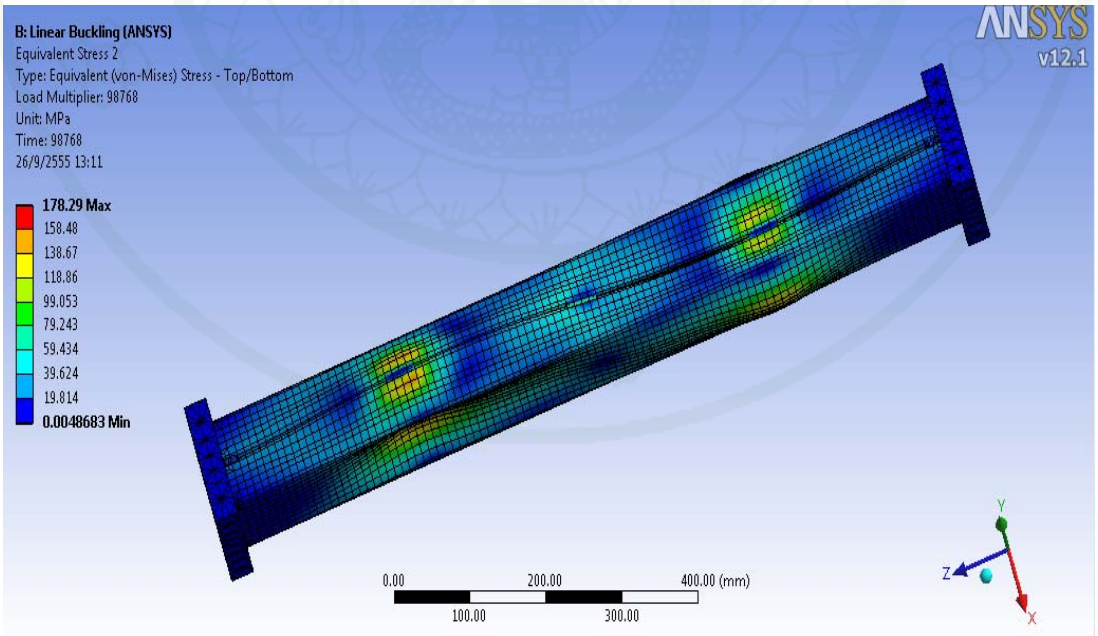

Figure 93 Mode 2 Local buckling load 9,876 Kg.

3. BC100@500

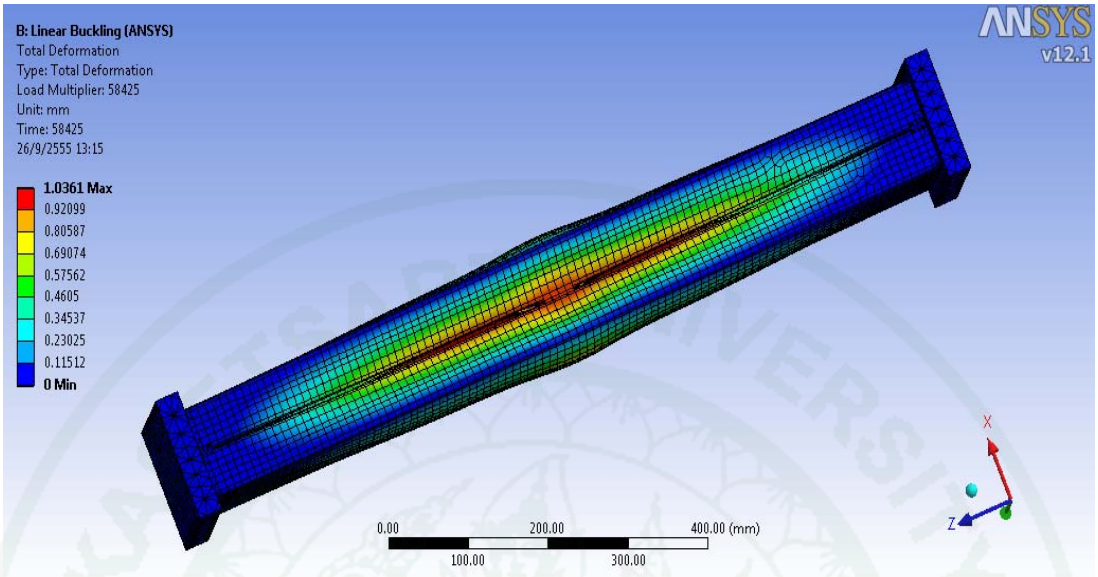

Figure 94 Mode 1 Local buckling 5,842 Kg.

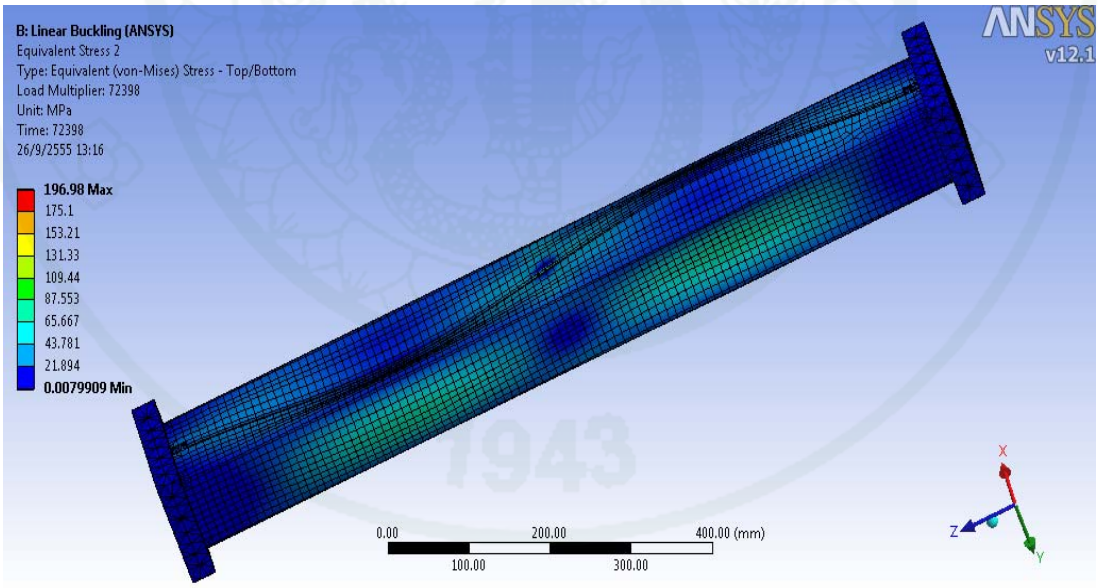

Figure 95 Mode 2 Local buckling 7,240 Kg.

4. BC150@125

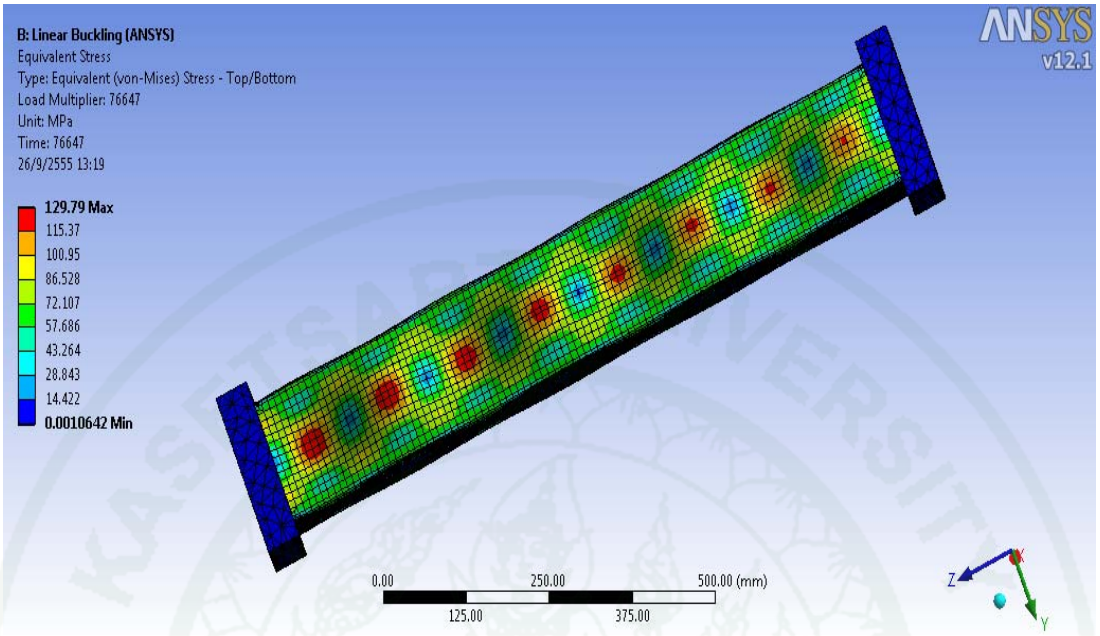

Figure 96 Mode 1 Local buckling 7,664 Kg.

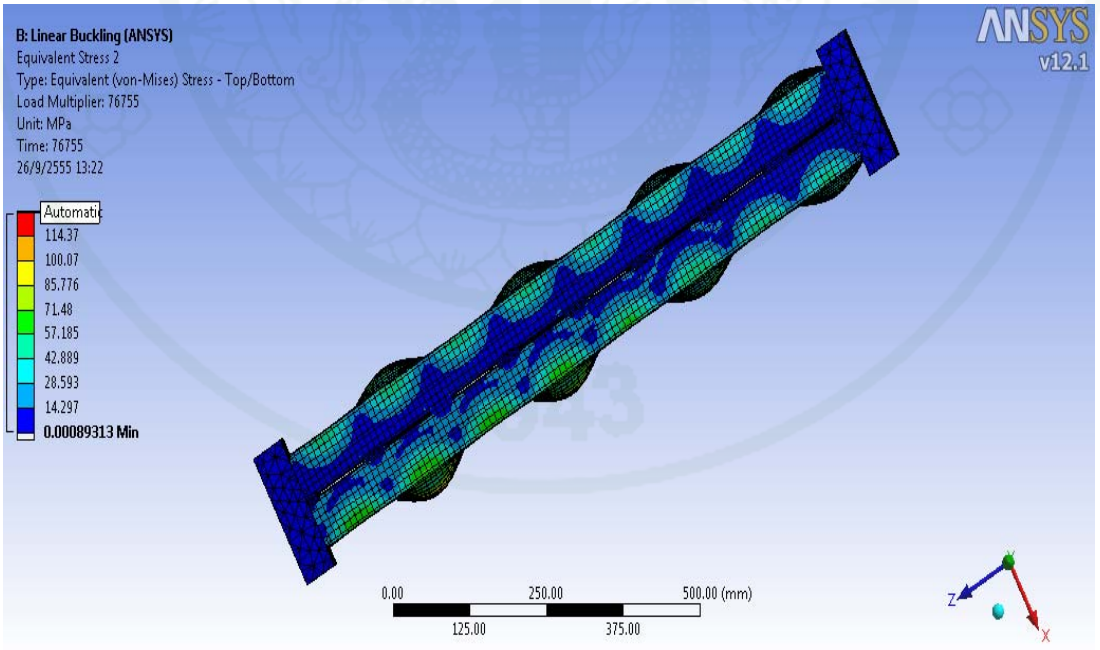

Figure 97 Mode 2 Local buckling 7,675 Kg.

5. BC150@250

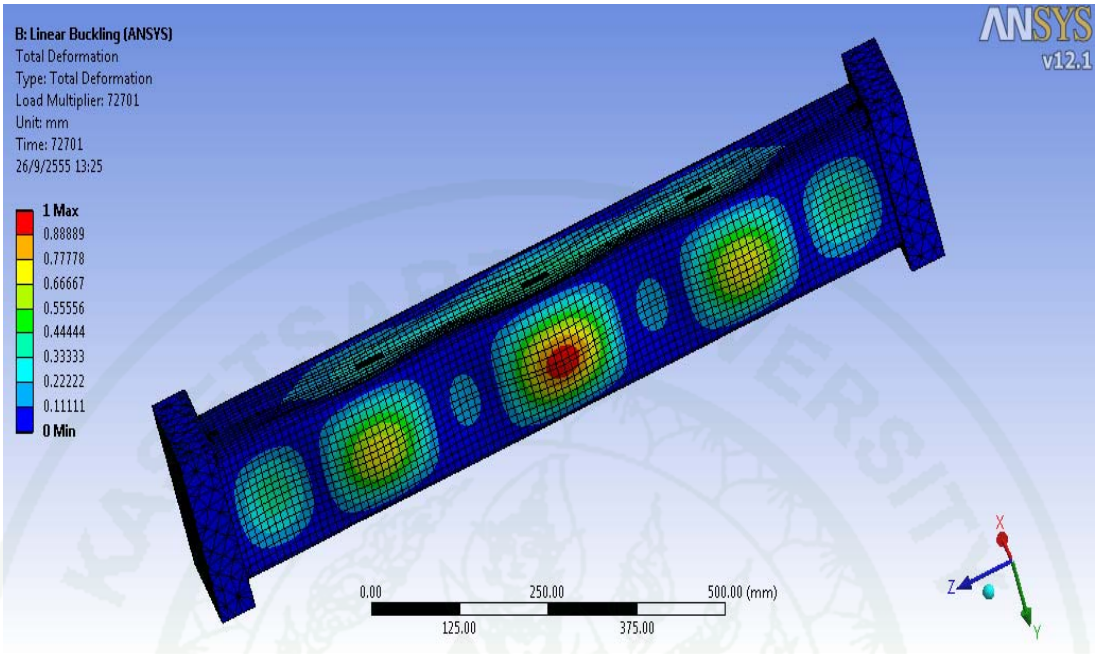

Figure 98 Mode 1 Local buckling 7,270 Kg.

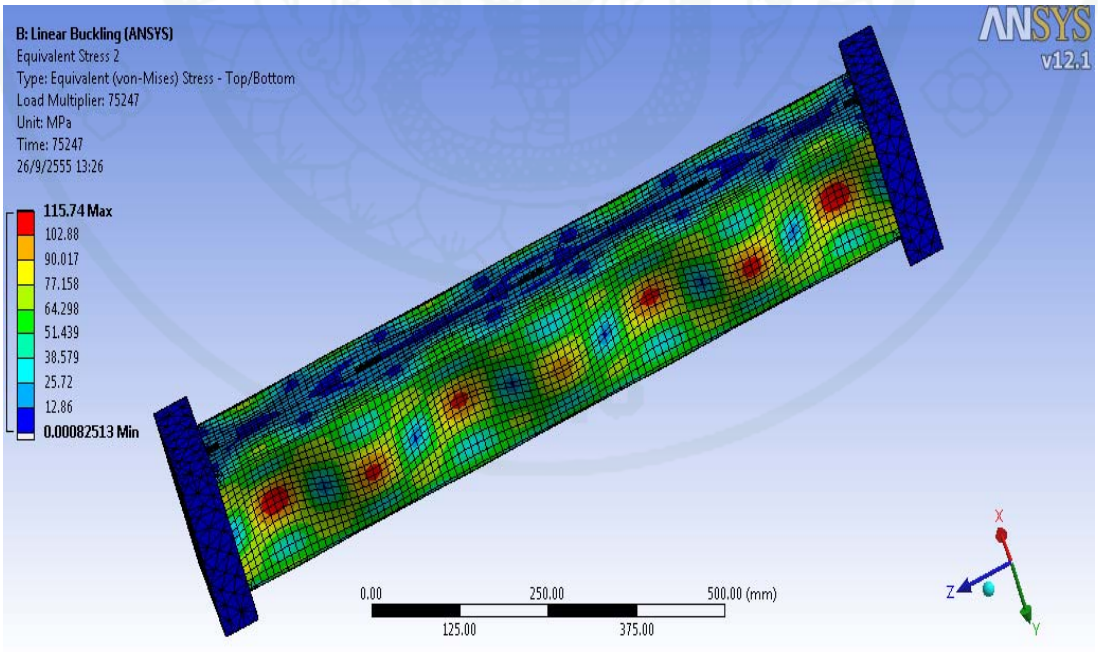

Figure 99 Mode 2 Local buckling 7,524 Kg.

6. BC150@500

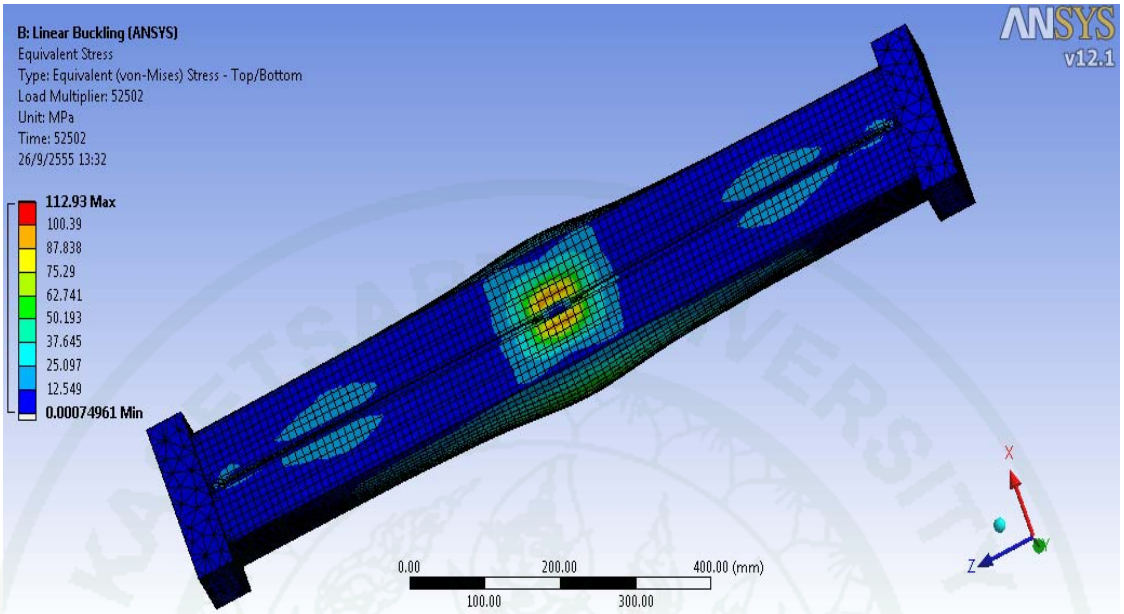

Figure 100 Mode 1 Local buckling 5,250 Kg.

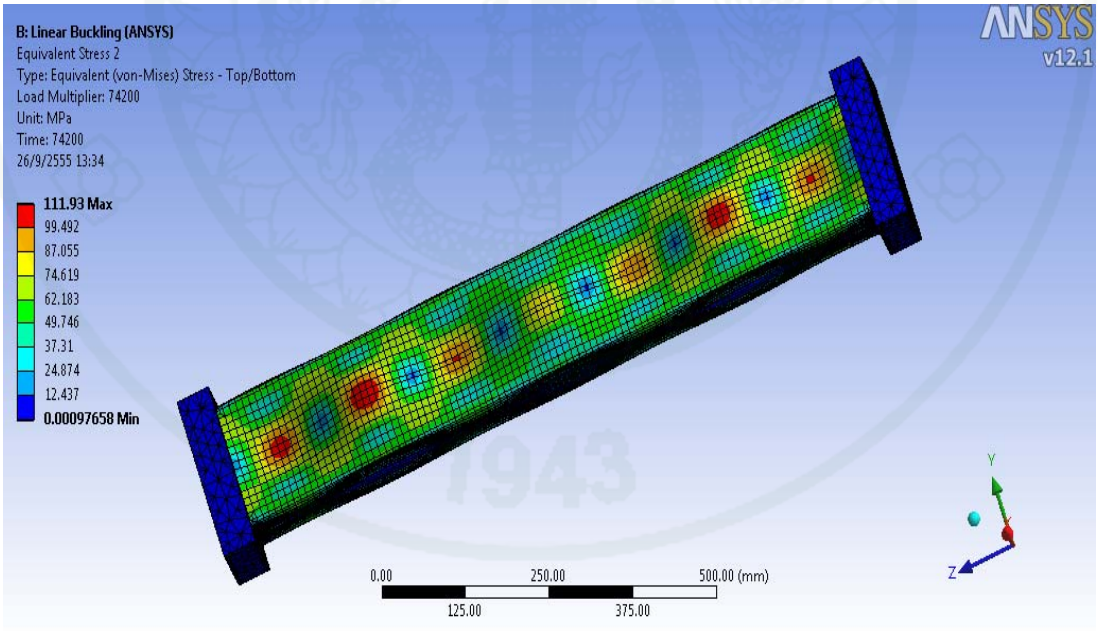

Figure 101 Mode 2 Local buckling 7,420 Kg.

7. BC200@125

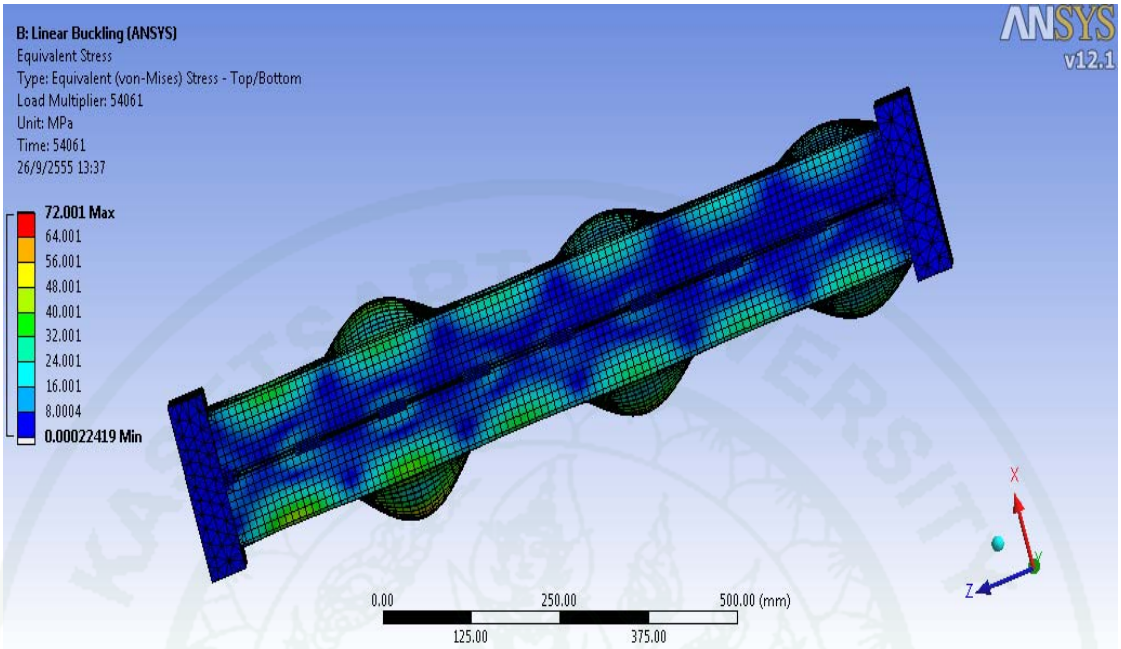

Figure 102 Mode 1 Local buckling 5,400 Kg.

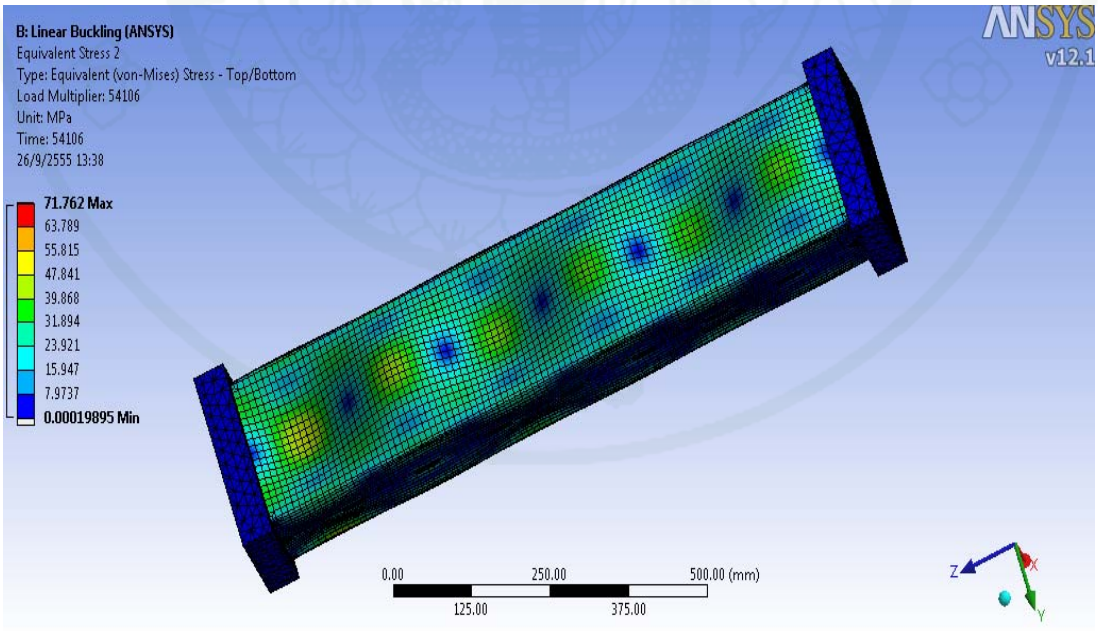

Figure 103 Mode 2 Local buckling 5,410 Kg.

8. BC200@250

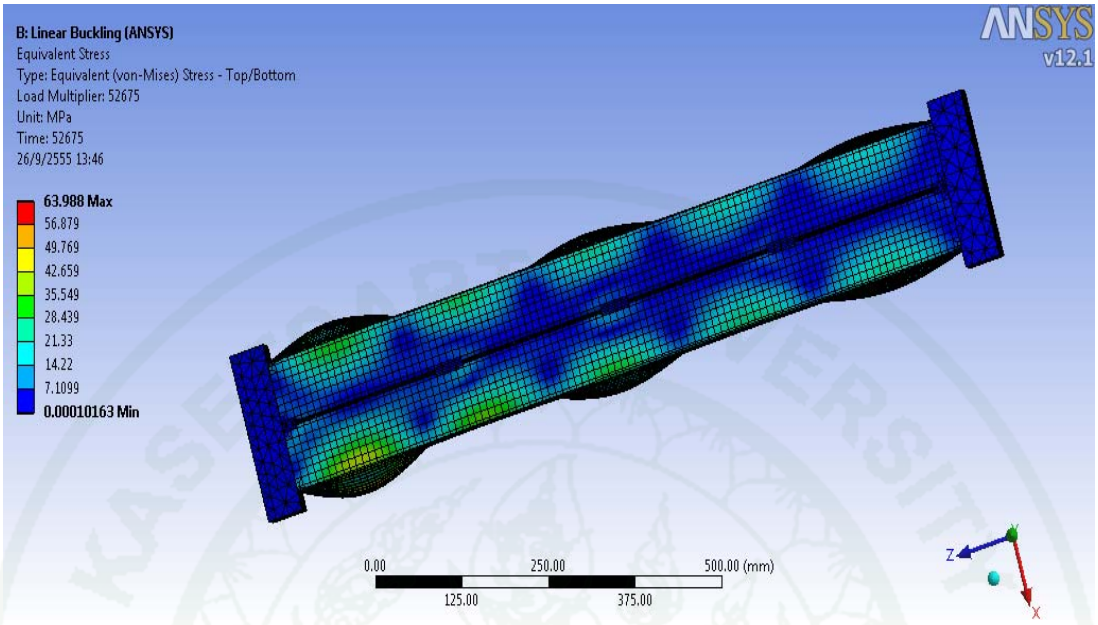

Figure 104 Mode 1 Local buckling 5,267 Kg.

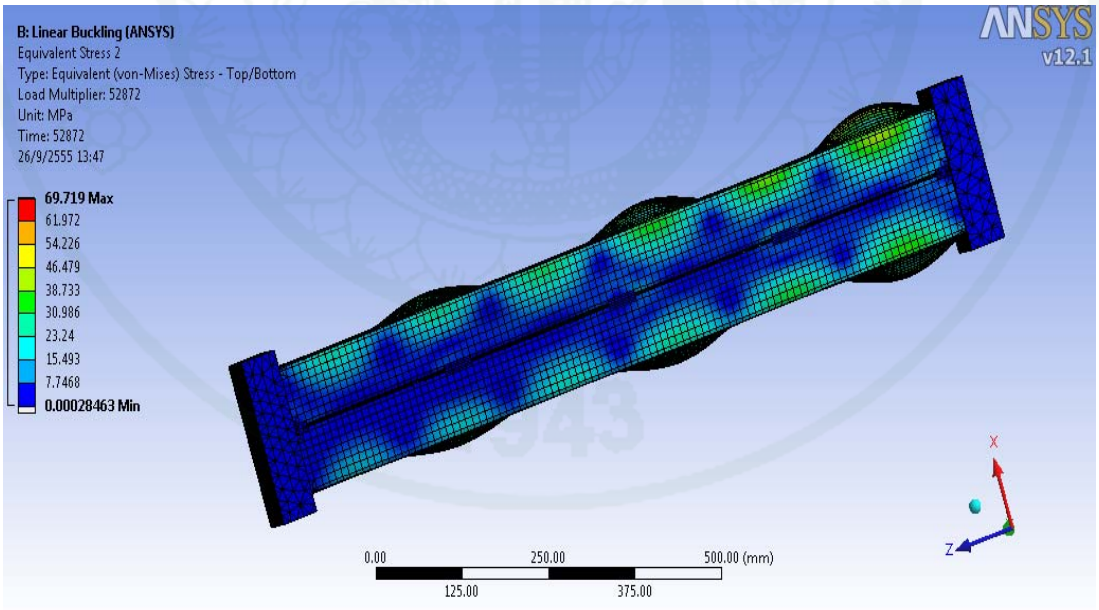

Figure 105 Mode 2 Local buckling 5,287 Kg.

9. BC200@500

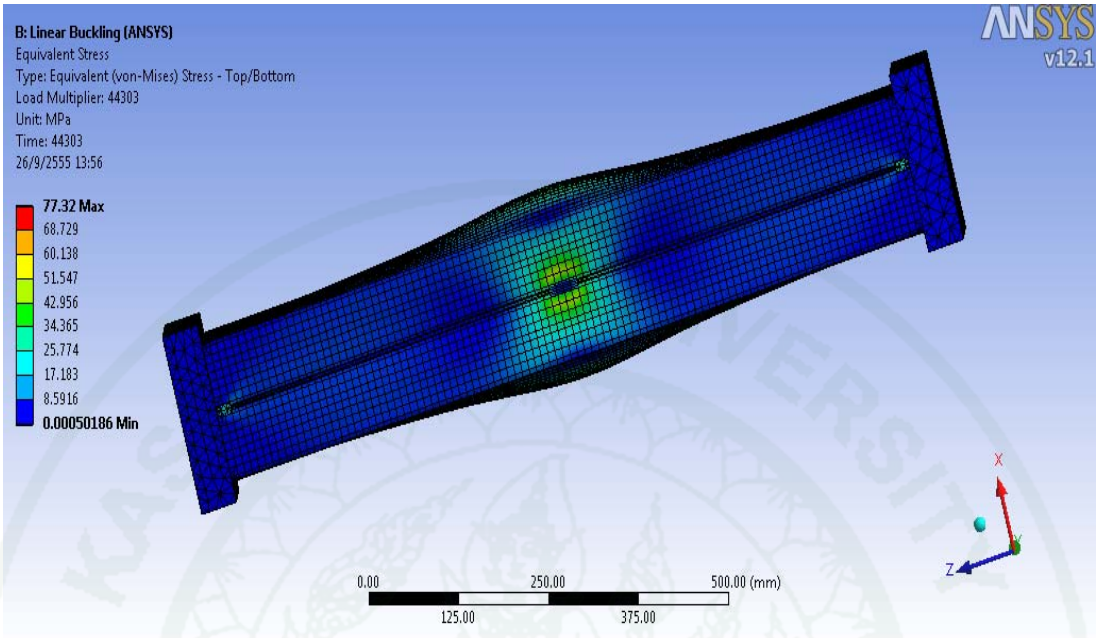

Figure 106 Mode 1 Local buckling 4,430 Kg.

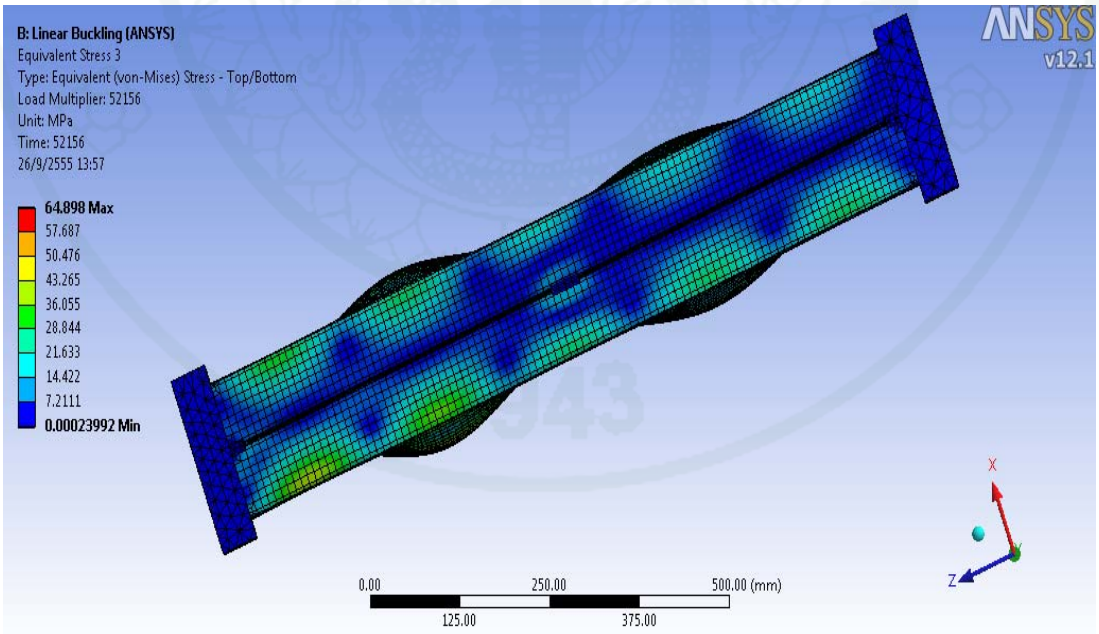

Figure 107 Mode 2 Local buckling 5,215 Kg.

Conclusion resulted of Finite element method.

Finite element method, a numerical method, is used here to solve differential equation. The equation can sometimes be complex, and the numerical answer will be taken to model or predict the structural behaviors of cold-formed steel. The results are presented in 3-dimensional pictures and the analytical interpretation in color shades of stress. Then the interpretation will be used in finding out critical limits, stress, and failure patterns of the structure. Being compared with the experimental result in laboratory, the result of finite element method can be verified that it is correct and suitable for practical use.

Table 8 Conclusion resulted of Finite element method.

No.	Specimens	Weld spacings (cm.)	Local bucking load (Kg.) Model 1	Local bucking load (Kg.) Model 2
1	BC100@125	12.5	11,340	12,240
2	BC100@250	25	7,722	9,876
3	BC100@500	50	5,842	7,240
4	BC150@125	12.5	7,664	7,675
5	BC150@250	25	7,270	7,524
6	BC150@500	50	5,250	7,420
7	BC200@125	12.5	5,400	5,410
8	BC200@250	25	5,267	5,287
9	BC200@500	50	4,430	5,215

From this figure as shown Local buckling loaded of specimen from FEM method by ANSYS program between mode1 and mode2 .For BC100 all weld spacings have highest local buckling loaded more than BC150 and BC200 because BC100 have w/t ratio less than BC150 and BC200.

For BC200 all weld spacings have lowest local buckling loaded because BC200 have w/t ratio more than BC150 and BC100 . For w/t ratio identify to local buckling mode, if highest w/t ratio it easy for occurred local buckling mode more than low w/t ratio which followed to theory of local buckling mode.

The conclusion for strength design criteria of specimens following AISI section D1.2 specification.

Figure 108 as shown the strength of specimens for BC100 all weld spacing , BC150 all weld spacing and BC200 all weld spacing can expected strength of specimen from AISI2007 Section D1.2 by using modified slenderness ratio in formular and shown calculation of compression load at appendix c.

Specimens	Weld spacings (cm.)	a/ri	(KL/r)o	0.5(KL/r)o	Satisfy AISI D1.2 condition	(KL/r)m	λc	Full Area (A)	Fn	Effective Area (Ae) at stress Fn	Pn (AISI)
	(a)				a/ri < 0.5(KL/r)o		λc < 1.5 (Inelastic buckling) λc > 1.5 (Elastic buckling)	(cm^2)	(ksc.)	(cm^2)	(Kg_f)
BC100@125	12.5	6.68	12.5	6.25	not satisfy (a/ri > 0.5(KL/r)o)	14.7	0.87 (Inelastic buckling)	6.46	3920.74	4.7	18,430
BC100@250	25	13.36	12.5	6.25	not satisfy (a/ri > 0.5(KL/r)o)	18.3	0.9 (Inelastic buckling)	6.46	3847.31	4.73	18,200
BC100@500	50	26.74	12.5	6.25	not satisfy (a/ri > 0.5(KL/r)o)	29.51	1.03 (Inelastic buckling)	6.46	3463	4.97	17,210
BC150@125	12.5	5.41	9.7	4.85	not satisfy (a/ri > 0.5(KL/r)o)	11.11	0.29 (Inelastic buckling)	8.86	5216.49	4.72	24,620
BC150@250	25	10.82	9.7	4.85	not satisfy (a/ri > 0.5(KL/r)o)	14.54	0.34 (Inelastic buckling)	8.86	5145	4.78	24,580
BC150@500	50	21.64	9.7	4.85	not satisfy (a/ri > 0.5(KL/r)o)	23.72	0.49 (Inelastic buckling)	8.86	4978.17	4.87	23,750
BC200@125	12.5	4.68	8.06	4.03	not satisfy (a/ri > 0.5(KL/r)o)	9.33	0.22 (Inelastic buckling)	11.1	5291.71	4.83	25,610
BC200@250	25	9.36	8.06	4.03	not satisfy (a/ri > 0.5(KL/r)o)	12.36	0.26 (Inelastic buckling)	11.1	5244.34	4.84	25,330
BC200@500	50	18.73	8.06	4.03	not satisfy (a/ri > 0.5(KL/r)o)	20.39	0.39 (Inelastic buckling)	11.1	5059.12	4.89	24,740

Figure 108 The conclusion result for strength design criteria following AISI section D1.2 specification.

Figure 108 as shows the conclusion result for strength design criteria following AISI section D1.2 specification.

All specimens do not satisfy condition of AISI section D1.2, because to satisfy condition is $a/ri < 0.5(KL/r)o$, but all specimens are short (100 cm.) when comparing weld spacing (a). This length of specimens should be used to weld spacing at 8-10 cm. to satisfy AISI condition.

The modified slenderness ratio (KL/r)m have highest value at big weld spacing @500 of all groups. The (KL/r)m increased differently with (KL/r)o when weld spacing is increased and has effect to reduce stress (Fn) of specimens.

λc is identified value to inelastic buckling ($\lambda c < 1.5$) and elastic buckling ($\lambda c > 1.5$) . All specimens are inelastic buckling and weld spacing @500 has λc highest following value in Figure 108 .

Ae is effective area at stress Fn of built-up section and (a) is weld spacings. Ae and (a) have relationship if a is wider and effects to Ae at stress Fn, which is bigger as in calculation formula of Ae at stress Fn as seen in calculation sheet at appendix c.

CONCLUSION

Conclusions of research

From the resulted of research, it can be seen that the load capacity of the specimens is directly affected by weld spacing. Results from the laboratory, Code AISI calculation, and finite element analysis all lead to the same conclusion, as followings:

1. The experimental results for built-up section depends on weld spacings. According to the experimental result, the longer the weld spacings are the lower the load capacity is. However, after more specimens are added into the test, if the weld spacings are shorter than L/4 (L: Length of specimen = 100 cm.), the load capacity becomes lower too. It can be concluded by this experiment that weld spacing of 25 cm (@250) result in the highest loading capacity of all sizes of sections. It is reasonably believed that longer weld spacings result in lower loading capacity. However, relatively too short weld spacings also result in the same way as the weld spacing which are longer than 25 cm. That is because when the specimens made of the thin cold-formed steel plate were joined with too many seam welds, more the residual stress was generated . Consequently, the loading capacity was quite low. On the other hand, when the specimens which were joined with longer weld spacings were compressed, the weld spacings became widened, resulting in lower loading capacity compared to shorter welds spacings. As for stress distribution, the focus was at the locations joined by seam welds. The plate near the seam weld only moved slightly since, the stress at that position was transferred to seam weld. Consequently, the stress there was quite lower than other positions.

2. In term of cost, since the cost of built-up section concludes welding expense, it becomes higher than box-shaped section with similar size and thickness. However, the costs of built-up section members depend on weld spacing, size and thickness of steel, as well as overall work.

3. As for AISI 2007 section D1.2, (similarly for The Engineering Institute of Thailand (EIT), 2010) the use of modified slenderness ratio (KL/r)m also depends on the condition of AISI 2007 section D1.2. The experimental resulted indicates that the equation of AISI 2007 section D1.2 can applied to all kinds of built-up section. Because of the resulted from compression tested with AISI 2007 section D1.2 are similarly. Thus, there should be further research to reach the better conclusion.

4. For the finite element analysis, the behavior and the load capacities obtained from the finite analysis results can be comparable to the experimental test results. The local buckling loads could be predicted from the finite element analysis.

Recommendations for research

This study covers almost all of the topics regarding the built up column, provided that it gives extensive details and experiments; however, there is still room for improvement as listed below**.**

1. To improve the accuracy of the experiment, the specimens must be carefully welded to the base plates, i.e. perpendicular to both the top plate and the bottom plate. In addition, the base plates should have the thickness of no less than 25 mm, since thin plate will give rise to inaccurate results.

2. Prior to the test, each strain gauge installed for measuring the stress of the specimen should be examined whether it has the correct gauge number and the proper capacity, and that it is placed in the correct position.

3. For further study of this work, the specimens used in the experiment should be longer than 100 cm for comparison purpose.

4. Residual stress should also be considered in future research concerning cold formed steel built up column, since the residual stress from welding and manufacturing process is the major factor affecting buckling load of the specimens.

LITERATURE CITED

American Welding Society. 2008. **AWS D1.3 Structural Welding Code-Sheet Steel.** American Welding Society, Florida.

AS/NZS 4600 Australian/New Zealand Standard (AS/NZS). 2007. **Cold-formed steel structures, 4 th edition.** Australian steel institute, Sydney**.**

AISI standard. 2007. **North American specification for the design of cold-formed steel structural members 2007 edition.** AISI institute, Washington D.C**.**

Bleich, F. 1952. **"Buckling Strength of Metal Structures".** McGraw–Hill, New York .

Cook, R., D. Malkus, M. Plesha M and J. Witi . 2003. **"Concept and Applications of Finite Element Analysis" Fourth Edition**. John Wiley and Sons, Inc., Maadison.

Ghoraba, M. 1997. "Design of cold-formed steel built-up post member" **Journal of Constructional Steel Research** 45(4): 1003–1012.

Gregory, J., T. Hancock, M. Murray and D.S. Ellifritt. 2001. **Cold-Formed Steel Structures to the AISI Specification**. Marcel Dekker, New York.

Guo, Y., A. Zhu, Y. Pi and F. Tin-Loi . 2007. "Experimental study on compressive strengths of thick-walled cold-formed sections" **Journal of Constructional Steel Research** 63 (8): 718–723.

Kwona, Y., N. Kimb and G.J. Hancock. 2007. "Compression tests of welded section columns undergoing buckling interaction" **Journal of Constructional Steel Research** 63 (2):1590–1602.

Kwona, Y., N. Kimb and G.J. Hancock. 2009. "Compression tests of high strength cold-formed steel channels with buckling interaction." **Journal of Constructional Steel Research** 65 (9): 278–289.

Iwamoto, I., Y. Kimura and T. Ogawa. 1978. "Tests of Cold-Formed Lipped C-Section Members Subject to Compresssion". **Journal of Structural Engineering** 107(3): 930-941.

Liu, J., D. Lue and C. Lin. 2009. "Investigation on slenderness ratios of built-compression members" **Journal of Constructional Steel Research** 65(2): 237–248.

Lue, D., T. Yen and J. Ling. 2006. "Experimental investigation on built-up columns" **Journal of Constructional Steel Research** 62(8): 1325–1332.

Logan, D. 1976. "**A First Course in the Finite Element Method" Third Edition.** Wisconsin, Platteville**.**

Reyes, W. and A.Guzman.2011. " Evaluation of the slenderness ratio in built-up cold-formed box sections". **Journal of Construction Steel Research** 67(2011): 929-935.

Schafer, B.W. and S. Adany. 2006. "Buckling analysis of cold-formed steel members using CUFSM : conventional and constrained finite strip methods" **18th International Specialty Conference on Cold-Formed Steel Structures** 14(5): 107-119.

Stone, T.A. and R.A. LaBoube. 2005 "Behavior of cold-formed steel built-up I-sections" **Thin-Walled Structures** 43(4): 1805–1817.

The Engineering Institute of Thailand (EIT). 2010. **Design standarad of cold-formed steel building 1st edition**. Global graphic Co., Ltd., Bangkok.

Timoshenko, S.P. and J.M. Gere. 1961. **Theory of Elastic Stability**. McGraw-Hill Book Company, New York.

Weng, C.C. and T. Pekoz. 1990. "Compression tests of cold-formed steel columns." **Journal of Structural Engineering** 116(8): 1230-1246.

Whittle, J. and C. Ramseyer. 2009. "Buckling capacities of axially loaded, cold-formed, built-up C-channels.**" Thin-Walled Structures** 47(10): 190-201.

Young, B. 2004. "Design of channel columns with inclined edge stiffeners". **Journal of Constructional Steel Research** 60(2): 97-183.

_____. 2008. "Research on cold-formed steel columns" **Thin-Walled Structures** 46(4): 731–740

_____, M. ASCE, and J. Chen. 2008. "Design of Cold-Formed Steel Built-Up Closed Sections with Intermediate Stiffeners" **Journal of Structural Engineering © ASCE** 45(3): 727-737.

Yu, Wei-Wen. 1924a. **Cold-formed Steel Design, 4 th Ed**., Wiley, New York.

_____. 1924b**. Cold-formed Steel Design, 3 rd Ed**., Wiley, New York.

APPENDICES

Appendix A

Step of using ANSYS program

Step 1. Geometry model

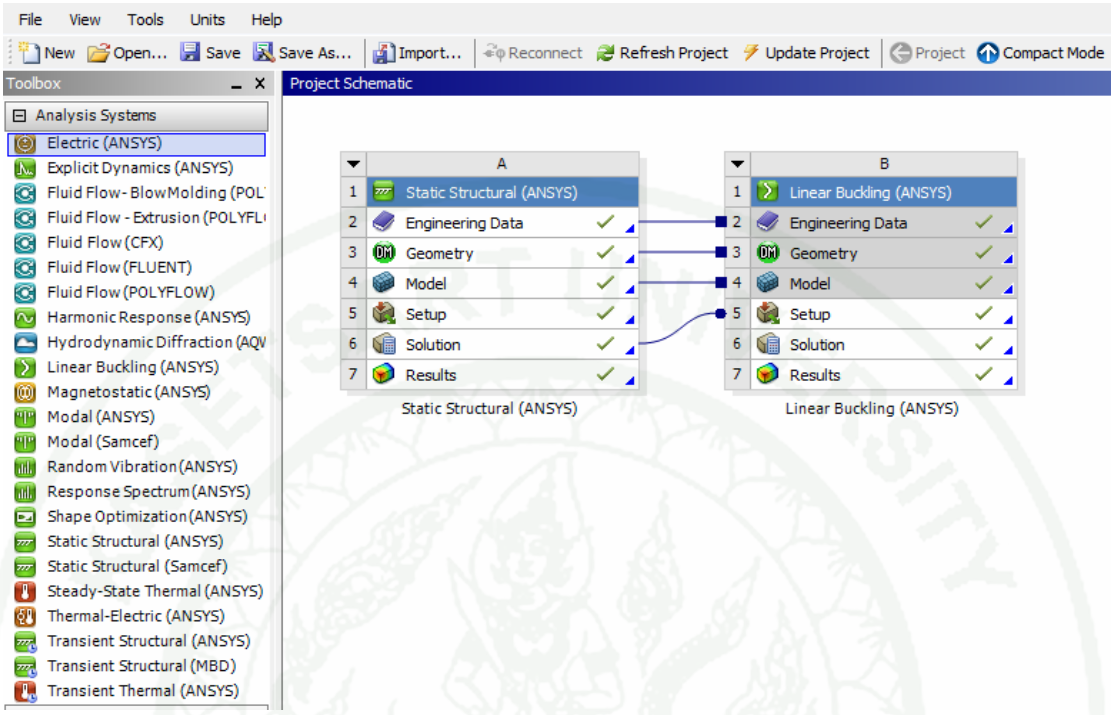

- From open ANSYS program, click choose Static Structural (Ansys) from the left tab menu.

- Click choose Geometry for built up model.

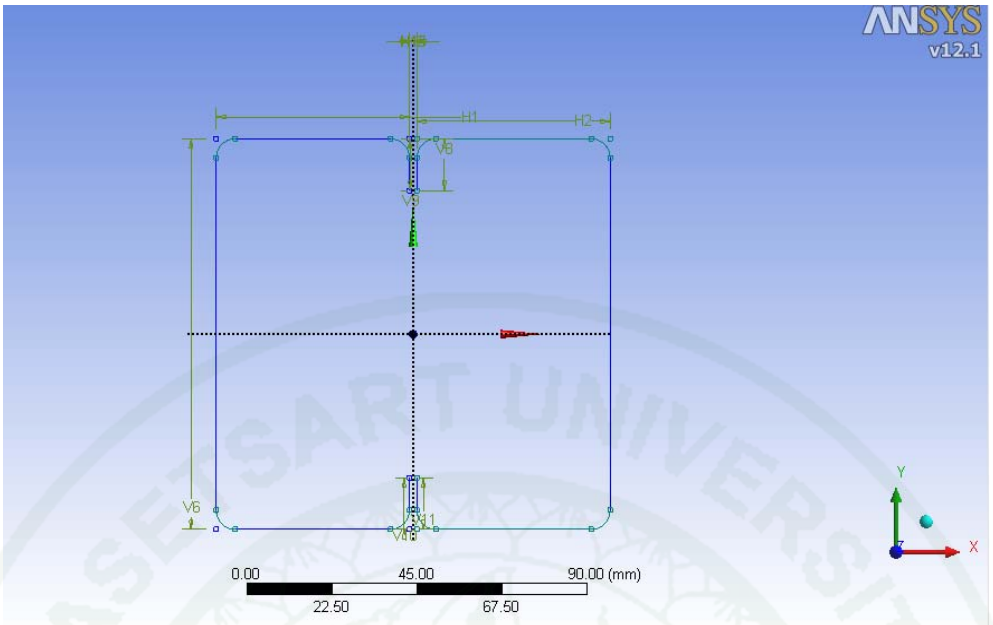

- Choose sketching tab for built up column geometry model.

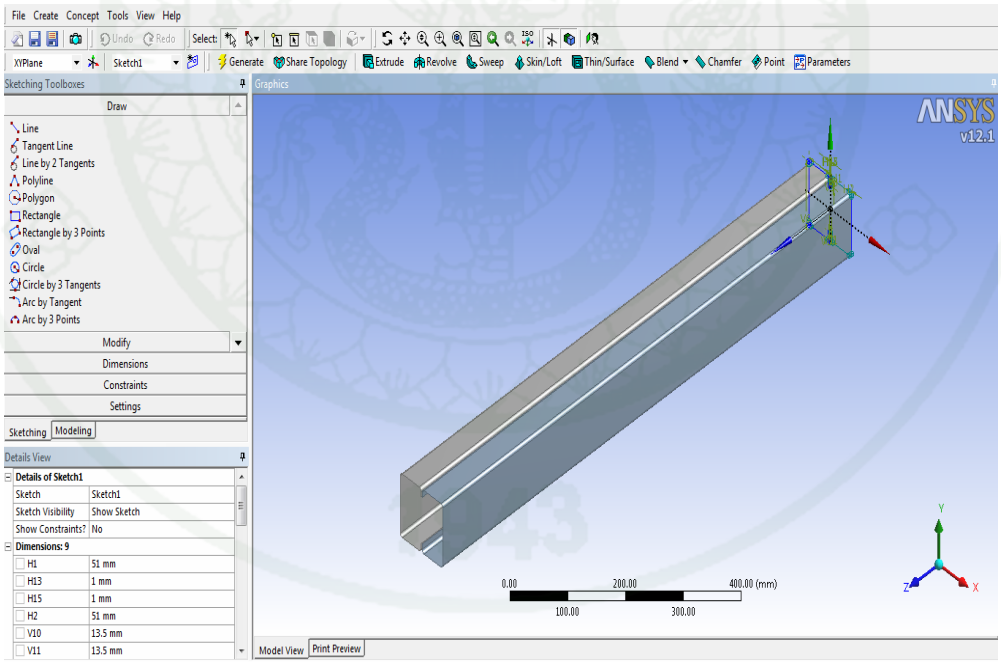

- Choose extrude menu (length 1000 mm.) to shell element of specimen.

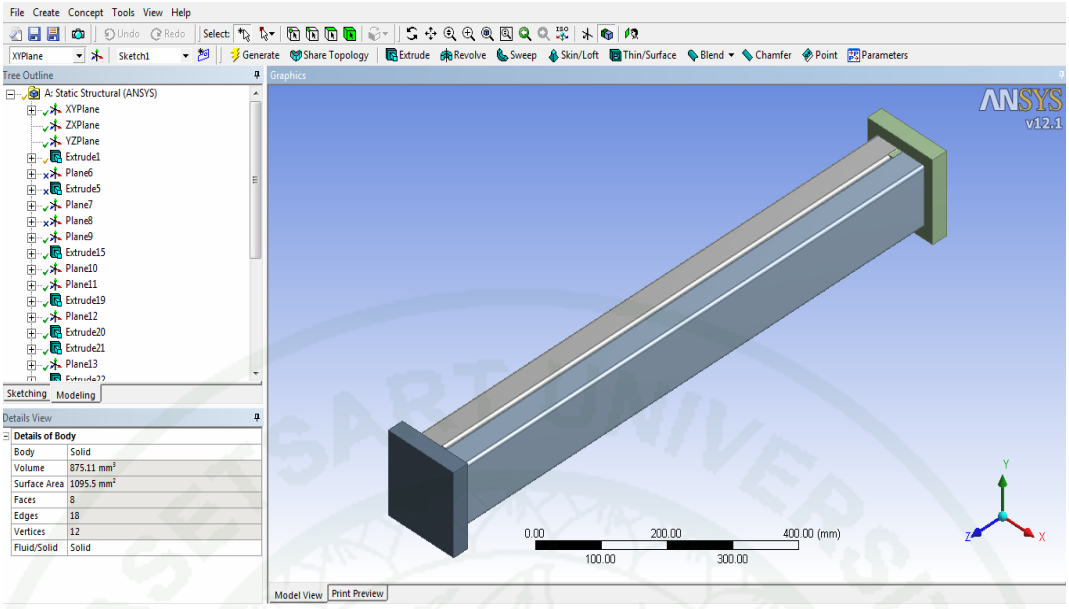

- Choose sketching tab for drawing baseplate and then extrude its (length 30 mm.) for thickness in both supports.

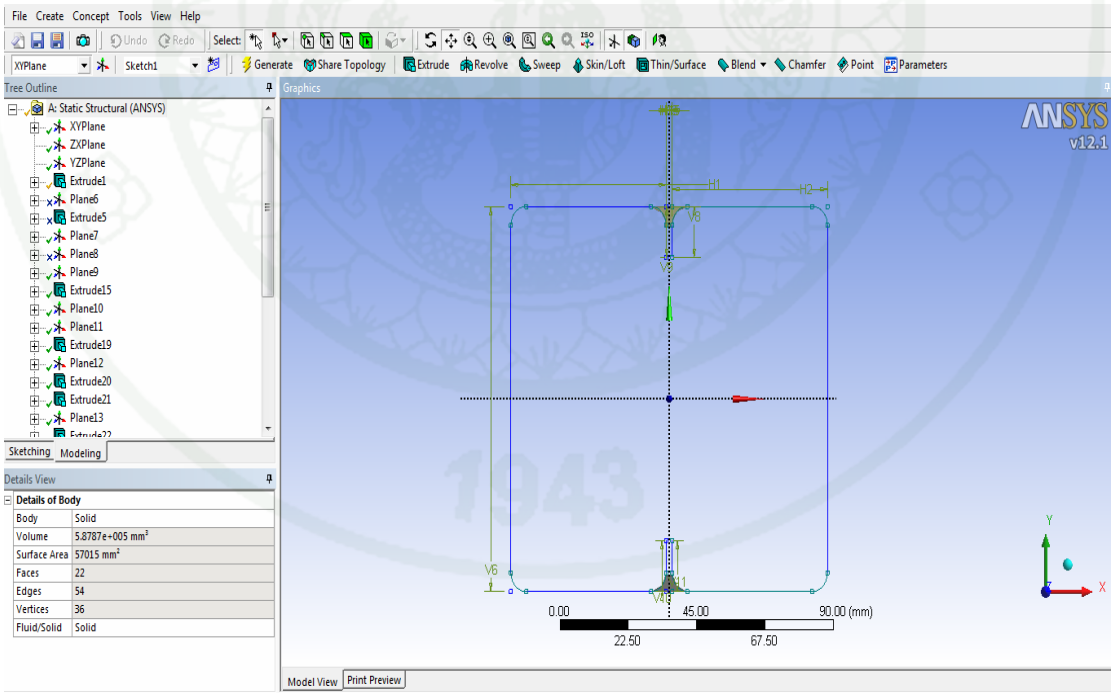

- Choose sketching tab for drawing welding section and then extrude its (length 20 mm.) for welding lengths.

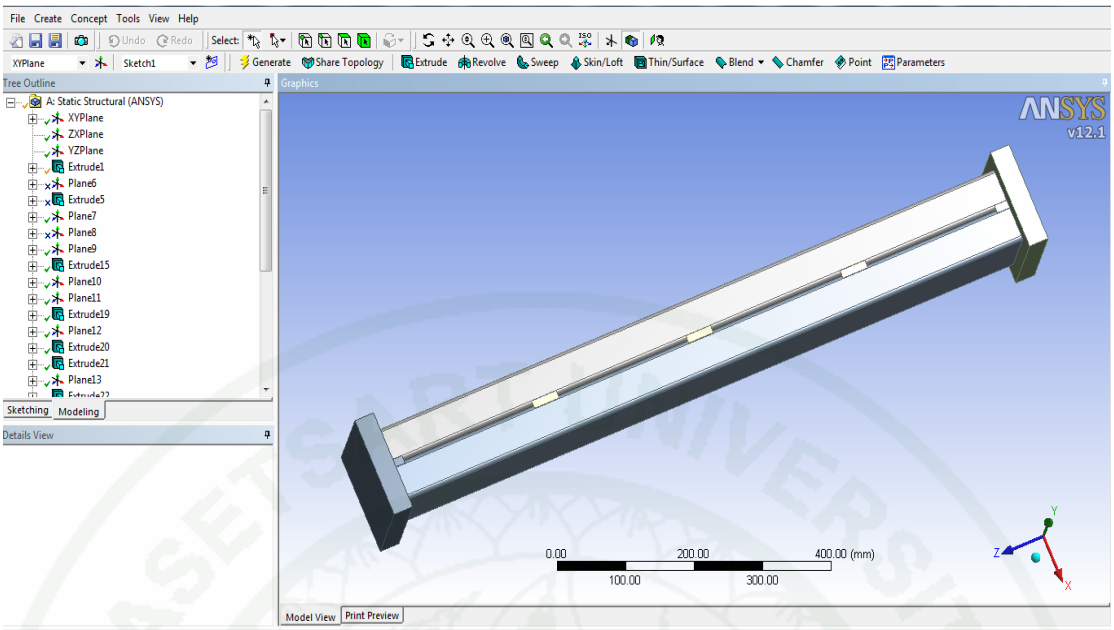

- Extrude welding point until complete all position and generate its.

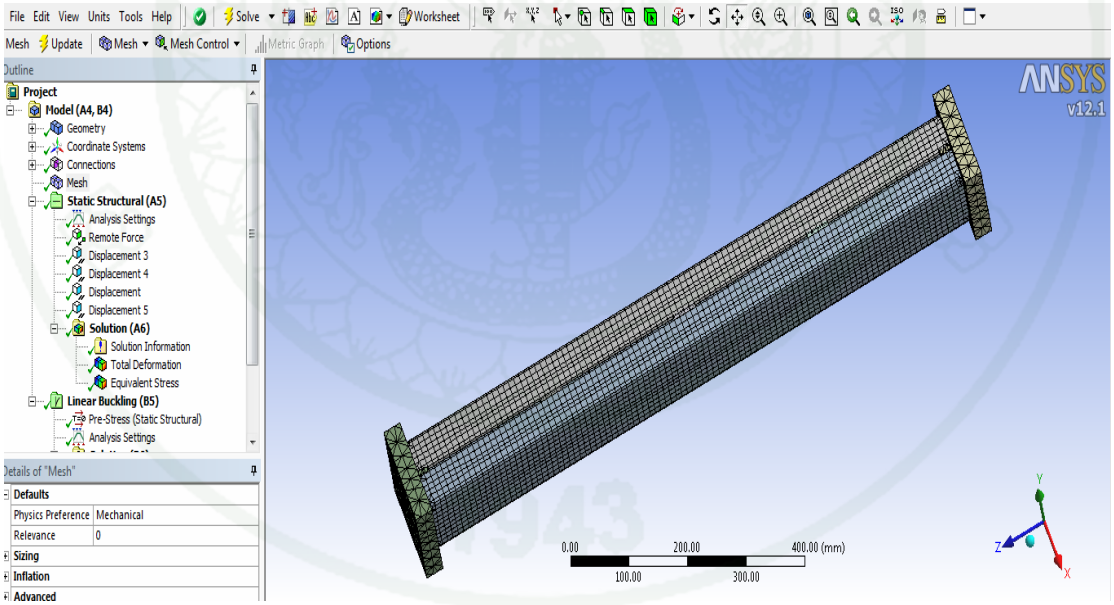

- Open the model menu and then assign mesh sizing about 10 mm. and generate its.

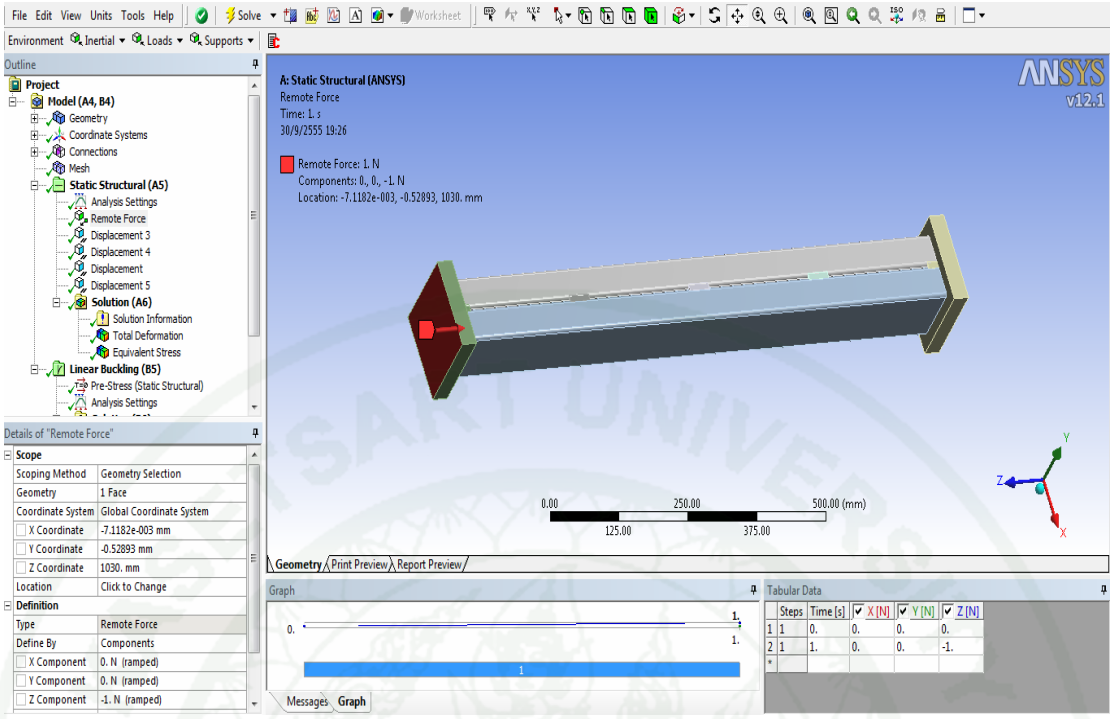

- Assign remote force 1 N. at one side of baseplate for concentric loaded in static structural menu.

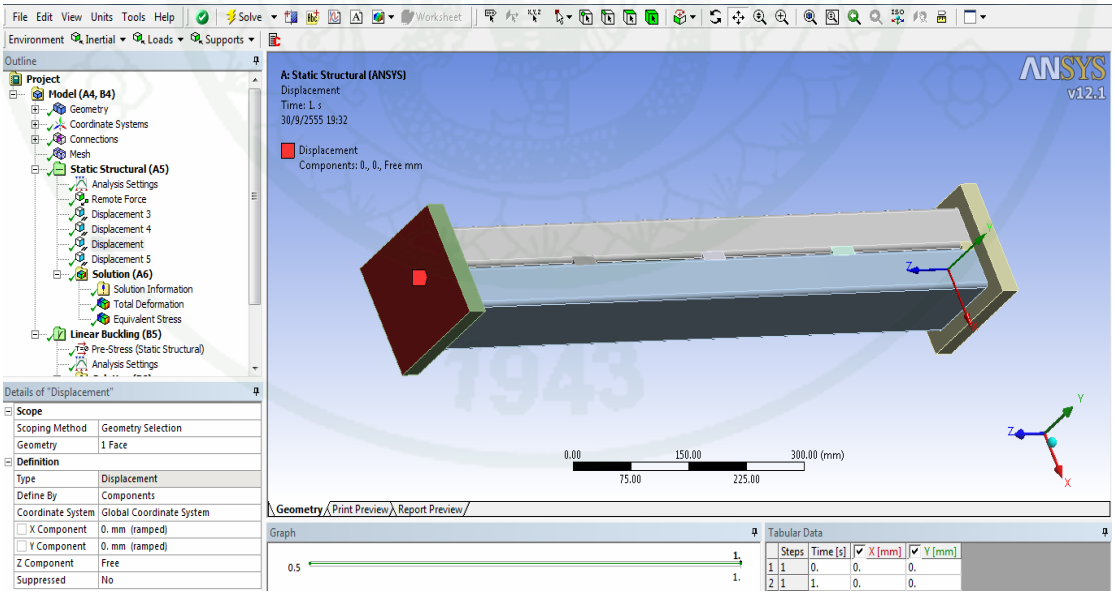

- Assign boundary condition at top baseplate with remote force to x , y direction are constant and z is free respectively.

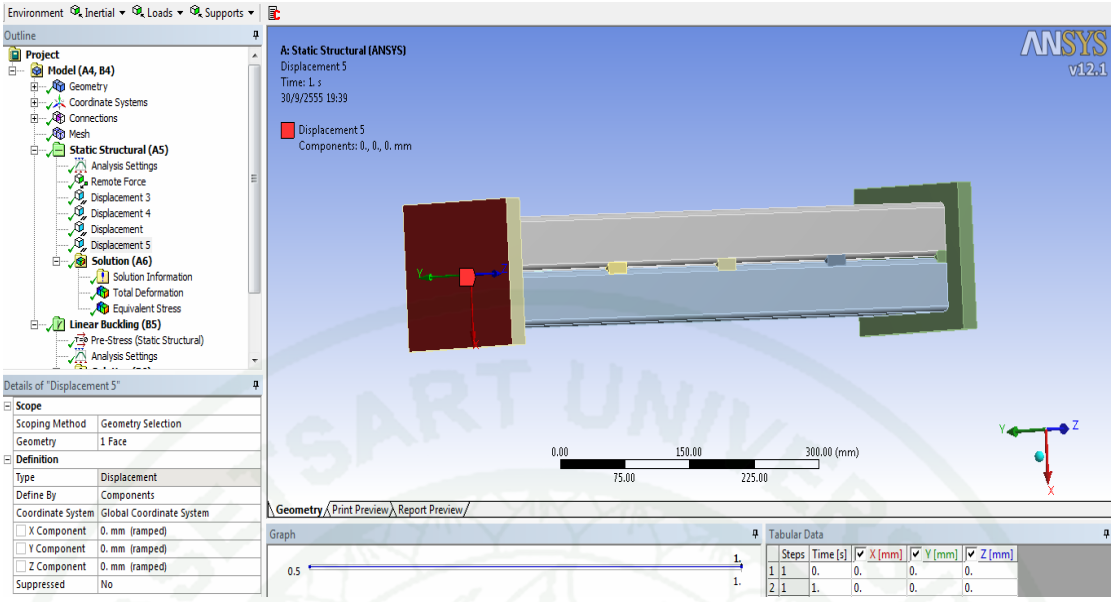

- Assign boundary condition at bottom baseplate with remote force to x , y ,z are constant all.

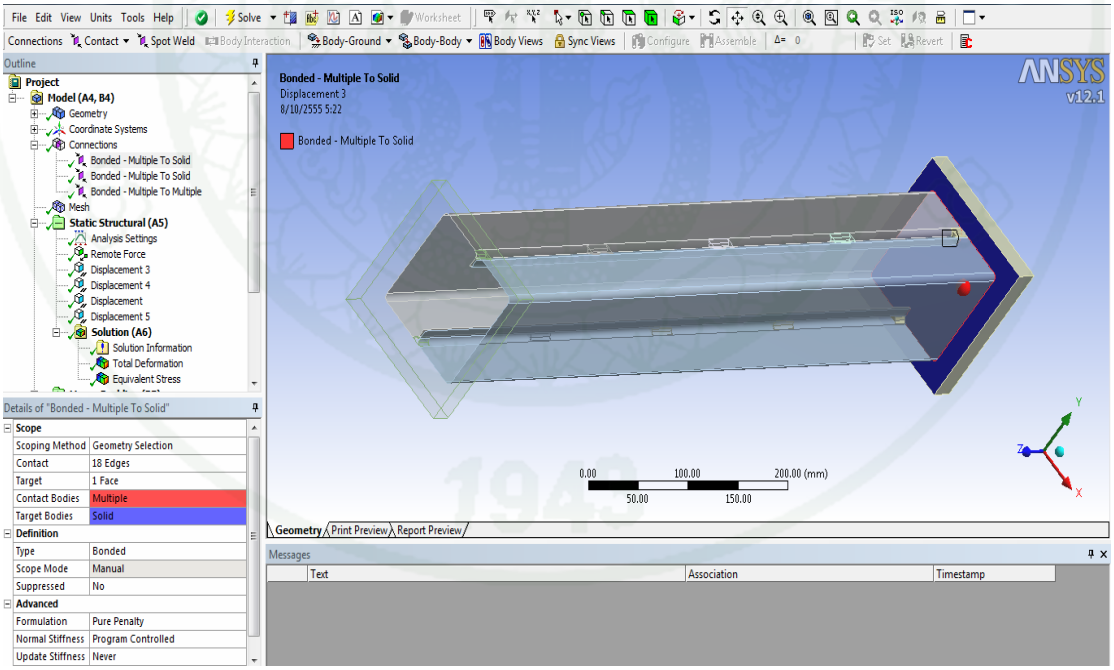

- From menu bar, choose contacted bonded for connected between the solid element (baseplate) with shell element (specimen) at top and bottom bastplate for transferred stress between shell with solid.

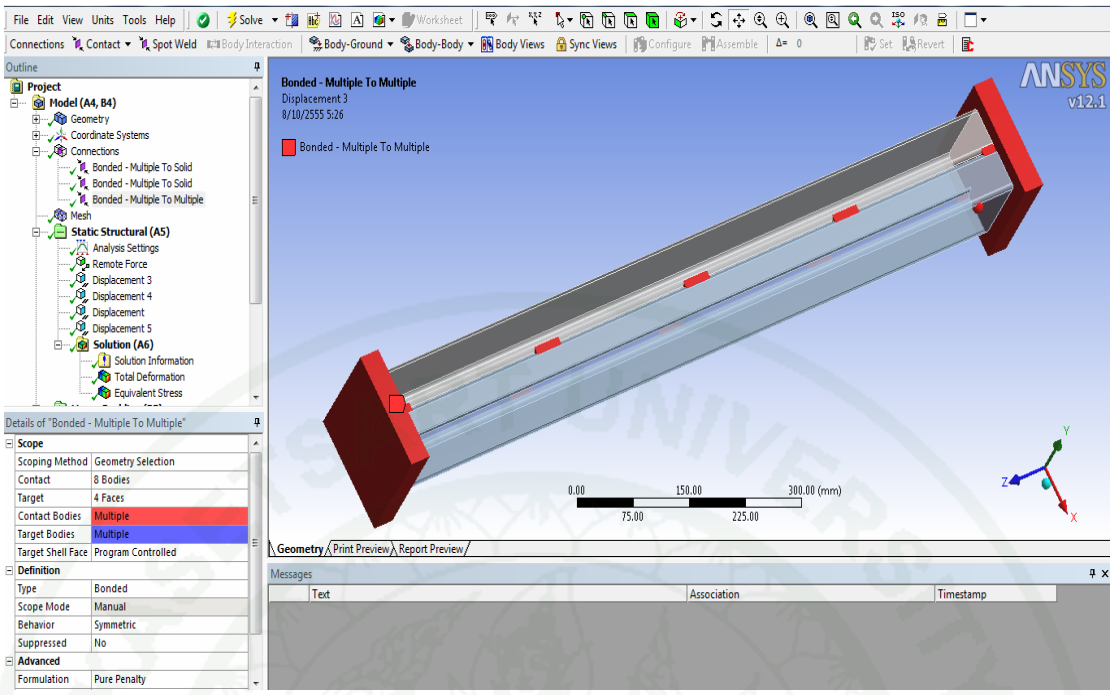

- From menu bar , choose contacted bonded for connected between the solid element (seam welding) with shell element (specimen) at all seam welding for transferred stress between shell with solid.

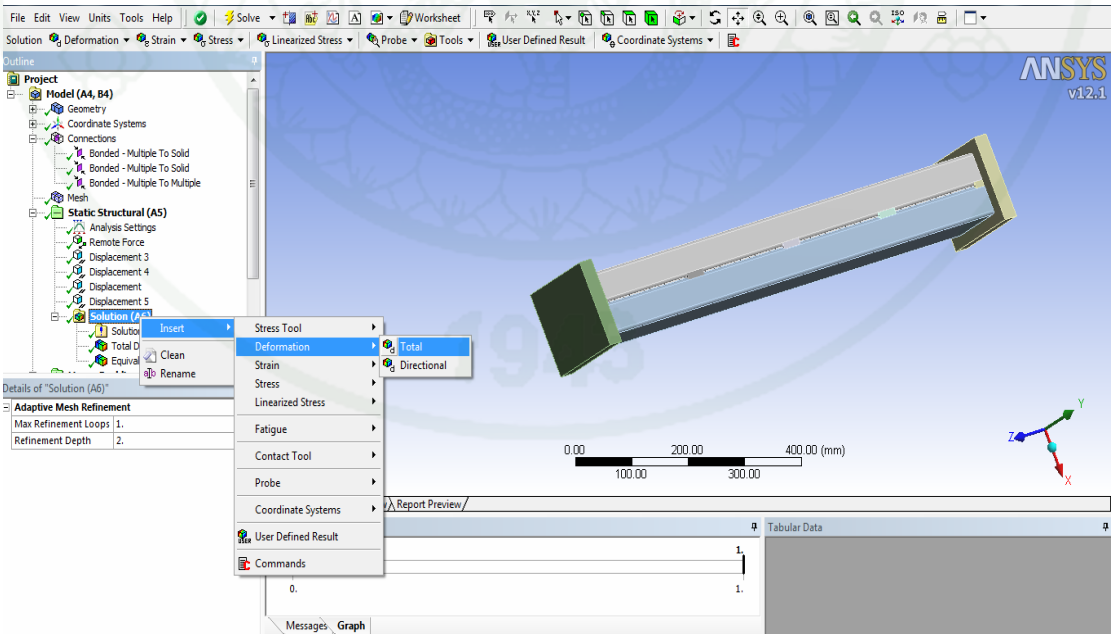

- From solution menu in the left tab, choose insert menu and then choose total deformation .

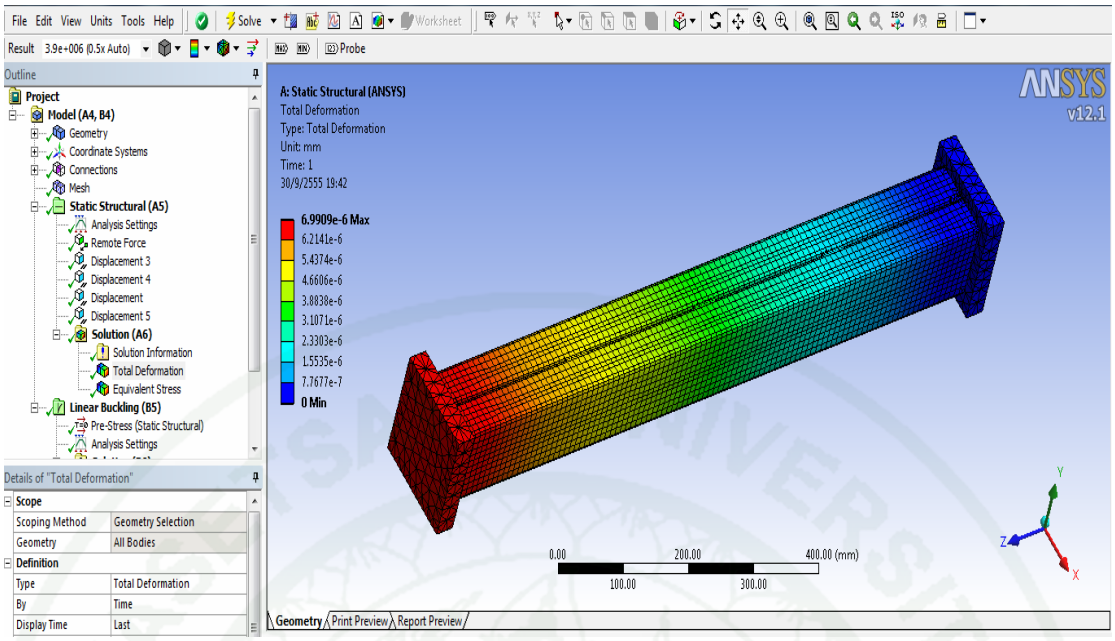

- Run static structural mode for total deformation resulted.

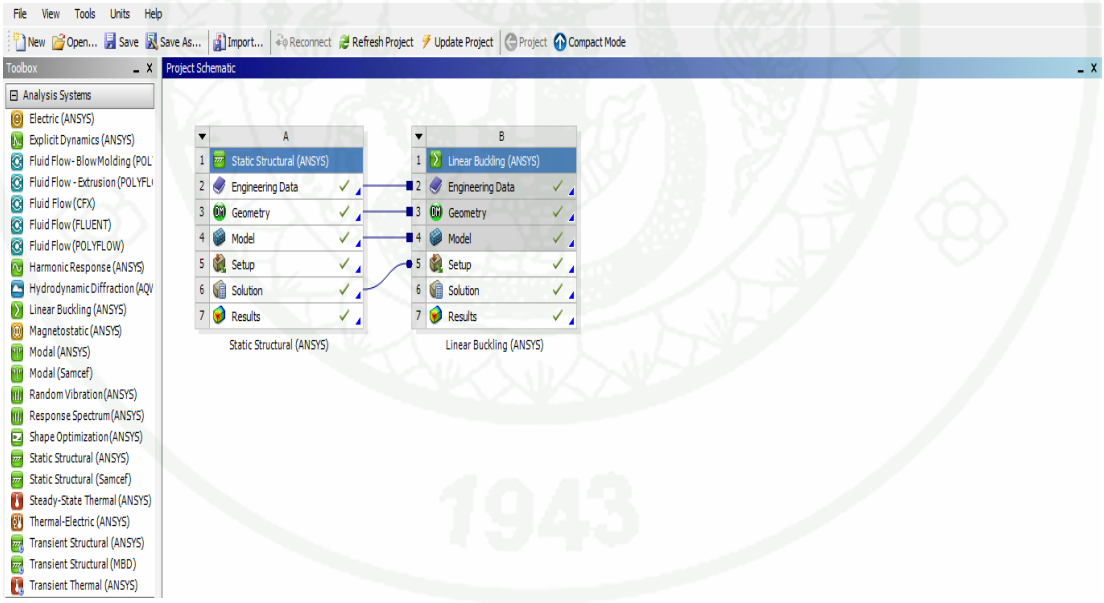

- From static structural (Ansys) mode, right click for open Linear buckling (Ansys) mode .

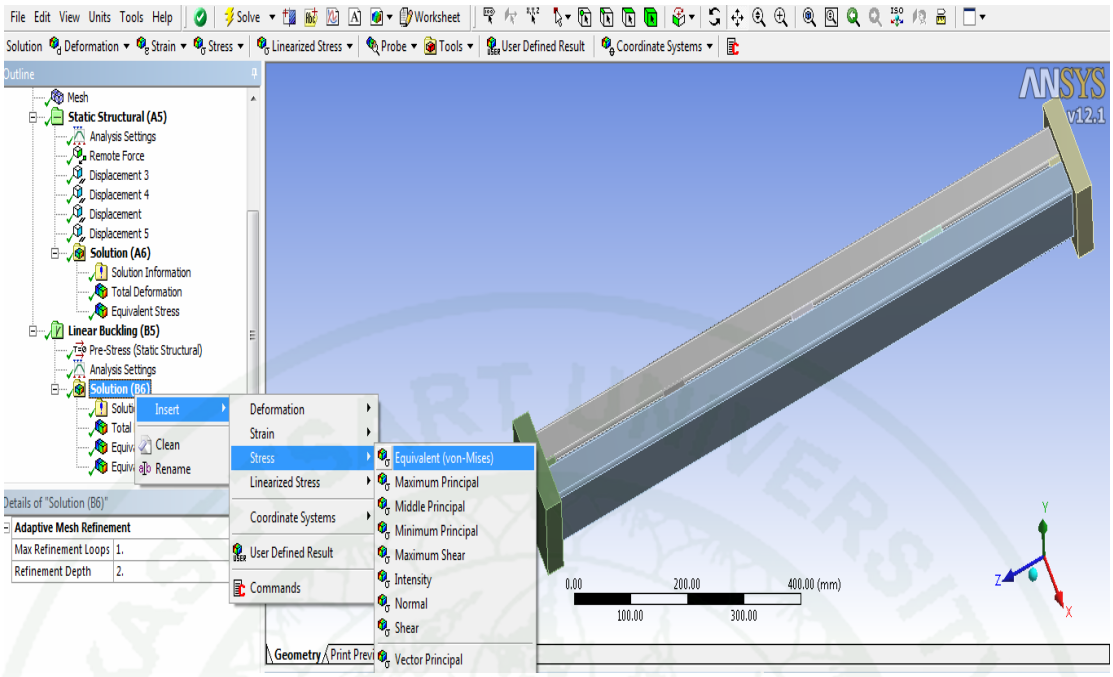

-From Linear buckling , choose solution tab for insert Equivalent stress mode1 and mode 2 and then choose total deformation for linear buckling mode.

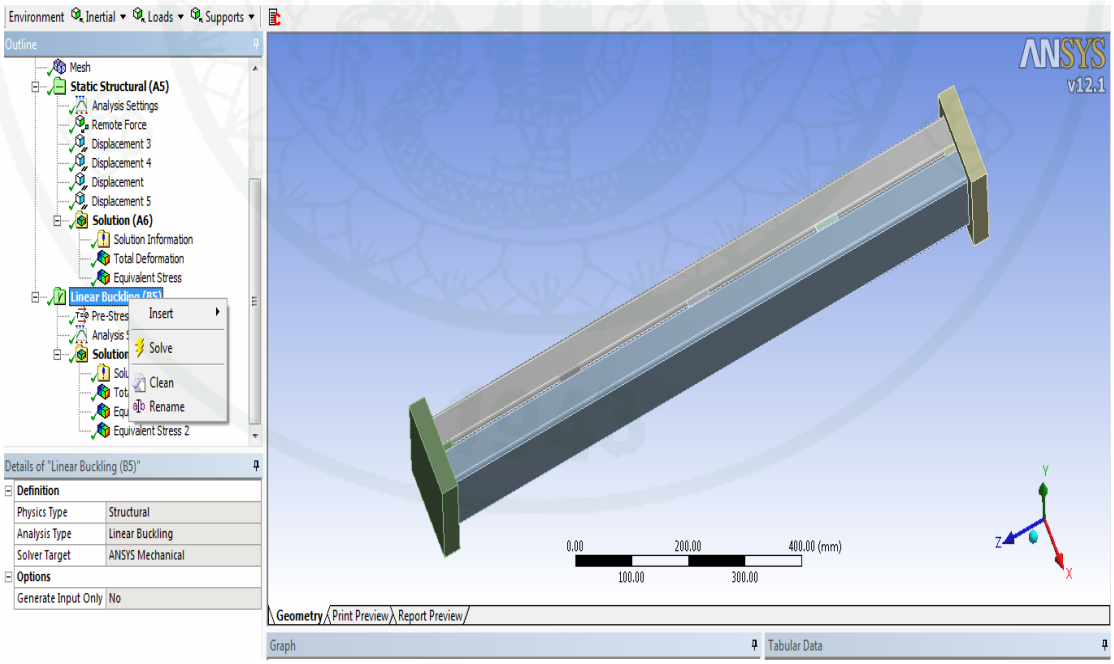

- Right click on Linear buckling mode and choose solve demand for run it.

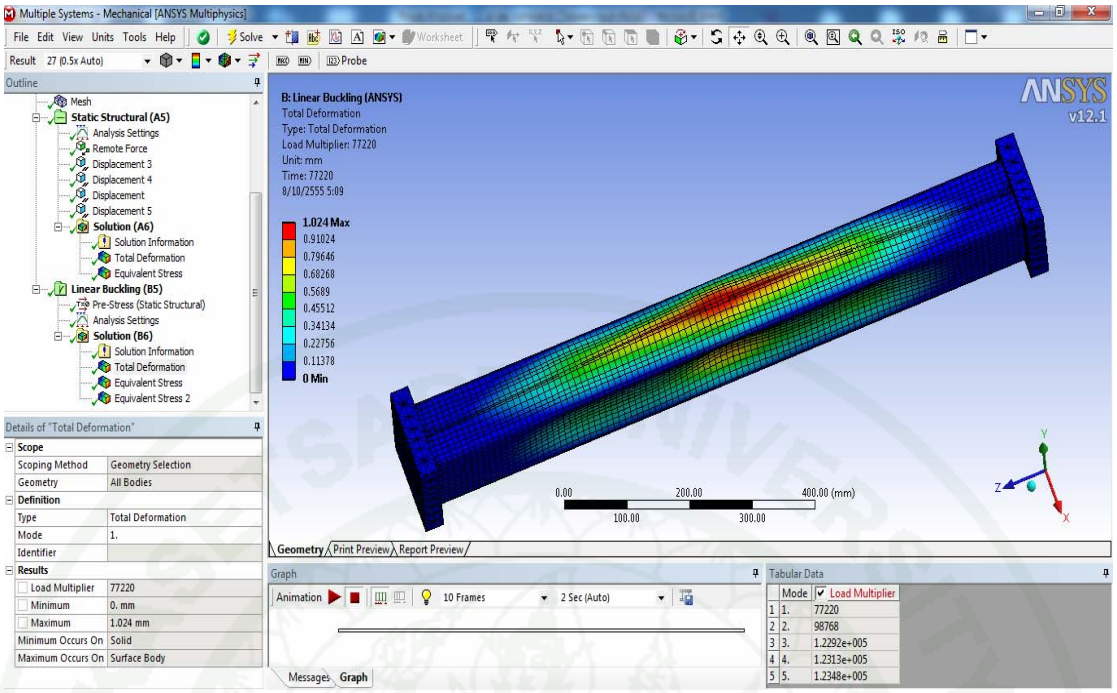

- After run Linear buckling mode, choose total deformation bar for resulted in buckling deformation shape .

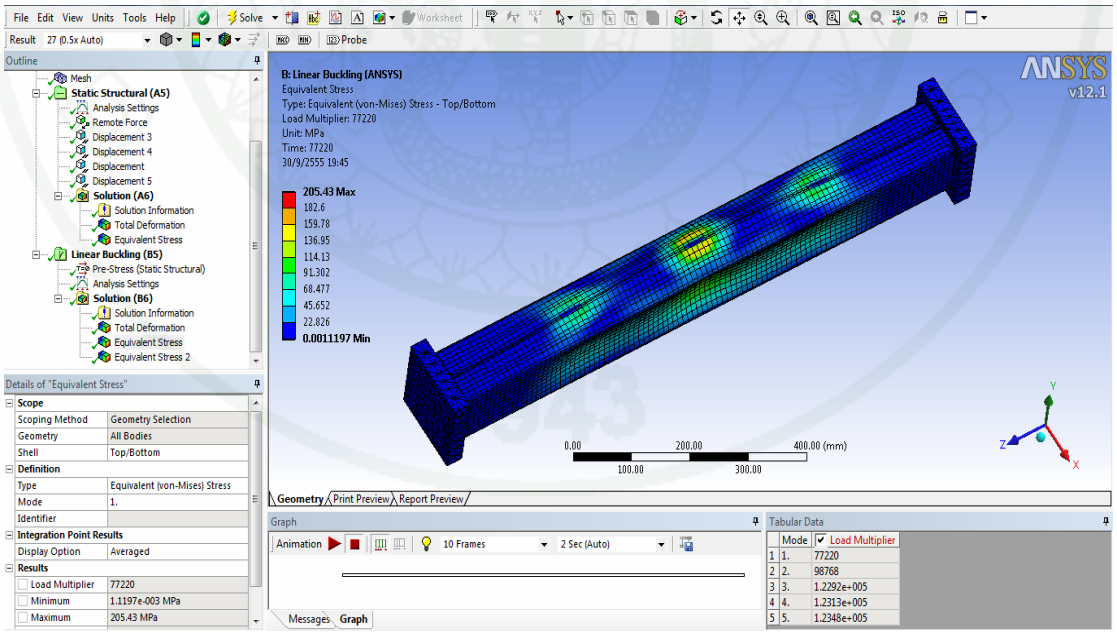

- From solution tab of Linear buckling, choose equivalent stress mode1 for resulted of stress mode 1 and local buckling loaded resulted as shown in table at corner of screen.

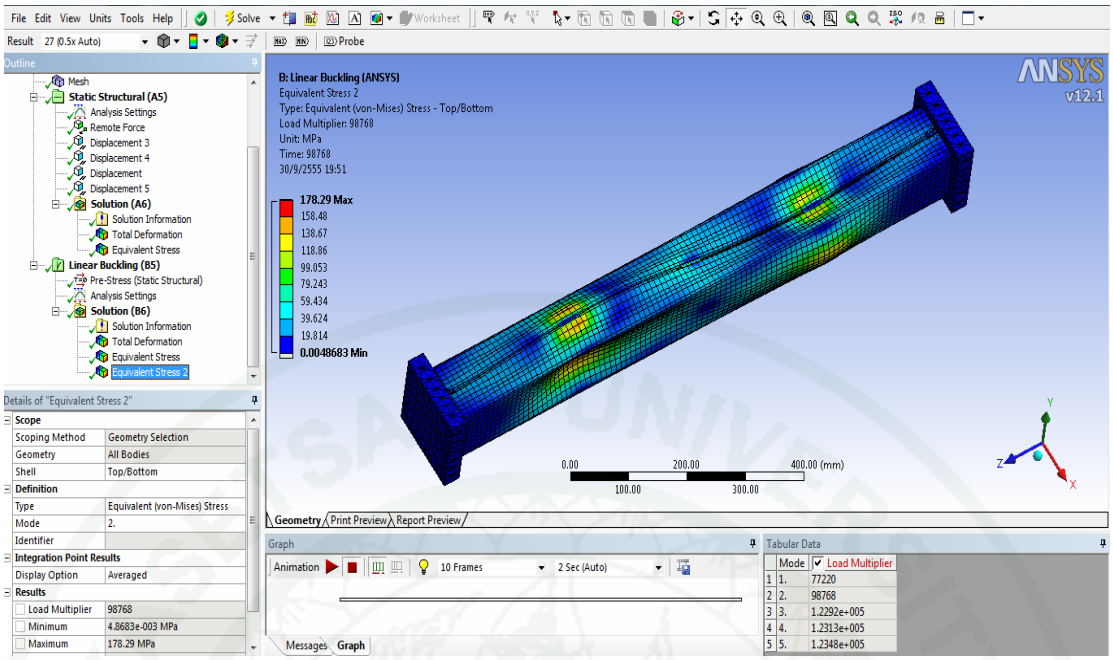

- From solution tab of Linear buckling, choose equivalent stress mode 2 for resulted of stress mode 2 and local buckling loaded resulted as shown in table at corner of screen.

Appendix B

Failure behaviors of specimens

1. BC100@125

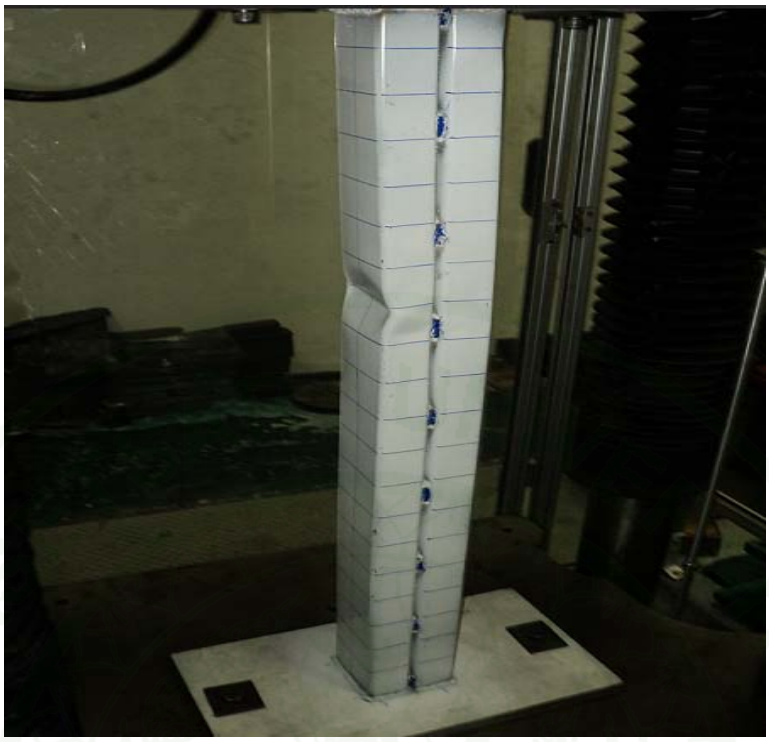

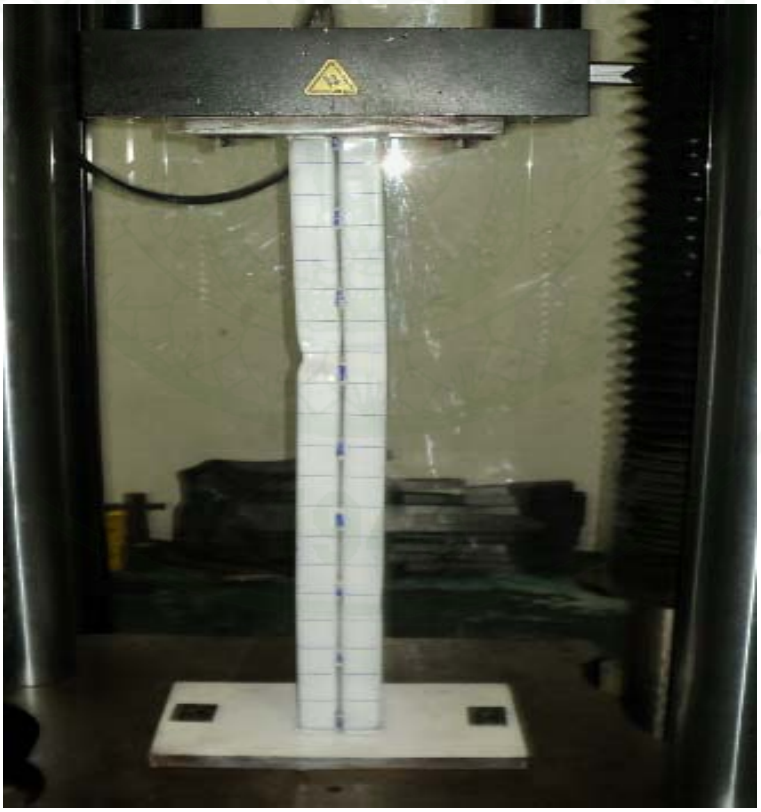

2. BC100@250

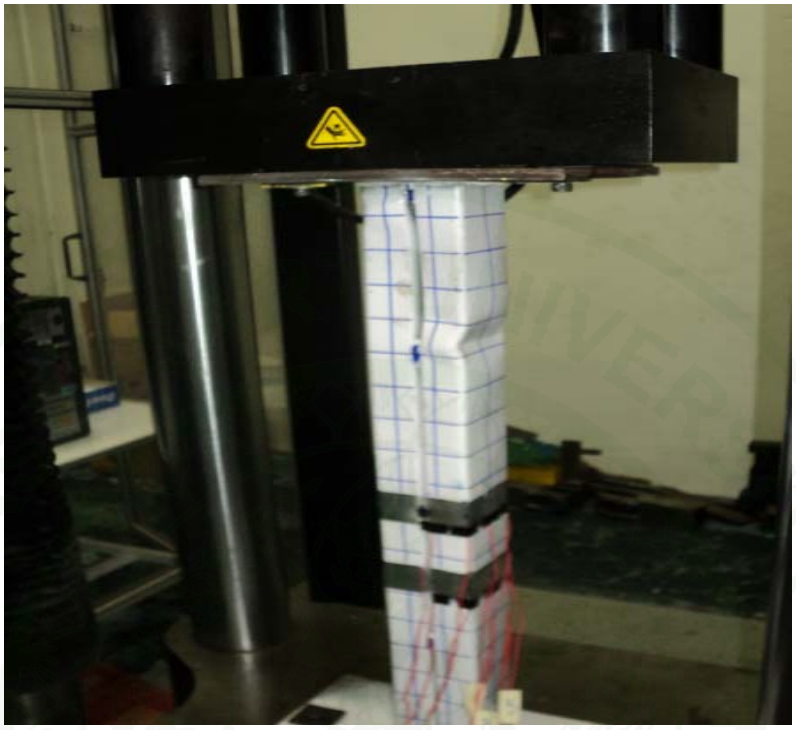

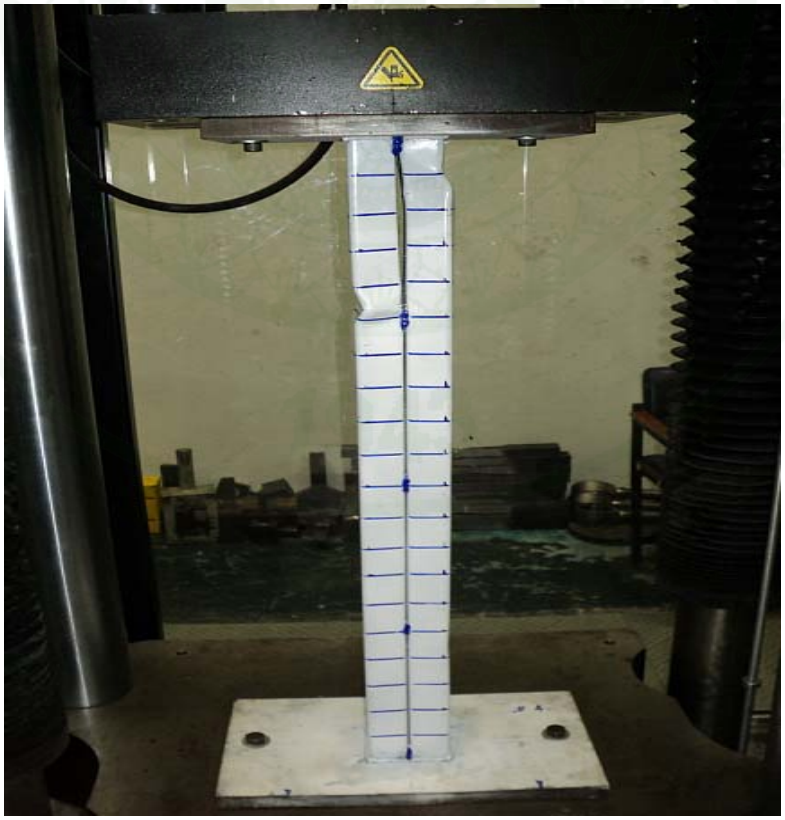

3. BC100@500

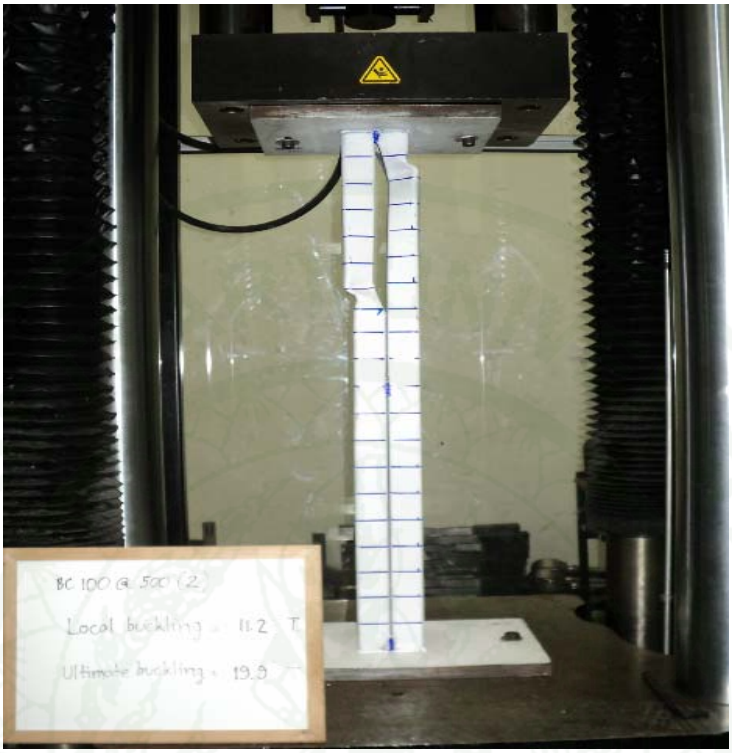

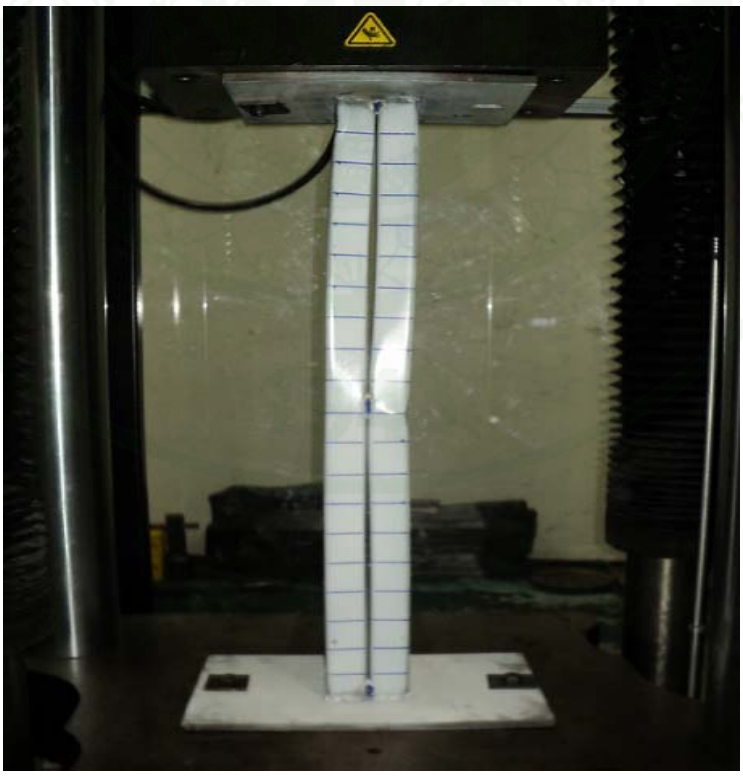

4. BC150@125

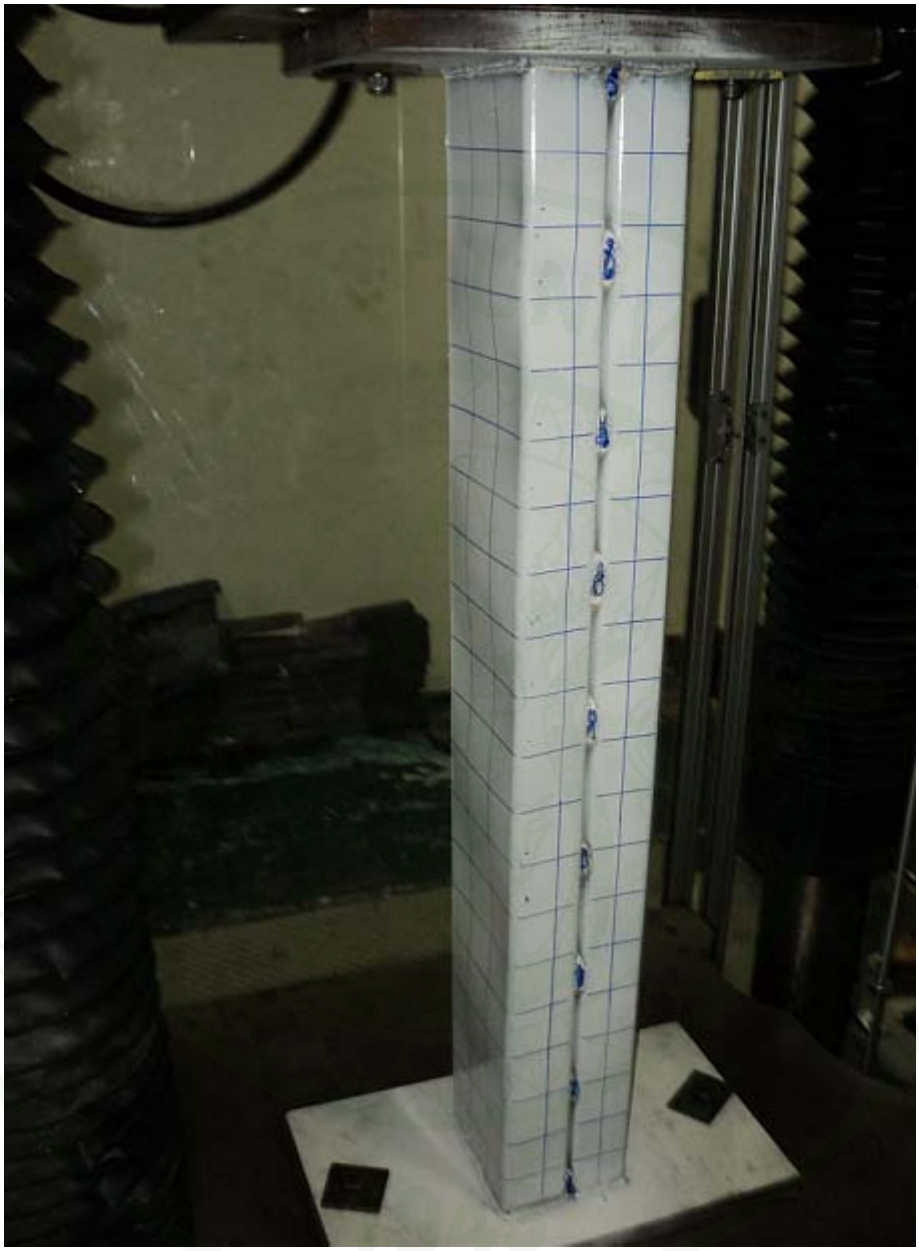

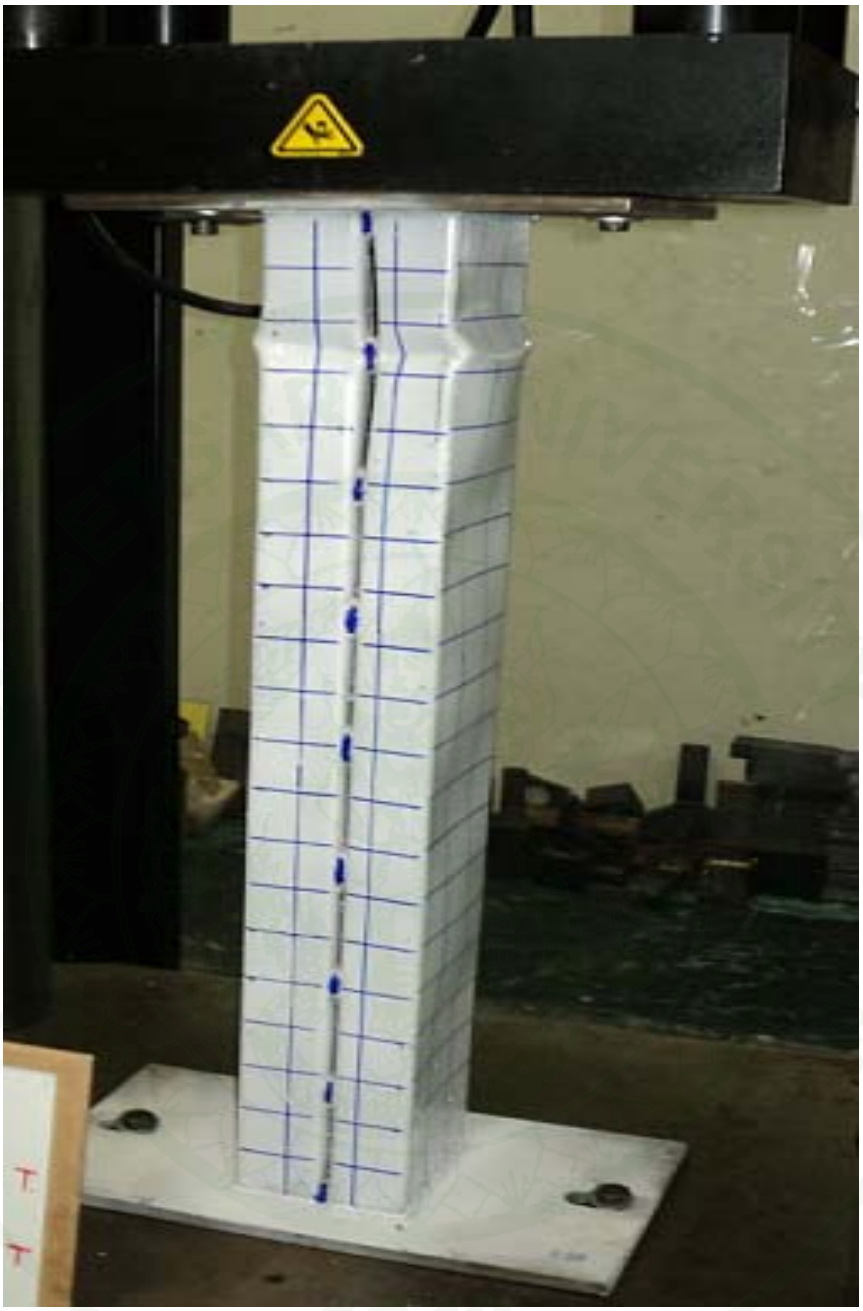

5. BC150@250

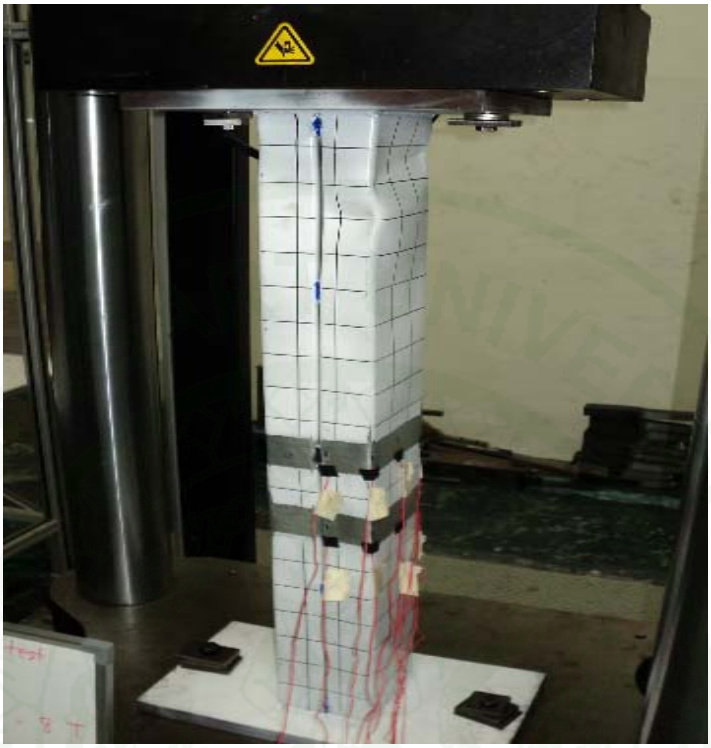

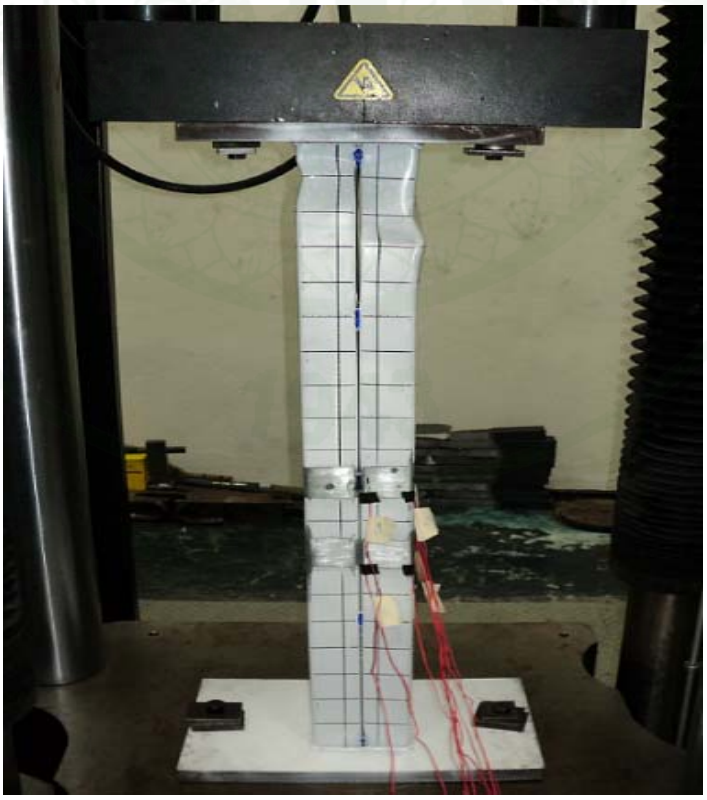

6. BC150@500

7. BC200@125

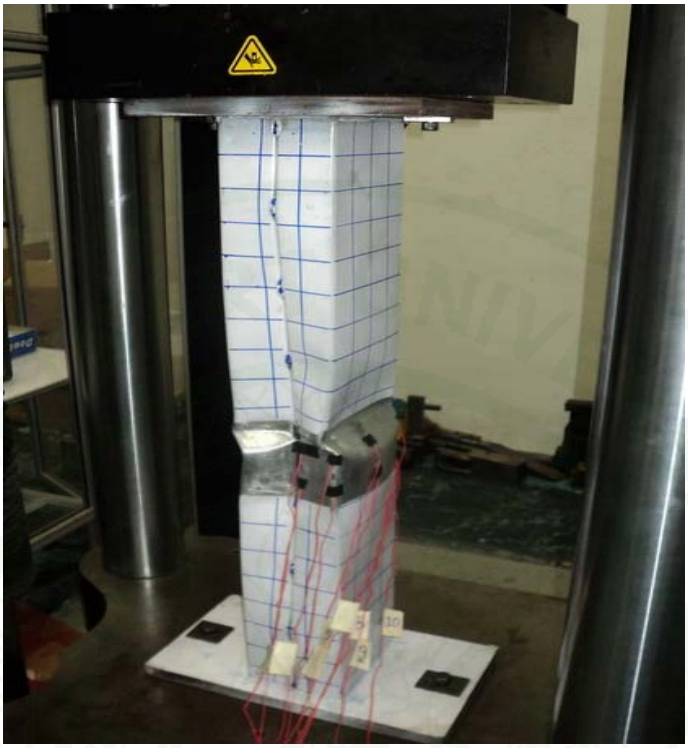

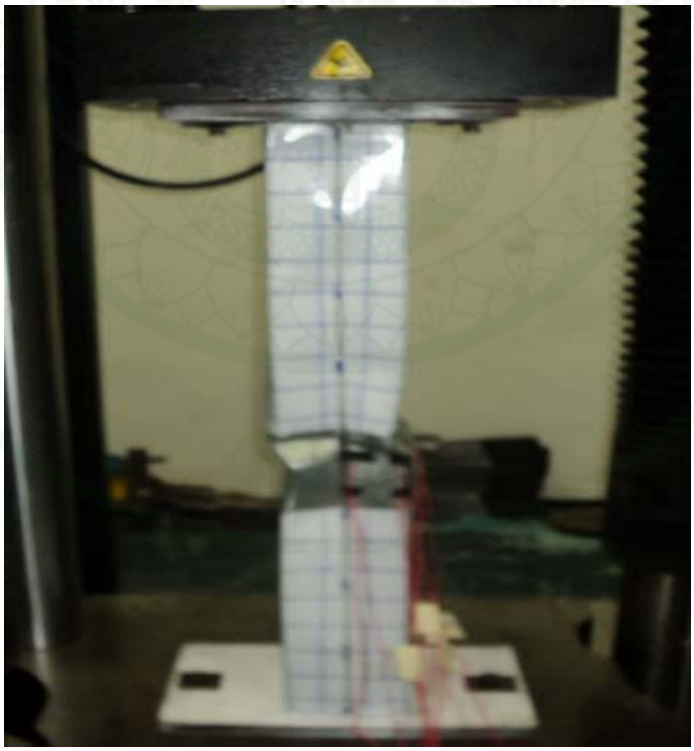

8. BC200@250

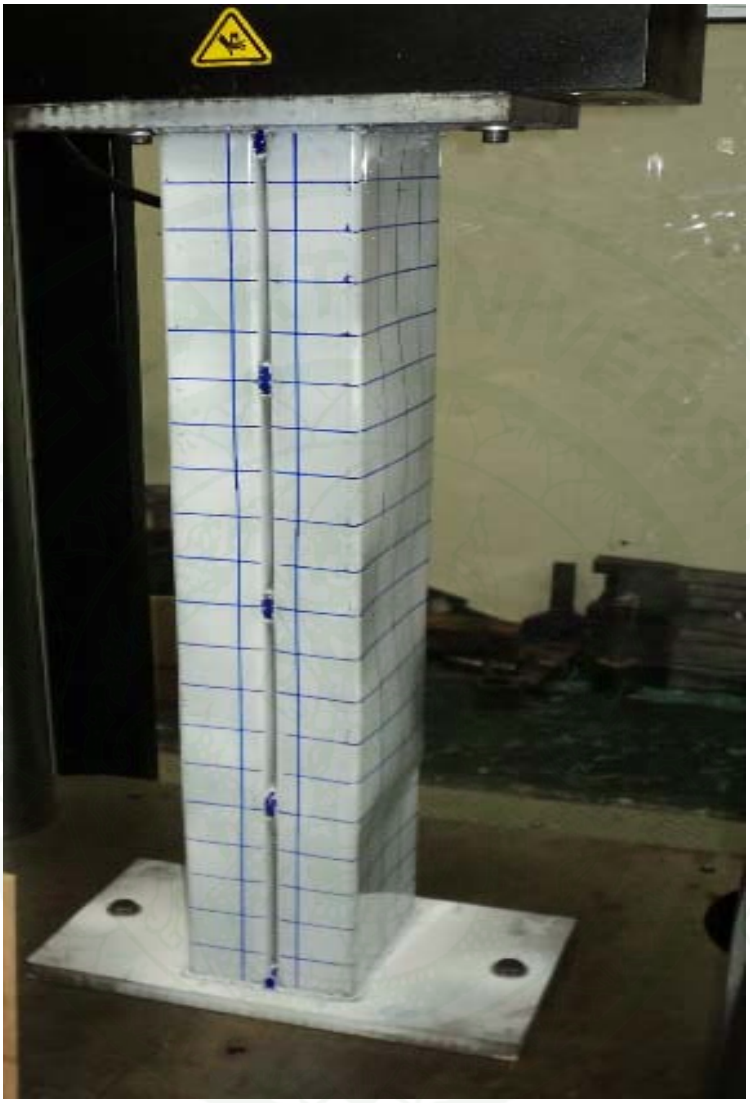

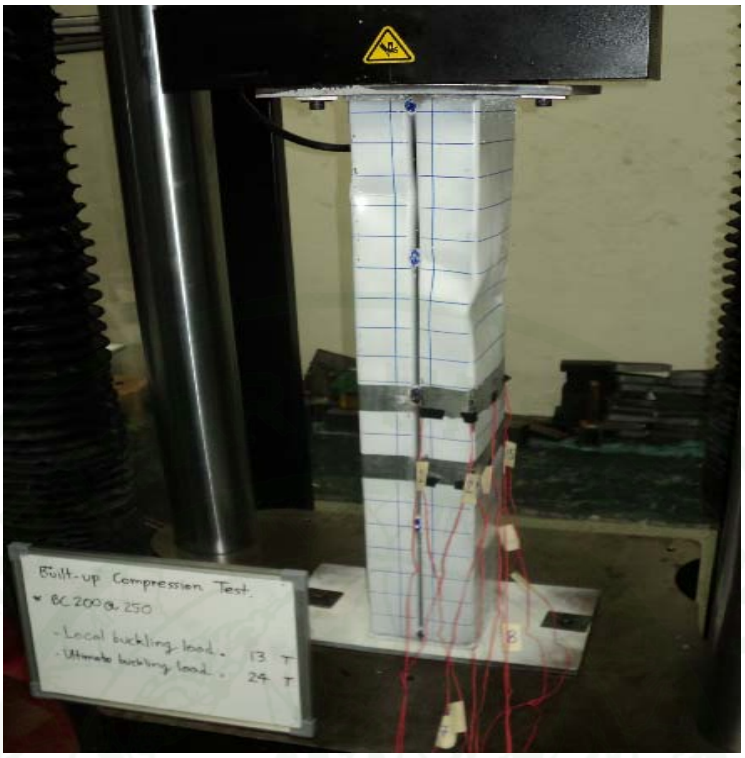

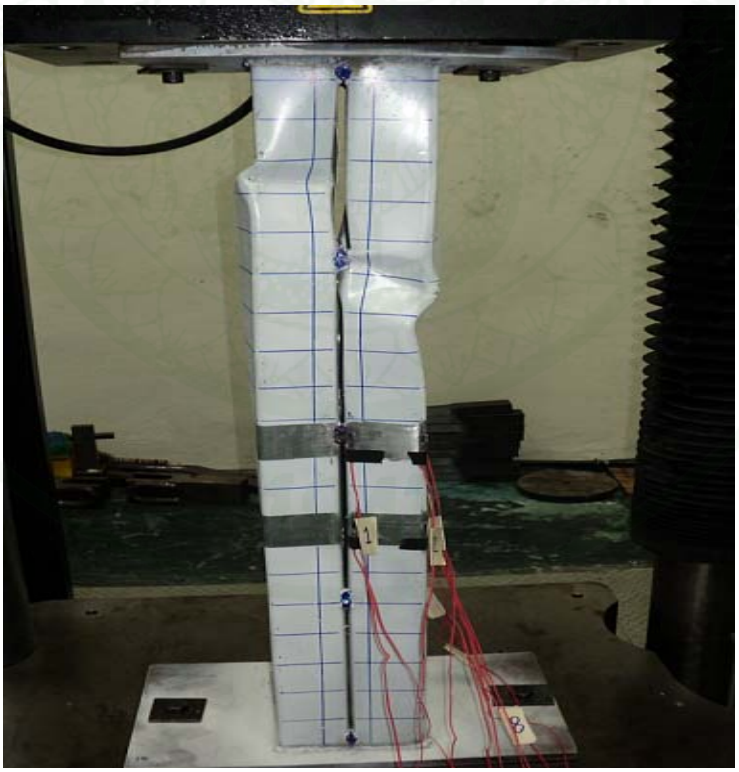

9. BC200@500

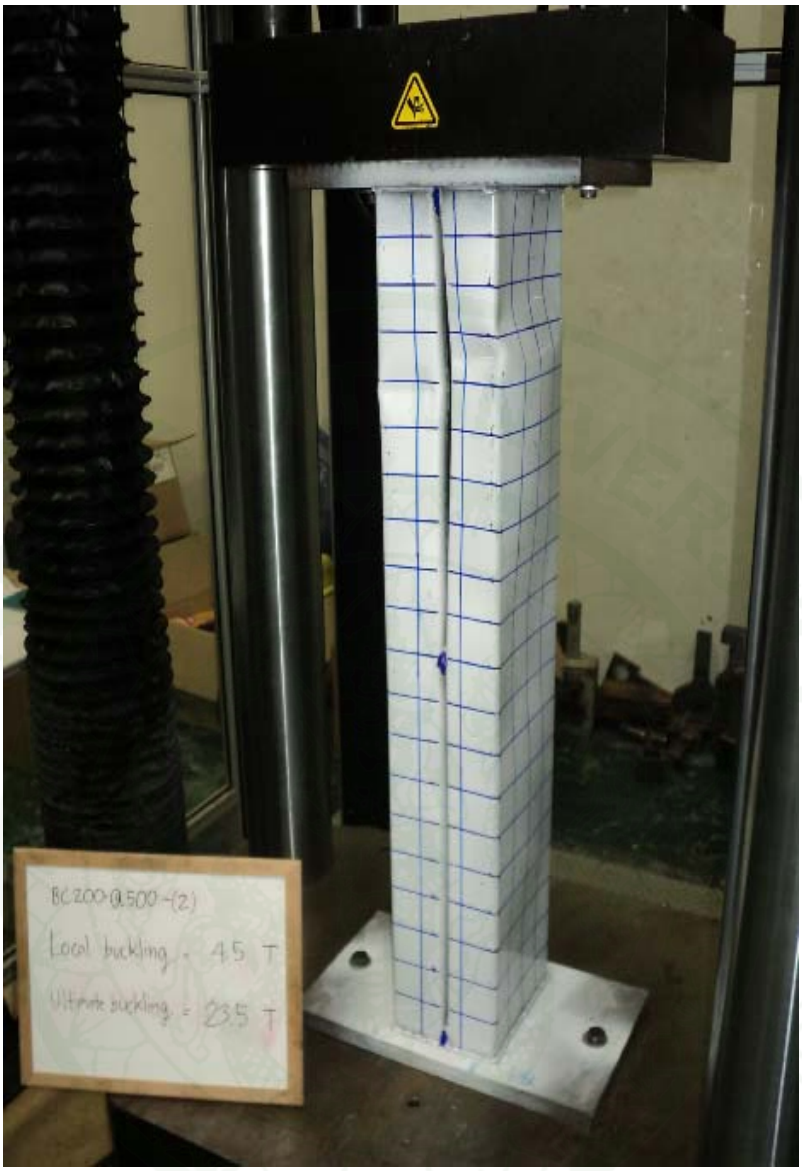

Appendix C

Compression load calculation.

Example of
Compression load calculation.

1. C100 (Single section)
2. BC100@500 (Built up section)
3. BC150@250 (Built up section)
4. BC200@125 (Built up section)

Compression load calculation.

1. C 100 (Single section)

Properties

Dimension (DxWxt)	Length(mm)	Section area (mm^2)	Ix (mm^4)	Iy (mm^4)	r_y (mm)	r_x (mm)
102x51x13.5	1000	323	$0.537x10^6$	$0.112x10^6$	18.7	40.8

Fe_1 (Flexural buckling); $= \dfrac{\pi^2 E}{(KL/r)^2}$

$= \dfrac{\pi^2 x 2.1 x 10^6}{(0.5x100/1.87)^2}$

$= 28987.65$ ksc.

Fe_2 (Torsional buckling)

$$Fe_2 = \frac{1}{A_g r_0^2}\left[GJ + \frac{\pi^2 ECw}{(KtLt)^2}\right]$$

$r_0 = \sqrt{r_x^2 + r_y^2 + X_0^2}$

G = Shear modulus

J = Torsion constant

Cw = Warping Constant

Ag = Gross section area

$$Fe2 = \frac{1}{323 \times 47.68^2}\left[7946.93 \times 242 + \frac{\pi^2 \times 2.1 \times 10^4 \times 241 \times 10^6}{1000^2}\right]$$

Fe2 = 7064.28 ksc.

Fe_3 (flexural - torsional buckling)

$$\mathbf{Fe_3} = \frac{1}{2B}\left[(\sigma ex + \sigma t) - \sqrt{(\sigma ex + \sigma t)^2 - 4\beta \sigma ex \sigma t}\right]$$

since $\sigma ex = \frac{\pi^2 E}{(KxLx/rx)^2}$

$$\sigma ex = \frac{\pi^2 \, x2.1x10^6}{(0.5x100/4.08)^2}$$

$\therefore$ σex = 138008.85 ksc

Substituted value into equation ; by σt = 7064.28 (Fe_2)

$\therefore$ **Fe_3** = 6813.73 ksc (**Fe3 is controlled)**

$$\lambda c = \sqrt{\frac{Fy}{Fe}}$$

$$\lambda c = \sqrt{\frac{5400}{6813.73}}$$

λc = 0.89 < 1.5 (Inelastic buckling)

$$Fn = (0.658^{\lambda_c^2}) \, Fy$$

Fn = 3,875.56 ksc

Effective Area Ae at stress Fn

1. Lip = 13.5 mm

W_1 = 13.5 – (5+1.5) = 7 mm

2. Flange = 51 mm.

W_2 = 51-2(5+1.5) = 38 mm.

3. Web = 102 mm.

W_3 = 102-2(6.5) = 89 mm.

1. Effective Width of Compression flange

$$\frac{w}{t} = \frac{38}{1.5} = 25.33$$

$$S = 1.28\sqrt{E/f}$$

$$S = 1.28\sqrt{2.1x10^4/38.75}$$

$$S = 29.80 \quad , \quad \frac{s}{3} = 9.93$$

$$S > \frac{w}{t}$$

$$Ia = 399\left\{\left[(w/t)/S\right] - \sqrt{Ku/4}\right\}^3 t^4$$

$$= 399\left\{\left[\frac{25.33}{29.80}\right] - \sqrt{0.43/4}\right\}^3 \left(1.5^4\right)$$

$$= 399\{0.85 - 0.327\}^3 (1.5)^4$$

$$= 288.96 \text{ mm}^4$$

$$Is = d^3t/12 = \left(\frac{7^3 x1.5}{12}\right) = W_1{}^3t/12 = 42.87 \text{ mm}^4$$

$$C_2 = Is/Ia$$

$$= \frac{42.87}{288.96}$$

$$= 0.148 < 1.0$$

$$C_1 = 2\text{-}C_2 = 2\text{-}0.148 = 1.852$$

$$D/W_2 = \frac{13.5}{38} = 0.355$$

Since $D/W_2 < 0.80$

$$ka = 5.25\text{-}5(0.355) = 3.475 < 4.0$$

$$k = C_2{}^n(ka\text{-}ku) + ku$$

$$= (0.148)^{0.5}(3.475\text{-}0.43)+0.43$$

$$= 1.60$$

USE $k = 1.60$ to compute the effective width of compression flange

$$\lambda = \frac{1.052}{\sqrt{k}}\left(\frac{W_2}{t}\right)\sqrt{\frac{f}{E}}$$

$$= \frac{1.052}{\sqrt{1.60}}\left(\frac{38}{1.5}\right)\sqrt{\frac{38.75}{2.1x10^4}}$$

$$= 0.91 > 0.673$$

$$\rho = \left(1-\frac{0.22}{\lambda}\right)/\lambda$$

$$\rho = \left(1-\frac{0.22}{0.91}\right)/0.91$$

$$b = \rho w_2 = 0.833 \text{ x } 38 = 31.66 \text{ mm.}$$

2. Effective Width of Edge stiffener

$$\frac{w}{t} = \frac{7}{1.5} = 4.67 < 14 \quad \text{OK}$$

$$\lambda = \frac{1.052}{\sqrt{k}}\left(\frac{w_1}{t}\right)\sqrt{\frac{f}{E}}$$

$$= \frac{1.052}{\sqrt{0.43}}(4.67)\sqrt{\frac{38.75}{2.1x10^4}}$$

$$= 0.322 < 0.673$$

$$d^1_s = w_1 = 7$$

$$d_s = C_2 d^1_s = 0.148 \times 7 = 1.036 < d^1_s \quad \text{OK}$$

3. Effective Width of Web element

$$\frac{w}{t} = \frac{89}{1.5} = 59.33$$

$$\lambda = \frac{1.052}{\sqrt{k}}\left(\frac{w_1}{t}\right)\sqrt{\frac{f}{E}}$$

$$\lambda = 1.341 > 0.673$$

$$\rho = \left(1-\frac{0.22}{\lambda}\right)/\lambda = 0.62$$

$$b = \rho w_3 = 0.62 \times 89 = 55.48 \text{ mm.}$$

$$\text{Ae of C100} = 323\text{-}\left[2(38-31.66)+2(7-1.036)+(89-55.48)\right]x1.5$$

$$= 235.81 \text{ mm}^2 = 2.36 \text{ cm}^2$$

Since ; $Pn = Ae \times Fn$

$$Pn = 2.36 \times 3{,}875$$

Pn = 9,145 Kg.

Pn = 9. 14 Ton. (**flexural – torsional**)

Compute of Pn based on Distortional buckling

$$P_n = \left[1 - 0.25\left(\frac{P_{crd}}{P_y}\right)^{0.6}\right]\left(\frac{P_{crd}}{P_y}\right)^{0.6} P_y$$

Pcrd = AgFd

Py = AgFy

$$Fd = \frac{k\phi fe + k\phi we + k\phi}{k\phi fg + k\phi wg}$$

$$k_{\phi fe} = \left(\frac{\pi}{L}\right)^4\left[EI_{xf}(x_{0f} - h_x)^2 + EC_{wf} - E\frac{I_{xyf}^2}{I_{yf}}(x_{0f} - h_x)^2\right] + \left(\frac{\pi}{L}\right)^2 GJ_f$$

$$k_{\phi we} = \frac{Et^3}{6h_0(1-\mu^2)}$$

$$\tilde{k}_{\phi fg} = \left(\frac{\pi}{L}\right)^2\left\{A_f\left[(x_{0f} - h_x)^2\left(\frac{I_{xyf}}{I_{yf}}\right)^2 - 2y_{0f}(x_{0f} - h_x)\times\left(\frac{I_{xyf}}{I_{yf}}\right) + h_x^2 + y_{0f}^2\right] + I_{xf} + I_{yf}\right\}$$

$$\tilde{k}_{\phi wg} = \left(\frac{\pi}{L}\right)^2\left(\frac{th_0^3}{60}\right)$$

k_ϕ = 0 (Unrestrained)

since

$$L_{cr} = \left\{\frac{6\pi^4 h_0(1-\mu^2)}{t^3}\left[I_{xf}(x_{0f} - h_x)^2 + C_{wf} - \frac{I_{xyf}^2}{I_{yf}}(x_{0f} - h_x)^2\right]\right\}^{1/4}$$

Substitute value into equation ; Lcr = 400.9 mm.

; Since (Lm = Ly = 1000 mm.) > Lcr , use L = 400.9 mm.

Substitute value into equation ; get

$$k\phi fe = 127.09$$

$$k\phi we = 127.26$$

$$k\phi fg = 6.874$$

$$k\phi wg = 1.618$$

$$Fd = \frac{k\phi fe + k\phi we + k\phi}{k\phi fg + k\phi wg}$$

$$Fd = 3934.76 \text{ ksc}$$

Therefore;

$$Pcrd = AgFd$$

$$Pcrd = 3.23 \times 3934.76 = 12709.28 \text{ kg.}$$

$$Py = AgFy$$

$$Py = 3.23 \times 5400 = 17442 \text{ kg.}$$

Substitute Pcrd and Py into equation ; $P_n = \left[1 - 0.25\left(\frac{P_{crd}}{P_y}\right)^{0.6}\right]\left(\frac{P_{crd}}{P_y}\right)^{0.6} P_y$

$$Pn = \left[1 - 0.25(12709.28/17442)^{0.6}\right](12709.28/17442)^{0.6}17442$$

Distortional buckling load Pn = 11438.65 Kg. = 11.43 Ton

Since

Pn = 9.14 Ton (flexural - torsional) < 11.43 Ton (Distortional)

Therefore the governing Pn = 9. 14 Ton. (flexural - torsional) controlled

2. BC 100 @ 500 (Built-up)

Properties of BC100@500

Length(cm)	Weld spacing (a) (cm)	Section area (cm^2)	Ix (cm^4)	Iy (cm^4)	r_y (cm)	r_x (cm)
100	500	6.46	115.24	103.83	4	4.22

Modified slenderness ratio

$$\left(\frac{KL}{r}\right)_m = \sqrt{\left(\frac{KL}{r}\right)_0^2 + \left(\frac{a}{r}\right)^2}$$

$\left(\frac{KL}{r}\right)_0$ = Overall slenderness of built-up mumber

r_i = Minimum radius of gyration on individual member of built-up

$\left(\frac{KL}{r}\right)_m$ = Modified slenderness ratio

a = Weld spacing

$$\left(\frac{KL}{r}\right)_m = \sqrt{\left(\frac{0.5x1000}{40}\right)^2 + \left(\frac{500}{18.7}\right)^2}$$

$$\left(\frac{KL}{r}\right)_m = 29.51$$

Fe_1 (Flexural buckling); $= \dfrac{\pi^2 E}{(KL/r)_m^2}$

$= \dfrac{\pi^2 x 2.1 x 10^6}{(29.51)^2}$

$= 23800.20$ ksc.

Fe_2 (Torsional buckling stress between fasteners)

$$Fe_2 = \frac{1}{A_g r_0^2}\left[GJ + \frac{\pi^2 ECw}{(a)^2}\right]$$

Use properties of single section; (Unit; mm.)

$r_0 = \sqrt{r_x^2 + r_y^2 + X_0^2}$

G = Shear modulus

J = Torsion constant

Cw = Warping Constant

a = Weld spacing

Ag = Gross section area

$$Fe = \frac{1}{323 x 60.2^2}\left[7946.93 x 242 + \frac{\pi^2 x 2.1 x 10^4 x 241 x 10^6}{500^2}\right]$$

Fe = 17068.7 ksc.

Fe_3 (flexural-torsional buckling stress between fasterers)

$$\mathbf{Fe_3} = \frac{1}{2B}\left[(\sigma ex+\sigma t)-\sqrt{(\sigma ex+\sigma t)^2-4\beta\sigma ex\sigma t}\right]$$

since $\sigma ex = \frac{\pi^2 E}{(KxLx/rx)^2}$

$$\sigma ex = \frac{\pi^2 \text{ x } 2.1\text{x}10^6}{(100/1.87)^2}$$

$\therefore$ $\sigma ex = 7247.73$ ksc

Substituted value into equation ; by $\sigma t = 17068.7$ (Fe_2)

$\therefore$ $Fe_3 = 5087.48$ ksc.

$\therefore$ **Minimum of Fe is Fe_3 (flexural-torsional buckling stress between fastener)**

$Fe_3 = 5087.48$ ksc..

$$\lambda c = \sqrt{\frac{Fy}{Fe}}$$

$$\lambda c = \sqrt{\frac{5400}{5087.48}}$$

$\lambda c = 1.03 < 1.5$ (Inelastic buckling)

$Fn = (0.658^{\lambda_c^2})\,Fy$

$Fn = 3463$ ksc

Effective Area Ae at stress Fn

1. Lip = 13.5 mm

W_1 = 13.5 – (5+1.5) = 7 mm

2. Flange = 51 mm.

W_2 = 51-2(5+1.5) = 38 mm.

3. Web = 102 mm.

W_3 = 102-2(6.5) = 89 mm.

1. Effective Width of Compression flange

$$\frac{w}{t} = \frac{38}{1.5} = 25.33$$

$$S = 1.28\sqrt{E/f}$$

$$S = 1.28\sqrt{2.1x10^4/34.63}$$

$$S = 31.52 \ , \ \frac{s}{3} = 10.50$$

$$S > \frac{w}{t}$$

$$Ia = 399\left\{\left[(w/t)/S\right] - \sqrt{Ku/4}\right\}^3 t^4$$

$$= 399\left\{\left[\frac{25.33}{31.52}\right] - \sqrt{0.43/4}\right\}^3 \left(1.5^4\right)$$

$$= 399\{0.80 - 0.33\}^3 (1.5)^4 = 214.60 \text{ mm}^4$$

$$Is = d^3t/12 = \left(\frac{7^3 x1.5}{12}\right) = W_1^3 t/12 = 42.87 \text{ mm}^4$$

C_2 = Is/Ia

$$= \frac{42.87}{214.60}$$

$= 0.2 < 1.0$

$C_1 = 2\text{-}C_2 = 2\text{-}0.2 = 1.8$

$D/W_2 = \frac{13.5}{38} = 0.355$

Since $D/W_2 < 0.80$

$ka = 5.25\text{-}5(0.355) = 3.475 < 4.0$

$k = C_2^n(ka\text{-}ku) + ku$

$= (0.20)^{0.5}(3.475\text{-}0.43)+0.43$

$= 1.79$

USE $k = 1.79$ to compute the effective width of compression flange

$$\lambda = \frac{1.052}{\sqrt{k}}\left(\frac{W_2}{t}\right)\sqrt{\frac{f}{E}}$$

$$= \frac{1.052}{\sqrt{1.79}}\left(\frac{38}{1.5}\right)\sqrt{\frac{34.63}{2.1x10^4}}$$

$= 0.80 > 0.673$

$$\rho = \left(1-\frac{0.22}{\lambda}\right)/\lambda$$

$$\rho = \left(1-\frac{0.22}{0.80}\right)/0.80$$

$b = \rho w_2 = 0.90 \times 38 = 34.43$ mm.

2. Effective Width of Edge stiffener

$$\frac{w}{t} = \frac{7}{1.5} = 4.67 < 14 \quad \text{O:K}$$

$$\lambda = \frac{1.052}{\sqrt{k}}\left(\frac{w_1}{t}\right)\sqrt{\frac{f}{E}}$$

$$= \frac{1.052}{\sqrt{0.43}}(4.67)\sqrt{\frac{34.63}{2.1x10^4}}$$

$$= 0.30 < 0.673$$

$$d^1_s = w_1 = 7$$

$$d_s = C_2 d^1_s = 0.2 \times 7 = 1.4 < d^1_s \quad \text{OK}$$

3. Effective Width of Web element

$$\frac{w}{t} = \frac{89}{1.5} = 59.33$$

$$\lambda = \frac{1.052}{\sqrt{k}}\left(\frac{w_1}{t}\right)\sqrt{\frac{f}{E}}$$

$$\lambda = 1.27 > 0.673$$

$$\rho = \left(1-\frac{0.22}{\lambda}\right)/\lambda = 0.65$$

$$b = \rho w_3 = 0.65 \times 89 = 57.85 \text{ mm.}$$

$$\text{Ae of BC100} = 646\text{-}\left[4(7-1.4)+4(38-34.43)+2(89-57.85)\right]x1.5$$

$$= 497.53 \text{ mm}^2$$

$$= 4.97 \text{ cm}^2$$

Since ; Pn = Ae x Fn

Pn = 4.97 x 3,463

Pn = 17.21 Ton.

3. BC 150 @ 250 (Built-up)

Properties of BC150@250

Length(cm)	Weld spacing (a) (cm)	Section area (cm^2)	Ix (cm^4)	Iy (cm^4)	r_y (cm)	r_x (cm)
100	25	8.86	338.55	235.35	5.15	6.18

Modified slenderness ratio

$$\left(\frac{KL}{r}\right)_m = \sqrt{\left(\frac{KL}{r}\right)_0^2 + \left(\frac{a}{r}\right)^2}$$

$\left(\frac{KL}{r}\right)_0$ = Overall slenderness of built-up mumber

r_i = Minimum radius of gyration on individual member of built-up

$\left(\frac{KL}{r}\right)_m$ = Modified slenderness ratio

a = Weld spacing

$$\left(\frac{KL}{r}\right)_m = \sqrt{\left(\frac{0.5x1000}{51.5}\right)^2 + \left(\frac{250}{23.1}\right)^2}$$

$$\left(\frac{KL}{r}\right)_m = 14.54$$

Fe_1 (Flexural buckling); $= \dfrac{\pi^2 E}{(KL/r)_m^2}$

$= \dfrac{\pi^2 x 2.1 x 10^6}{(14.54)^2}$

$=$ 98037.05 ksc.

Fe_2 (Torsional buckling stress between fasteners)

$$Fe_2 = \frac{1}{A_g r_0^2}\left[GJ + \frac{\pi^2 ECw}{(a)^2}\right]$$

Use properties of single section; (Unit; mm.)

$r_0 = \sqrt{r_x^2 + r_y^2 + X_0^2}$

G = Shear modulus

J = Torsion constant

Cw = Warping Constant

a = Weld spacing

Ag = Gross section area

$$Fe = \frac{1}{443 x 79.73^2}\left[7946.93 x 332 + \frac{\pi^2 x 2.1 x 10^4 x 1070 x 10^6}{250^2}\right]$$

Fe = 126095.14 ksc.

Fe_3 (flexural-torsional buckling stress between fasterers)

$$\mathbf{Fe_3} = \frac{1}{2B}\left[(\sigma ex+\sigma t)-\sqrt{(\sigma ex+\sigma t)^2-4\beta\sigma ex\sigma t}\right]$$

since $\sigma ex = \frac{\pi^2 E}{(KxLx/rx)^2}$

$$\sigma ex = \frac{\pi^2 x 2.1 x 10^6}{(100/6.02)^2}$$

$\therefore$ σex = 75111.14 ksc

Substituted value into equation ; by σt = 126095.14 (Fe_2)

$\therefore$ Fe_3 = 47071.84 ksc.

$\therefore$ Minimum of Fe is Fe_3 (flexural-torsional buckling stress between fastener)

Fe_3 = 47071.84 ksc..

$$\lambda_c = \sqrt{\frac{Fy}{Fe}}$$

$$\lambda_c = \sqrt{\frac{5400}{47071.84}}$$

λ_c = 0.34 < 1.5 (Inelastic buckling)

$$Fn = (0.658^{\lambda_c^2})\, Fy$$

Fn = 5145 ksc

Effective Area Ae at stress Fn

1. Lip = 15.5 mm

W_1 = 15.5 – (5+1.5) = 9 mm

2. Flange = 64 mm.

W_2 = 64-2(5+1.5) = 51 mm.

3. Web = 152 mm.

W_3 = 152-2(6.5) = 138.5 mm.

1. Effective Width of Compression flange

$\frac{w}{t}$ = 51/1.5 = 34

$S = 1.28\sqrt{E/f}$

$S = 1.28\sqrt{2.1x10^4/51.45}$

$S = 25.86$, $\frac{s}{3} = 8.62$

$\frac{w}{t} > S$

$Ia = \left\{\left[115\left(\frac{w}{t}\right)/S\right]+5\right\}t^4$

$Ia = \left\{\left[\frac{115x34}{25.86}\right]+5\right\}1.5^4$

Ia = 790.75

D = 15.5

$d = D-(f-t) = 15.5-(5+1.5) = 9$ mm.

$\frac{d}{t} = \frac{9}{1.5} = 6 < 14$ (Maximum d/t)

$Is = d^3t/12$

$= 9^3 \times 1.5/12$

$= 91.125$

$C_2 = Is/Ia$

$= \frac{91.125}{790.75} = 0.115 < 1.0$

$D/W_2 = \frac{15.5}{51} = 0.304 < 0.8$

$\therefore ka = 5.25 - 5(D/W_2)$

$ka = 5.25 - 5(0.304)$

$ka = 3.73$

$k = C_2^n(ka-ku) + ku$

$k = 0.115^{0.333}(3.73-043)+0.43$

$k = 2.03$

$$\lambda = \left(1.052/\sqrt{2.03}\right)(34)\left(\sqrt{\frac{51.45}{2.1x10^4}}\right)$$

$$\lambda = 1.24 > 0.673$$

$$b = \rho w$$

$$b = \left[\left(1-\frac{0.22}{1.24}\right)/1.24\right]x51$$

$$b = 33.83 \text{ mm.}$$

2. Effective Width of Edge stiffener

$$\lambda = \frac{1.052}{\sqrt{k}}\left(\frac{w_1}{t}\right)\sqrt{\frac{f}{E}}$$

$$\lambda = \frac{1.052}{\sqrt{0.43}}(6)\sqrt{\frac{51.45}{2.1x10^4}}$$

$$\lambda = 0.47 < 0.673$$

$$d'_s = d = 9 \text{ mm.}$$

$$d_s = C_2 d'_s = 0.115 \times 9 = 1.03$$

3. Effective Width of Web Element

$$\frac{w}{t} = \frac{138.5}{1.5} = 92.33 < 500 \quad \text{OK}$$

$$\lambda = \frac{1.052}{\sqrt{k}}\left(\frac{w_3}{t}\right)\sqrt{\frac{f}{E}}$$

$$\lambda = \frac{1.052}{\sqrt{4}}(92.33)\sqrt{\frac{51.45}{2.1x10^4}}$$

$$\lambda = 2.40 > 0.673$$

$$\rho = \left(1-\frac{0.22}{\lambda}\right)/\lambda$$

$$\rho = \left(1-\frac{0.22}{2.40}\right)/2.40$$

$$\rho = 0.38$$

$$b = \rho w_3 = 0.38 \times 138.5 = 52.63 \text{ mm.}$$

$\therefore$ Ae of BC150@250 = 886-[4(9-1.03)+4(51-33.83)+2(138.5-52.63)]x 1.5

$$= 477.55 \text{ mm}^2 = 4.78 \text{ cm}^2$$

Since ; Pn = Ae x Fn

Pn = 4.78 x 5145

Pn = 24.58 Ton

4. BC 200 @ 125 (Built-up)

Section properties

Length(cm)	Weld spacing (a) (cm)	Section area (cm^2)	Ix (cm^4)	Iy (cm^4)	r_y (cm)	r_x (cm)
100	12.5	11.10	734.79	426.96	6.20	8.13

Modified slenderness ratio

$$\left(\frac{KL}{r}\right)_m = \sqrt{\left(\frac{KL}{r}\right)_0^2 + \left(\frac{a}{r}\right)^2}$$

$\left(\frac{KL}{r}\right)_0$ = Overall slenderness of built-up mumber

r_i = Minimum radius of gyration on individual member of built-up

$\left(\frac{KL}{r}\right)_m$ = Modified slenderness ratio

a = Weld spacing

$$\left(\frac{KL}{r}\right)_m = \sqrt{\left(\frac{0.5x1000}{62}\right)^2 + \left(\frac{125}{26.7}\right)^2}$$

$$\left(\frac{KL}{r}\right)_m = 9.33$$

Fe_1 (Flexural buckling); $= \frac{\pi^2 E}{(KL/r)_m^2}$

$$= \frac{\pi^2 x 2.1x10^6}{(9.33)^2}$$

= 238098 ksc.

Fe_2 (Torsional buckling stress between fasteners)

$$Fe_2 = \frac{1}{A_g r_0^2}\left[GJ + \frac{\pi^2 ECw}{(a)^2}\right]$$

Use properties of single section; (Unit; mm.)

$r_0 = \sqrt{r_x^2 + r_y^2 + X_0^2}$

G = Shear modulus

J = Torsion constant

Cw = Warping Constant

a = Weld spacing

Ag = Gross section area

$$Fe = \frac{1}{555 x 98.63^2}\left[7946.93 x 416 + \frac{\pi^2 x 2.1 x 10^4 x 3060 x 10^6}{125^2}\right]$$

Fe = 751873.47 ksc.

Fe_3 (flexural-torsional buckling stress between fasterers)

$$\mathbf{Fe_3} = \frac{1}{2B}\left[(\sigma ex + \sigma t) - \sqrt{(\sigma ex + \sigma t)^2 - 4\beta\sigma ex\sigma t}\right]$$

since $\sigma ex = \frac{\pi^2 E}{(KxLx/rx)^2}$

$$\sigma ex = \frac{\pi^2 x 2.1 x 10^6}{(100/7.97)^2}$$

$\therefore$ σex = 131653.24 ksc

Substituted value into equation ; by σt = 751873.47 ksc (Fe_2)

$\therefore$ Fe_3 = 112035.75 ksc.

$\therefore$ **Minimum of Fe is Fe_3 (flexural-torsional buckling stress between fastener)**

$Fe_3 = 112035.75$ ksc.

$$\lambda_c = \sqrt{\frac{Fy}{Fe}}$$

$$\lambda_c = \sqrt{\frac{5400}{112035.75}}$$

$\lambda_c = 0.22 < 1.5$ (Inelastic buckling)

$$Fn = (0.658^{\lambda_c^2}) Fy$$

$Fn = 5291.71$ ksc

Effective area Ae at stress Fn

1. Lip element = 15.5 mm
   $W_1 = 15.5 - (5+1.5) = 9$ mm

2. Flange element = 76 mm.
   $W_2 = 76-2(5+1.5) = 63$ mm.

3. Web element = 203 mm.
   $W_3 = 203-2(6.5) = 190$ mm.

1. Effective Width of Compression flange

$$\frac{w}{t} = \frac{63}{1.5} = 42$$

$$S = 1.28\sqrt{E/f} = 1.28\sqrt{2.1x10^4 / 52.91}$$

$$S = 25.50 \quad , \frac{s}{3} = 8.50$$

$$\frac{w}{t} > S$$

$$Ia = \left\{\left[115\left(\frac{w}{t}\right)/S\right]+5\right\}t^4$$

$$Ia = \left\{\left[\frac{115x42}{25.50}\right]+5\right\}1.5^4$$

$$Ia = 984.21$$

$D = 15.5$

$d = D-(f-t) = 15.5-(5+1.5) = 9$ mm.

$$\frac{d}{t} = \frac{9}{1.5} = 6 < 14 \text{ (Maximum d/t)}$$

$Is = d^3t/12$

$= 9^3 \times 1.5/12$

$= 91.125$

$C_2 = Is / Ia$

$$= \frac{91.125}{984.21} = 0.092 < 1.0$$

$$D/W_2 = \frac{15.5}{63} = 0.246 < 0.8$$

$\therefore$ $ka = 5.25 - 5(D/W_2)$

ka = 5.25 – 5(0.246)

ka = 4.02 > 4.0

∴ ka = 4.0

$k = C_2^n(ka-ku) + ku$

$k = 0.1^{0.333}(4-043)+0.43$

k = 2.09

$\lambda = \left(1.052/\sqrt{2.09}\right)(42)\left(\sqrt{\frac{52.91}{2.1x10^4}}\right)$

λ = 1.53 > 0.673

b = ρw

$b = \left[\left(1-\frac{0.22}{1.53}\right)/1.53\right]x63$

b = 35.26 mm.

2. Effective Width of Edge stiffener

$\lambda = \frac{1.052}{\sqrt{k}}\left(\frac{w1}{t}\right)\sqrt{\frac{f}{E}}$

$\lambda = \frac{1.052}{\sqrt{0.43}}(6)\sqrt{\frac{52.91}{2.1x10^4}}$

λ = 0.483 < 0.673

d^1_s = d = 9 mm.

d_s = $C_2 d^1_s$ = 0.092 x 9 = 0.828

3. Effective Width of Web Element

$\frac{w}{t} = \frac{190}{1.5} = 126.67 < 500$ OK

$\lambda = \frac{1.052}{\sqrt{k}}\left(\frac{w_3}{t}\right)\sqrt{\frac{f}{E}}$

$\lambda = \frac{1.052}{\sqrt{4}}(126.67)\sqrt{\frac{52.91}{2.1x10^4}}$

$\lambda = 3.34 > 0.673$

$\rho = \left(1-\frac{0.22}{\lambda}\right)/\lambda$

$\rho = \left(1-\frac{0.22}{3.34}\right)/3.34$

$\rho = 0.28$

b = ρw_3 = 0.28 x 190 = 53.2 mm.

$\therefore$ Ae = 1110-[4(9-0.828)+4(63-35.26)+2(190-53.2]x 1.5

= 484.13 mm^2 = 4.84 cm^2

Since ; Pn = Ae x Fn

Pn = 4.84 x 5291.71

Pn = 25611.87 Kg . = 25.61 Ton.

CURRICULUM VITAE

NAME : Mister. Siripob Kakaew

BIRTH DATE : June 28, 1980

BIRTH PLACE : Nonthaburi, Thailand

EDUCATION :

YEAR	INSTITUTE	DEGREE/DIPLOMA
2004	Kmutt.	B.E (Civil engineering.)

POSITION/TITLE : Structure Engineer

WORK PLACE : Freelance